SYNTHESIS, CHARACTERIZATION, AND REACTIVITY OF ZIRCONIUM (IV), TANTALUM (V), AND TUNGSTEN (VI) AMIDO COMPLEXES CONTAINING POLYDENTATE LIGANDS

By

PERCEFONI DOUFOU

A DISSERTATION PRESENTED TO THE GRADUATE SCHOOL
OF THE UNIVERSITY OF FLORIDA IN PARTIAL FULFILLMENT
OF THE REQUIREMENTS FOR THE DEGREE OF
DOCTOR OF PHILOSOPHY

UNIVERSITY OF FLORIDA

1997

Στους γονεις μου Γεωργιο και Χρυσανθη και την αδερφη μου Αθηνα–Μαρκια

To my parents George and Chrysanthe, and my sister Athena-Marcia

ACKNOWLEDGMENTS

I am eternally grateful to my parents who have instilled in me the desire to learn and to improve myself, and to my sister Athena who has been my best friend always. Their love, support and advice has given me strength throughout my life and especially during my years in graduate school.

I would like to extend my thanks to my research advisor Dr. James M. Boncella for his help and guidance throughout my graduate work in the University of Florida. I am sure the lessons I have learned from Jim will have a great influence on my life in chemistry. I also greatly appreciate the advice and encouragement that I have received from the other members of my committee, Dr. Russell Drago, Dr. David Richardson, Dr. Kenneth Wagener, and Dr. Anthony Brennan. In addition, I would like to thank Dr. Lisa McElwee-White for various helpful discussions, and Dr. Khalil Abboud for solving the crystal structures included in this dissertation and for patiently helping me understand them and interpret them.

Past and present fellow group members have provided a stimulating and fun work environment. Those people are Laura Blosch, Larry Villanueva, Will Vaughan, Dan Vanderlende, Mary Cajigal, Jerrold Miller, Steve Wang, Carlos Ortiz, David Knoeppel, Leigh Huff, and Ryan Mills. Special thanks to Perla Izsak for her friendship in and out of lab, and to Jon Penney for graciously answering all my computer questions and for always managing to "turn my frown upside down."

Tammy Davidson has been a dear friend and I want to thank her for always being there for me sharing good and bad times. I also wish to thank Augusta Dimou, Elizabeth Talmage, Gianna Thomatou, Niko Ganatsio and Ahmet Nadeem for their friendship, and for providing an enjoyable break from chemistry.

Finally, I would like to express my deepest appreciation to Dr. Faisal Shafiq whose friendship has meant so much to me personally and professionally. He has been a continuous source of motivation with his contagious enthusiasm about chemistry, his good advice, and his unique perspectives on life.

TABLE OF CONTENTS

ACKNOWLEDGEMENTS iii

ABSTRACT vii

CHAPTERS

1 INTRODUCTION AND BACKGROUND 1

Stabilization and Active Site Control of High-Oxidation State Early Transition Metal Complexes by use of Polydentate Ligands 1
Cyclopentadienyl and Hybrid-Cyclopentadienyl Ligands 2
Polydentate Ligands containing Nitrogen Functionalities 12

2 SYNTHESIS, STRUCTURE AND EXAMINATION OF PROTON TRANSFER IN W(VI) ALKYLIDYNE AMIDO COMPLEXES 3

Introduction 26
Attempted Ligand Removal from $TpW(CC(CH_3)_3)Cl_2$ and $Tp'W(CC(CH_3)_3Cl$ and Attempted Preparation of Monoalkyl Complexes 27
Synthesis of Hydro(1-pyrazolyl)borate (Tp) Neopentylidyne Amido Complexes 29
Synthesis of a Hydro(3,5-dimethyl-1-pyrazolyl)borate (Tp') Neopentylidyne Amido Complex 38
Variable Temperature and NOe Studies for Tp Amido Complexes **3**, **6-8** 43
Tautomerization Studies involving W(VI) Tp and Tp' Amido Alkylidyne Complexes 44
Conclusions 53

3 SYNTHESIS OF BISAMIDO-CYCLOPENTADIENYL AND (BIS)SULFAMIDE CHELATING LIGANDS AND THEIR USE IN THE SYNTHESIS OF ZIRCONIUM (IV) AND TANTALUM (V) METAL COMPLEXES 55

Synthesis of a Trianionic Bisamido-cyclopentadienyl Ligand 55
Reactions of **10** with Various Metal Complexes 57
(Bis)Sulfamides as Ligands 69
Attempted Deprotonation of $SO_2(NHR)_2$ (R = t-butyl (**14**), CHMePh (**15**) 72
Addition of **14** and **15** to Various Group IV-VI Alkyl, Imido, and Amido Metal Complexes 73
Attempted Conversion of **17** and **18** to their Halide and Alkyl Derivatives 82
Conclusions 85

4 EXPERIMENTAL PROCEDURES....87

Materials and Methods....87
Photolyses....88
TpW(NHPh)(CC(CH$_3$)$_3$)Cl (**3**)....88
TpW(NHPh-p-Br)(CC(CH$_3$)$_3$)Cl (**4**)....89
TpW(NHPh-3,5(CF$_3$)$_2$)(CC(CH$_3$)$_3$)Cl (**5**)....89
TpW(NH$_2$)(CC(CH$_3$)$_3$)Cl (**6**)....90
TpW(NHPh)$_2$(CC(CH$_3$)$_3$) (**7**)....90
Tp'W(NHPh)(CC(CH$_3$)$_3$)Cl (**8**)....91
Addition of H$_2$O to **3**, **4**, **5**, and **6**....92
Addition of a) NHCl$_4$, b) NEt$_3$HCl, c)HCl to Solutions of **3** that did not Tautomerize to TpW(NPh)(CHC(CH$_3$)$_3$)Cl (**9**)....92
1,2-(NH(C$_6$H$_5$)(N'H((C$_5$H(CH$_3$)$_4$)Si(CH$_3$)$_2$)C$_6$H$_4$ (**10**)....93
Alternate Synthesis of o-C$_6$H$_4${NH(C$_6$H$_5$)N'H[Si(CH$_3$)$_2$(C$_5$(CH$_3$)$_4$H)]} (**10**)....93
o-C$_6$H$_4${N(C$_6$H$_5$)N'[Si(CH$_3$)$_2$(C$_5$(CH$_3$)$_4$)]}Zr(N(CH$_3$)$_2$)(NH(CH$_3$)$_2$) (**12**)....94
o-C$_6$H$_4${N(C$_6$H$_5$)N'[Si(CH$_3$)$_2$(C$_5$(CH$_3$)$_4$)]}Zr(Cl)(NH(CH$_3$)$_2$)$_2$ (**13**)....94
Ta[N(CH$_3$)$_2$]$_3$[SO$_2$(NC(CH$_3$)$_3$)$_2$] (**17**)....95
Ta[N(CH$_3$)$_2$]$_3${SO$_2$[N[CH(CH$_3$)(C$_6$H$_5$)]]$_2$} (**18**)....96
Ta[N(CH$_3$)$_2$]$_3$[SO$_2$(NC(CH$_3$)$_3$)$_2$][Al(CH$_3$)$_3$]$_2$ (**19**)....96
Ta[N(CH$_3$)$_2$]$_3$[SO$_2$(NC(CH$_3$)$_3$)$_2$][Al(CH$_2$CH$_3$)$_3$]$_2$ (**20**)....97
Crystallographic Studies....98
X-ray Data Collection and Structure Refinement for Compounds **7** and **8**....97
X-ray Data Collection and Structure Refinement for Compounds **12** and **13**....98
X-ray Data Collection and Structure Refinement for Compound (**17**)....99

APPENDIX A....101

REFERENCES....151

BIOGRAPHICAL SKETCH....159

Abstract of Dissertation Presented to the Graduate School
of the University of Florida in Partial Fulfillment of the
Requirements for the Degree of Doctor of Philosophy

SYNTHESIS, CHARACTERIZATION, AND REACTIVITY OF ZIRCONIUM (IV), TANTALUM (V), AND TUNGSTEN (VI) AMIDO COMPLEXES CONTAINING POLYDENTATE LIGANDS

By

Percefoni Doufou

August, 1997

Chairman: James M. Boncella
Major Department: Chemistry

A number of tungsten (VI) amido alkylidyne complexes containing the chelating ligands Tp (hydrido(1-pyrazolyl)borate) and Tp' (hydrotris(3,5-dimethyl-1-pyrazolyl)borate) are described. Complexes of general formula, $TpW(CC(CH_3)_3)(Cl)(NHR)$ [R = Ph, p-Br-Ph, 3,5-bis-(CF_3), H], (**3-6**), were formed by reaction of $TpW(CC(CH_3)_3)(Cl)_2$ with the respective amide M^+NHR^- (M = Li, K). In the presence of excess Li^+NHPh^-compound $TpW(CC(CH_3)_3)(NHPh)_2$ (**7**) was isolated. The complex $Tp'W(CC(CH_3)_3)(Cl)(NHPh)$ (**8**) was synthesized by reaction of $(CH_3)_3SiN(H)Ph$ with $(DME)W(CC(CH_3)_3)(Cl)_3$ followed by addition of KTp'. Due to their electronic and coordinative saturation, these complexes display ligand centered reactivity such as proton transfer from the amido to the alkylidyne ligand of the complex, resulting in the formation of the corresponding imido-alkylidenes.

The trianionic ligand 1,2-$(NH(C_6H_5)(N'H((C_5H(CH_3)_4)Si(CH_3)_2)C_6H_4$ (**10**) and two dianionic (bis)sulfamide ligands $(SO_2(NHR)_2$ (R = t-butyl (**14**), CHMePh (**15**)) were

also synthesized. The amine elimination method was used in order to synthesize the cyclopentadienyl-diamido zirconium (IV) complexes *o*-$C_6H_4\{N(C_6H_5)N'[Si(CH_3)_2(C_5(CH_3)_4)]\}Zr(N(CH_3)_2)(NH(CH_3)_2)$ (**12**) and *o*-$C_6H_4\{N(C_6H_5)N'[Si(CH_3)_2(C_5(CH_3)_4)]\}Zr(Cl)(NH(CH_3)_2)_2$ (**13**), and tantalum (V) (bis)sulfamide complexes $Ta[N(CH_3)_2]_3[SO_2(NC(CH_3)_3)_2]$ (**17**) and $Ta[N(CH_3)_2]_3\{SO_2[N[CH(CH_3)(C_6H_5)]]_2\}$ (**18**). Single X-ray crystal studies were performed for three of these complexes, including *o*-$C_6H_4\{N(C_6H_5)N'[Si(CH_3)_2(C_5(CH_3)_4)]\}Zr(N(CH_3)_2)(NH(CH_3)_2)$ (**12**), *o*-$C_6H_4\{N(C_6H_5)N'[Si(CH_3)_2(C_5(CH_3)_4)]\}Zr(Cl)(NH(CH_3)_2)_2$ (**13**), and $Ta[N(CH_3)_2]_3[SO_2(NC(CH_3)_3)_2]$ (**17**). Attempted abstraction of the dimethylamido ligands from **17** by AlR_3 (R = Me, Et) resulted in the formation of adducts of the general formula $Ta(NMe_2)_3[SO_2(NC(CMe_3)_2].(AlR_3)_2$ (**19** when R = Me, **20** when R = Et). The synthesis of ligands **10**, **14**, and **15**, and of metal complexes containing them is related to the recent interest in high-oxidation state early transition metal complexes containing cyclopentadienyl-amido and chelating diamido ligands. Such complexes are of interest because of their demonastrated ability to polymerize olefins.

CHAPTER 1
INTRODUCTION AND BACKGROUND

Stabilization and Active Site Control of High-Oxidation State Early Transition Metal Complexes by use of Polydentate Ligands

The use of high oxidation state, early transition metal complexes (d^0 metals for the purpose of this introduction) has promoted in recent years a rich area of research for metal-mediated transformations. Such metal-mediated reactions include coordination polymerizations[1], electrophilic hydrocarbon activation[2], hydrogenation reactions[3], olefin metathesis reactions[4], and activation of small molecules such as N_2 and CO.[5] The high Lewis acidity of the d^0 early transition metals, combined, in most cases, with their coordinative and electronic unsaturation are important characteristics for many of these catalytically active species.[6]

Since the reactivity of these metal complexes is strongly related to their coordination environment, it is obvious that the choice of ancillary ligands is critical when designing a metal complex. Such ligands should, for example, be able to enhance the stability of metal complexes prone to decomposition, introduce a chiral environment thereby forcing a reaction to proceed regiospecifically, or block parts of the metal coordination sphere thus decreasing the number of possible active sites on a complex. The ligands also need to be easily functionalized in order to be tailored to individual reaction requirements.

In this vein, polydentate ligands are ideal for stabilizing and controlling the reactivity of high-oxidation state early transition metal complexes.[6] These ligands not only provide enhanced thermal and kinetic stability owing to the chelate effect, but their rigidity may also force limited and specific accessibility of reagents to the metal center. If the polydentate ligands are polyanionic, then they can reduce the coordination number of the

high-oxidation state metal complex without reducing its stability. Among the most common polydentate ligands for high oxidation Group III-VI metals are cyclopentadienyl rings,[7] functionalized cyclopentadienyl rings,[8] and ligands containing nitrogen[5d,6] and oxygen donors.[6,9] This introduction will only focus on cyclopentadienyl, functionalized cyclopentadienyl ligands, and ligands containing nitrogen functionalities since these types of ligands are more pertinent to the chemistry described in the following chapters. Moreover, the presentation of tris-pyrazolyl polydentate ligands will not be included in this chapter since, these ligands will be discussed more extensively in the introduction to Chapter 2.

Cyclopentadienyl and Hybrid-Cyclopentadienyl Ligands

The introduction of the cyclopentadienyl ligand as a new type of ancillary ligand resulted in an explosive growth of organotransition metal chemistry.[7b] Among the features that make this ligand so versatile are its relative kinetic and chemical stability upon coordination to a metal center, and the large array of synthetically accessible electronic and structural modifications (e.g. **Figure 1.1**).[10]

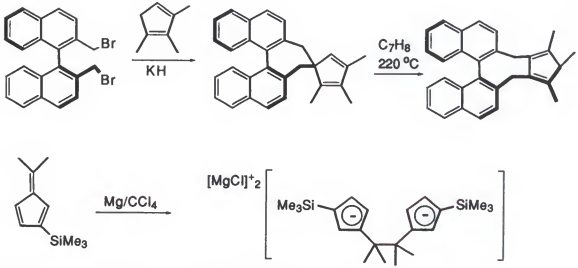

Figure 1.1 Examples of modifications that cyclopentadienyl ligands can undergo.

Cyclopentadienyl and functionalized cyclopentadienyl ligands have been especially useful in the synthesis and isolation of a great number of high-oxidation state early transition metal complexes.[7,8,10] Of those, Group III and IV cyclopentadienyl complexes have probably received the most attention due to their wide range of applications in homogeneous catalysis[6,11] and stereoselective syntheses.[10,12] Variations on the cyclopentadienyl ligand itself and on the number of cyclopentadienyl ligands attached to the metal have been shown to influence significantly the reactivity of these complexes and the structure of the resulting products. There is an enormous amount of literature on the synthesis and reactivity of early transition metal complexes containing cyclopentadienyl and functionalized cyclopentadienyl ligands. This introduction, however, will only cover a few specific examples concerning the chemistry related to cyclopentadienyl ligands.

Efforts to modify the steric/electronic properties of the cyclopentadienyl moiety have to a great extent been related to its importance as an ancillary ligand for metal complexes that catalyze olefin polymerizations.[1,13] (Bis)cyclopentadienyl complexes, particularly of Group IV (e.g. Cp_2MX_2 where M = Zr, Ti, X = Cl, Me), have become extremely important industrially.[14] They are highly active, homogeneous catalysts for olefin polymerization in the presence of methylaluminoxane (MAO). The advantage of the metallocene systems over classical heterogeneous olefin polymerization systems arises from the fact that the metallocenes are well defined, "single site" catalysts.[15] The well defined nature of these complexes has also allowed detailed mechanistic studies on the olefin polymerization reaction. Given the experimental evidence, the catalytic species of the Group IV metallocene systems is generally postulated to be a 14-electron metallocene alkyl cation.[14,16]

The most important benefit of using metallocene systems over classical systems in olefin polymerization is their ability to provide effective stereocontrol in the polymers produced by higher olefins and in the co-polymerization of different monomers.[17] The olefin insertion stereochemistry is dictated primarily by the cyclopentadienyl ligand

framework. For example, the zirconium complex shown in **Figure 1.2** can effectively produce polypropylene that contains isotactic and atactic stereoblocks, thus producing a very elastic polymer.[18] This type of polymerization is achieved by employing phenyl substituted indenyl rings which rotate about the metal-ligand bond axis with much slower rates compared to unsubstituted Cp rings. The slow rotation of the substituted indenyl rings causes this catalyst to isomerize slowly between chiral and achiral geometries thus producing blocks of different tacticity.

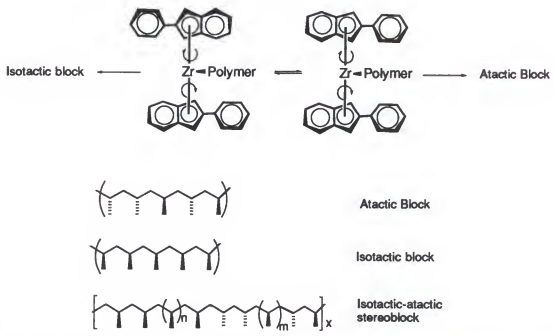

Figure 1.2 Stereoblock polymers produced by rotation of the indenyl rings around the Zr-Cp axis.

Achiral and chiral metallocenes, in which the two cyclopentadienyl rings are connected with bridges of variable lengths, are other types of systems that have also demonstrated remarkable control over polymer tacticity, block structure, and level of monomer incorporation.[10,14,19] In addition, these complexes have been used extensively

as stereoselective catalysts for a variety of other reactions (an example given in **Figure 1.3**) such as asymmetric hydrogenations,[3,20] epoxidations,[21] Diels-Alder reactions,[22] and dehydrogenative phenylsilane oligomerization.[23] The rigidity of the bridged cyclopentadienyl or substituted cyclopentadienyl rings due to hindered rotation relative to one another, combined in most cases with smaller Cp-M-Cp angles compared to unbridged systems are the controlling reactivity factors of these complexes.

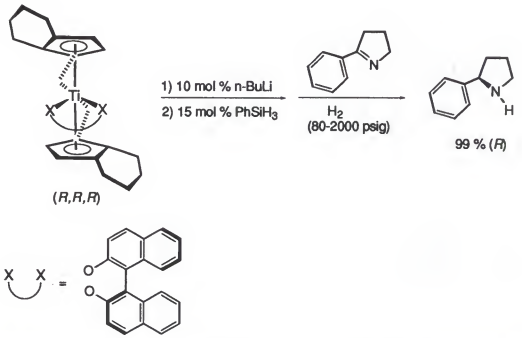

Figure 1.3 Example of stereoselective catalysis of imine hydrogenation using a chiral *ansa*-metallocene catalyst.[3c]

Substantial steric congestion around the metal-centered reaction site can still be a problem, however, even for bridged bis(cyclopentadienyl) systems.[8] Therefore, there has been an increasing interest in "constrained geometry" derivatives that contain a single cyclopentadienyl ring linked to additional pendent ligands such as amines, amides, alkoxides, and olefins.[8,14,24] These systems can further enhance the Lewis acidity and

electrophilicity of the metal center because of reduced steric crowding and electron count compared to their bis(cyclopentadienyl) analogs.[14] Another important feature that some of these ligands present is the formation of complexes that are neutral analogs of active cationic metallocene complexes for olefin polymerization.

Interest in the synthesis of various mixed Cp-amido ligand systems for early transition metal complexes has originated from the "Cp-SiNR" scandium systems that were first reported by Bercaw *et al.*. (**Figure 1.4**).[24a] Previous studies had demonstrated that scandanocene systems of the type Cp^*_2Sc-R, $[(C_5Me_4)_2SiMe_2]Sc$-R, and $[(C_5H_3CMe_3)_2SiMe_2]Sc$-R undergo facile ethylene insertion and β-H and β-R elimination.[25] These systems, however, were not active towards higher olefins. The dimeric complex $[(Cp(Me)_4SiMe_2NR)Sc(PMe_3)]_2(\mu\text{-}H)_2$ (**Figure 1.4**) on the other hand, cleanly catalyzes the oligomerization of propene, 1-butene, and 1-pentene although with rather slow rates.[24] The slow polymerization rates are partly compensated by very slow chain transfer rates thus giving a reasonably high molecular weight polymer. The difference between the (bis)cyclopentadienyl-Sc systems and the "Cp-SiNR"Sc system is that the amido ligand of the "Cp-SiNR" ligand renders the metal more accessible and more electron deficient, thus encouraging olefin insertion and hindering the β-H and β-R elimination steps.[24,25]

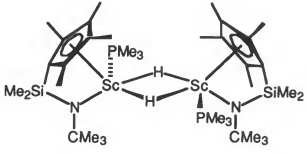

Figure 1.4 The half-sandwich "constrained geometry" system introduced by Bercaw.

Following Bercaw's observations on the scandanocene systems, researchers at Dow Chemical Co[26] and Exxon[27] have produced Group IV compounds of the general formula $(\eta^5\text{-}C_5R_4)SiR'_2(\eta^1NR'')MCl_2$ (where M = Ti, Zr, Hf, R = alkyl; R', R" = alkyl or aryl) that are highly active catalysts in the presence of MAO for the copolymerization of ethylene with 1-alkenes. The Cp(c)-M-N angle (Cp(c) = Cp centroid) in these systems is approximately 25-30° smaller than the Cp(c)-M-Cp(c) angle of the typical *ansa*-metallocenes which, combined with the more electron-deficient d^0 metal center, presumably promotes facile migratory olefin insertion into the metal-carbon bond of the growing polymer.

The usual synthetic approach to "Cp-SiNR" zirconium and titanium systems utilizes the reaction of the dilithio salt $[(C_5R_4)Si(NR')]^{-2}$ with the appropriate metal halide.[24,26,27] In some instances, this route leads to isolation of isomeric mixtures, especially when R = H on the Cp ring.[28] Petersen *et al.* [28] have utilized the amine elimination reaction in order to produce clean cyclopentadienyl-amido metal complexes. The neutral form of the ligand $[(C_5R_4H)Si(NHR')]$ can be introduced to the metal sphere by its reaction with corresponding Group IV homoleptic amides. The ancillary amides are then removed to give the desired dihalide complexes. This procedure has proven to be a convenient alternative synthetic method although in some cases, addition of acidic media (e.g. NEt_3HCl) in order to remove the NMe_2 ligands, has led to cleavage of the Si-N bond of the "Cp-SiNR" ligand (**Figure 1.5**). Such cleavage can be avoided if no Si-N bonds are present. For example, complexes of the type $[\{\eta^5\text{:}\eta^1\text{-}C_5H_4(CH_2)_3NMe\}MNMe_2]$ (M = Zr, Hf), in which the cyclopentadienyl and amido ligands are connected through an alkyl bridge, are more stable to protonolysis and give good yields of the corresponding dihalides.[29]

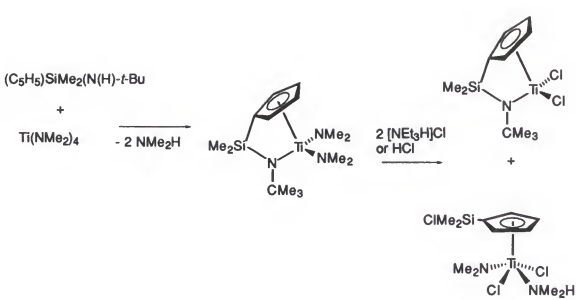

Figure 1.5 Synthesis of "Cp-SiNR" containing metal halide complexes by amine elimination and removal of the NMe_2 ligands by acidic media.

A number of functionalized cyclopentadienyl and fluorenyl ligands derived from the "Cp-SiNR" system have led to synthesis of various transition metal complexes with novel coordination spheres (e. g. **Figure 1.6 A-C**).[30]

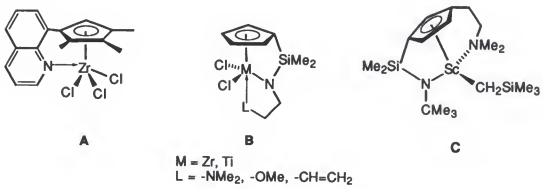

Figure 1.6 Different types of cyclopentadienyl complexes with pendent ligands.

Okuda *et al.* [31] for example, have prepared a chelating ligand in which a side chain with a semi-labile neutral ligand (NR_2, OR) is connected to the dianionic "Cp-SiNR" frame (**Figure 1.6 B**). Their reasoning for using the additional weak donor ligand is that depending on the reaction conditions, this ligand can either leave the metal exposed or increase its coordination number by interacting with it.

Two routes have been presented for preparing a metal complex that contains this type of ligand (**Figure 1.7**). One way is to prepare the complete polydentate ligand prior to its attachment to the metal center (**Figure 1.7** pathway (**a**)).[31b] The other way is to first prepare a half sandwich metal complex in which the cyclopentadienyl ligand can be further functionalized since it contains a reactive -$SiMe_2Cl$ group (**Figure 1.7** pathway (**b**)).[31a] The coordination mode of the neutral donor ligand differs in the Ti and Zr complexes.

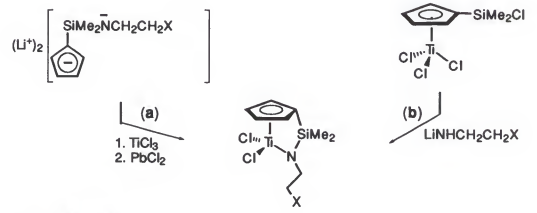

Figure 1.7 Two ways of preparing a metal complex containing a functionalized cyclopentadienyl ligand.

For complexes containing the functionalized cyclopentadienyl ligand shown in **Figure 1.7**, proton NMR spectra and crystal structure data confirm that the intramolecular

coordination of the -OMe and -NMe_2 fragments is stronger in the Zr complexes than in the Ti analogs.

Another important feature of the ligand system prepared by Okuda is the possibility of utilizing the chelate effect in order to prepare a ligand with a pendent olefin which could coordinate to the d^0 metal center. There is only one example of a d^0-olefin complex to date.[32] This type of complex would be very interesting since it could provide a structural model for olefin coordination to the metal center prior to the insertion step. Unfortunately, in Okuda's system there is no direct evidence that the olefin arm is coordinated to the metal center.[31]

A procedure similar to the one shown in **Figure 1.7** was also used to synthesize cyclopentadienyl ligands in which the pendent ligand is an alkoxide.[33] This "Cp-Si-O" type ligand has also been used to form dimers in which the cyclopentadienyl ligand is located on one metal center whereas the alkoxide part of the ligand is bridging the other metal center. The dimer shown in **Figure 1.8** is formed by hydrolysis of $[C_5H_4(SiMe_2Cl)]TiCl_3$. Further reaction with water can then give the monomeric species.

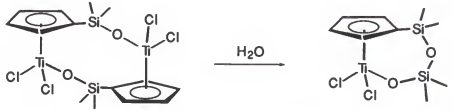

Figure 1.8 Dimeric and monomeric complexes containing a "Cp-SiO" type ligand.

Piers *et al.* have reported the synthesis of Sc and Zr complexes in which the cyclopentadienyl ligands are disubstituted, with amido and pendent neutral ligands on the 1

and 3 positions of the Cp ring (e.g. **Figure 1.6C**).[30c,34] The Sc complex shown in **Figure 1.6C** was prepared by an unusual one-pot reaction of $ScCl_3.3THF$, Me_3SiCH_2Li, and $CpH^{NMe}SiN(H)R$ (SiNR = -$SiMe_2$N-*t*-butyl; NMe = 3-$CH_2CH_2NMe_2$). An interesting metal complex arises from reaction of a similar ligand containing a pendent allyl chain.[34] Reaction of $Li_2Cp^{allyl}Si(CH_3)_2NR$ (R = *t*-butyl) with $ZrCl_4$ gives a "Cp-SiNR" ligand type metal complex in which the allyl chain is not coordinated to the metal center. The C=C bond of the allyl chain can be easily hydroborated while on the metal complex (**Figure 1.9**). The ultimate aim is to produce a zwitterionic complex, similar to those reported by Erker and others, in which the counterion is covalently attached to the metal complex.[35]

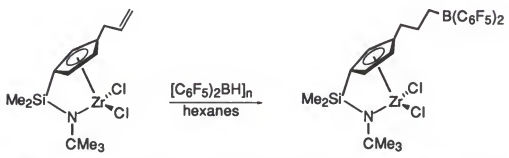

Figure 1.9 Hydroboration of the pendent allyl functionality on the "Cp-SiNR" ligand system.

Due to their industrial importance as potential olefin polymerization catalysts, most of the research concerning metal complexes with cyclopentadienyl-amido ligands has focused on Group IV metals. On the other hand, complexes of these ligands with Group V and VI metals are rare. Herman *et al.*[36] has reported the synthesis of Ta (V), Nb(V) and Mo(IV) complexes that contain a "Cp-SiNR" ligand. Their synthesis was achieved by

reaction of the homoleptic amides $Mo(NMe_2)_4$ and $M(NMe_2)_5$ (M = Nb, Ta) with $(C_5H_5)SiMe_2(NHPh)$. Interestingly, for the tantalum and niobium complexes, photolytic cleavage of the Si-N bond of the ligand was observed, resulting in the formation of an imido species (**Figure 1.10**).[36a] This type of transformation once again demonstrates that the "Cp-SiNR" type ligands may not be tolerant to certain reaction conditions.

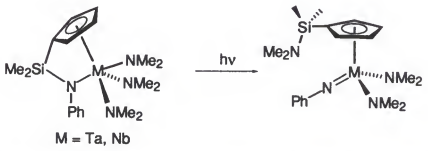

Figure 1.10 Photolytic cleavage of the Si-N bond of the chelate Cp-SiNR ligand

Polydentate Ligands Containing Nitrogen Functionalities

Polydentate, nitrogen containing ligands have been used as chelating ligands for a variety of early and late transition metal complexes. The ability of nitrogen to form particularly strong bonds with high-oxidation-state early-transition metals has been a significant factor in the widespread use of such ligands for the synthesis of d^0 metal complexes.[6,37] In addition, the substituents on the nitrogens of these ligands may provide steric protection of the metal center if needed. Various polydentate nitrogen compounds

have been employed as "spectator" ligands for Group IV-VII metal complexes, including tris-pyrazolylborates,[38] polyamidos,[39] and macrocycles.[2c,5d,40]

The use of cyclopentadienyl-amido type ligands as ancillary ligands for olefin polymerization[8] catalysts has prompted chemists to take a step further and investigate "metallocene like" chemistry with Group IV metal complexes containing chelating diamido ligands.[39f,41] These ligands can be viewed as electron deficient cyclopentadienyl ligands, and in principal, the coordination sphere of metal complexes containing such ligands may be more easily tuned compared to complexes that contain Cp rings.

Some preliminary observations provide additional support that amido and chelating amido complexes may be potential catalysts for olefin polymerization.[41a,42] Recent reports show that bulky un-chelated (bis)amido zirconimum complexes can be active olefin polymerization catalysts.[42] Complex $[(Me_3Si)_2N]_2ZrCl_2$ for example, can be activated with MAO and polymerize propylene to 90 % isotactic polypropylene.[42c] A similar complex, $[(Me_3Si)_2N]_2Zr(CH_2Ph)_2$, is also reported to be an active propylene catalyst in the presence of $[PhMe_2NH][B(C_6F_5)]$ producing atactic polymers.[42d] Moreover, a chelating titanium diamido complex (*vide infra*) has been shown to polymerize propylene.[41a]

The incorporation of these polyamido ligands into the metal sphere is accomplished by the usual methods of either reacting the deprotonated ligand with the appropriate metal halide, or by reaction of the protonated form of the ligand with homoleptic metal amido or alkyl complexes.[39e,f, 41,43] A significant number of chelating amido Group IV metal complexes have been synthesized recently. Some of the complexes synthesized contain chiral amido ligands to mimic the chemistry of the chiral *ansa*-metallocene complexes.[43b,44]

Various diamido complexes with and without additional neutral donor ligands have been synthesized.[39e,f,41,43-45] The structural similarities of most of these complexes with metallocene and *ansa*-metallocene type complexes are shown in **Figure 1.11**.

A = optional bridging atom
L = Cp, substituted Cp, NR
M =Ti, Zr, Hf
X = halogen, alkyl, amide
⬭ = bulky functionality when L ≠ Cp

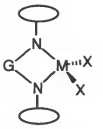

G = bridging alkyl chain, Ph, etc.
M =Ti, Zr, Hf
X = halogen, alkyl, amide
⬭ = bulky functionality on N

Figure 1.11 Structural comparison between metallocene complexes and metal complexes with chelating diamido ligands.

As shown in **Figure 1.11**, the functionalities on the nitrogens of the chelating ligand can partially shield the plane above and below the metal center, while still leaving a large part of the metal exposed. Moreover, the substituents on the amido nitrogens can be flexible enough so they can adapt to the size needs of the incoming substrate.

The structural data for some of these chelating diamido complexes demonstrate the similarities discussed above. For example, the rigid coordination of the $[ArN(CH_2)_3NAr]$ ligand in complex $[(ArN(CH_2)_3NAr)Zr(CH_2CMe_2Ph)(\eta^2\text{-}C_5H_4N)]$ ($Ar = 2,6\text{-}{}^{i}Pr_2C_6H_3$) and the enforced location of the aryl isopropyl groups protects the metal above and below the zirconium-diamide plane.[41b] This conformation leaves a "pocket" opposite to the ligand which is occupied by the $\text{-}CH_2CMe_2Ph$.

Another complex that can better demonstrate how the substituents on the nitrogen can provide a coordination environment similar to metallocenes is the complex $[Mes_2BNCH_2CH_2NBMes_2]Ti(CH_2Ph)Cl$ (**Figure 1.12**).[41c] In this complex, although the mesityl groups are slightly "off-centered" from the plane above and below the metal center due to puckering of the ethylene backbone, they still manage to provide some steric protection to the metal center. The authors suggest using larger groups on the nitrogens or

shortening the bridge in order to induce further metallocene-like character by providing more "lateral" protection to the metal center. The substituents on the nitrogens of this chelating diamido ligand (**Figure 1.12**) provide an additional advantage. The boron substituents on the nitrogens generate more electron deficiency on the metal center by competing with the metal for the nitrogen lone pair via a N-B π-interaction. The reactivity demonstrated by these borylamide metal complexes supports the enhanced electrophilicity of the metal center.[41c]

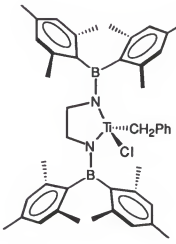

Figure 1.12 The bis(borylamide) complex prepared by Schrock *et al.*.[41c]

An additional way to direct the substituents towards the metal center can be the use of more rigid backbones,[43a,46] as shown in **Figure 1.13**. In this complex, the rigid pyridine backbone prevents any puckering of the ligand, therefore forcing the substituents on the amido nitrogens to completely shield the "lateral" of the metal. For the complex shown in **Figure 1.13** the protection of the metal center is so pronounced especially due to the large phenyl rings, that it is inactive as an alkyne cyclotrimerization catalyst. The congested coordination area allows only two alkynes to insert and form the corresponding metallacyclopentadienyl complex.[46]

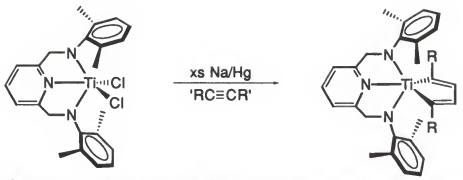

Figure 1.13 Use of a pyridine backbone to enforce the direction of the nitrogen substituents towards the metal center.

Preliminary studies on the polymerization activity of Group IV chelate diamido complexes as polymerization catalysts are quite promising. McConville *et al.* [41a] in a recent report have demonstrated that the titanium complex shown on Figure **1.14** is highly active in the presence of MAO or $B(C_6F_5)_3$ for the polymerization of α-olefins, producing polymers with narrow molecular weight distributions (M_w/M_n = 1.06-1.73). When MAO is used as a cocatalyst, the only chain termination mechanism appears to be chain transfer to aluminum. On the other hand, the $[RN(CH_2)_3NR]TiMe_2$-$B(C_6F_5)_3$ system achieves living aspecific polymerization of α-olefins with no chain termination or transfer observed even after several hours.[41a]

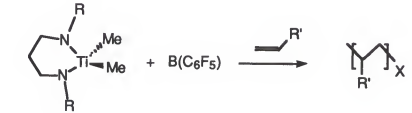

R = 2,6-iPr2C6H5
2,6-Me2C6H5

R' = n-Bu, n-Pr, n-Hex

Figure 1.14 The chelating diamido complex prepared by McConville *et al.*.[41]

As can be seen in **Figure 1.15**, the geometry of the diamido complex **B** is comparable to the commercially valuable "constrained geometry" complex **A**. The chelating diamide imposes a small N-Ti-N angle thereby allowing a large area of the metal center exposed to substituents. This may, in part at least, explain the unusual living polymerization of α-olefins observed for this complex and its dimethyl analog.[41a] Similar small N-M-N angles have also been observed for several other group IV diamide complexes thus demonstrating their potential to be successfully involved in "metallocene like" chemistry.[41b,c,43b]

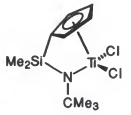

	L-Ti-L (deg)	Cl-Ti-Cl (deg)
A	107.6	102.97(7)

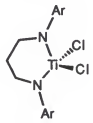

B	99.2(2)	107.77(9)

Ar = 2,6-$^{i}Pr_2C_6H_4$

Figure 1.15 Comparison of key structural data for the "Cp-SiNR" complex **A** and the chelating diamide complex **B**.

o-Phenylene diamine has also been successfully employed as a chelating ligand in the preparation of monomeric d^0 early transition metal diamido complexes.[39a] Tilley *et al.*[47] have prepared Zr, Ti and Ta complexes that contain the bulky *o*-$C_6H_4(NHSi^{i}Pr_3)_2$ ligand as possible alternative catalysts for dehydropolymerization of silanes, a reaction that

requires highly electrophilic monomeric metal hydrides as mediators. In addition to these Group IV and V metal complexes, the *o*-phenylene diamine ligand has been employed in the synthesis of high oxidation state tungsten and molybdenum complexes.[48,49] The *o*-phenylenediamine ligand can produce monomeric or dimeric complexes depending on the reaction conditions. (**Figure 1.16**). A significant contribution of this ligand has been the isolation of coordinatively and electronically unsaturated diamido W and Mo alkyl and alkylidene complexes (**Figure 1.16 B, C**).[49] These compounds are particularly interesting because of their relation to the olefin metathesis reaction,[4] including the metathesis polymerization of strained olefins (ROMP)[50] and acyclic dienes (ADMET).[51]

Addition of the dilithio salt *o*-$C_6H_4(NLiSiMe_3)_2$ to $W(NPh)Cl_4(Et_2O)$ affords high yields of *o*-$C_6H_4(NSiMe_3)_2W(NPh)Cl_2$.[49a] In contrast, the analogous Mo complex *o*-$C_6H_4(NSiMe_3)_2Mo(NPh)Cl_2$ can only be prepared by complete protonation of one of the imido ligands of $Mo(NPh)_2Cl_2(DME)$ by reaction with *o*-$C_6H_4(NHSiMe_3)_2$.[49c]

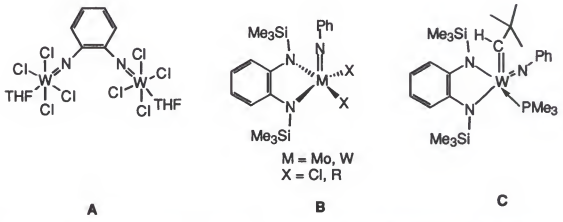

Figure 1.16. Various Group VI metal complexes containing terminal or bridging *o*-phenylediamido ligands.

An interesting discovery was made during kinetic studies of the formation of alkylidene complex **C** depicted in **Figure 1.16**. Labeling experiments revealed that in

the absence of PMe_3, one of the -$SiMe_3$ groups of the phenylene diamide ligand is reversibly metallated to produce a tungsten metallasilacycle complex in equilibrium with the free alkylidene species (**Figure 1.17**).[52] Upon addition of Lewis bases the metallacycle is then transformed to the corresponding five-coordinate alkylidene complex **C** (**Figure 1.17**). Complex **C** (**Figure 1.17**) is active towards olefin metathesis polymerization of strained olefins producing polymers with narrow polydispersities (M_w/M_n = 1.005-1.12).[53] The mechanistic studies may to an extent support the reasoning behind the narrow polydispersity of the polymers. The metallation of the ligand provides a favorable equilibrium between intermediates **A** and **B** (**Figure 1.17**), and may be protecting the catalytic site in **B** from undergoing other reactions that facilitate chain transfer or termination during polymerization. Complex **A** can, in a way, be considered the resting state of catalyst **B**.[52]

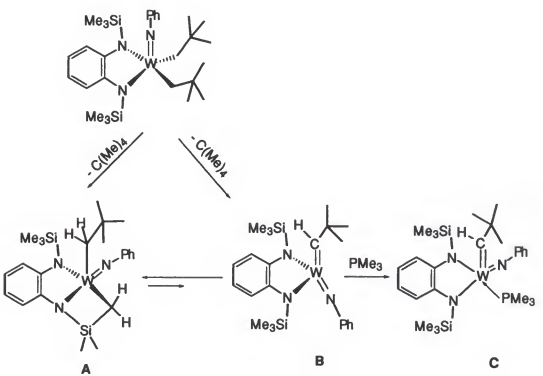

Figure 1.17 Protection of the alkylidene catalyst (**B**) by formation of a metallasilacycle complex (**A**).

Complexes with chiral diamido ligands have been isolated as well. The chiral complexes shown in **Figure 1.18** have been prepared in good yields via alkane elimination because a number of side products have been observed when halide metathesis was investigated.[43b,44] Although the ligand in complex **A** (**Figure 1.18**) is asymmetric, its asymmetry is not effectively transmitted to the coordination sphere of the Ti center. This is demonstrated by the positions of the -$SiMe_3$ groups which although they sit on a C_2 axis, are essentially coplanar. Since the -$SiMe_3$ groups are relatively small, there is no significant difference above and below the plane of the metal. In contrast, the C_2 symmetry of the ligand in **B** is more evident, because of the larger substituents on the amido nitrogens and the twisting of the backbone of the ligand. The reactivity of these two chiral complexes has not been tested extensively in order to see how the chirality of the ligand affects a particular reaction. Complex **B** can catalyze the polymerization of ethylene and the formation of low molecular weight, atactic polypropylene. The propylene produced by this complex, however, is low molecular weight and atactic.[44]

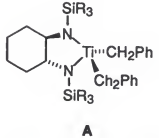

A

{(±)-*trans*-1,2(NSiR$_3$)$_2$-cyclohexane}

SiR_3 = $SiMe_3$, $SiMe_2Ph$, $SiMePh_2$

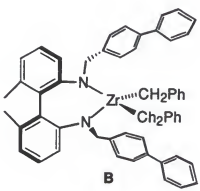

B

Figure 1.18 Metal complexes with chiral diamido ligands.

Tripodal amido ligands such as those shown in Figure (**Figure 1.19**) are another family of polyamides that are receiving attention.[39b,54] A key feature of these ligands is that they provide a sterically protected "pocket" which is formed by the large substituents on the amido nitrogens. The orbital arrangement enforced by these ligands is ideal for forming sterically protected d^0 complexes that contain M-X triple bond or a double and a single bond.[55] Tripodal amido systems have also been shown to stabilize heterobimetallic complexes that contain M-M' bonds without any additional bridging ligands.[54,56] Additionally, these ligands are fairly easily synthesized and deprotonated, and give high yields of trilithio salts that are soluble in hydrocarbons.[57]

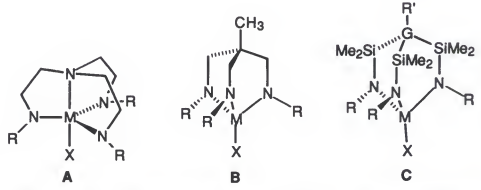

M = Group IV when M-X single bond, or Group V, VI when M-X multiple bond

Figure 1.19 Metal complexes containing tripodal chelating amides.

The influence of the tripodal amido ligands in the formation of Group V and VI metal complexes that contain multiple bonds with carbon, nitrogen, oxygen and other atoms has been extensively explored lately.[55,57] There are a number of Ta and V complexes containing ligands of type **A** (**Figure 1.19**) synthesized, which display some interesting reactivities. For example, a number of stable complexes with terminal (=N-H)

imidos were isolated in good yields (e.g. **Figure 1.20**).[55a] Complexes with imidos in which R =H are rather rare because usually they are very unstable.[58]

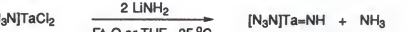

Figure 1.20 Formation of a tantalum complex containing a terminal =N-H group.

The same $[N_3N]TaCl_2$ starting material has also been used to synthesize phosphinidine and alkylidene complexes. The degree of steric pressure that the $[N_3N]$ framework imposes on the metal complex forces the formation of stable alkylidene complexes by α abstraction even when the alkyls contain β-hydrogens (**Figure 1.21**). When β-hydrogens are present, β-hydrogen abstraction is usually predominant resulting in the formation of olefin complexes.[55a]

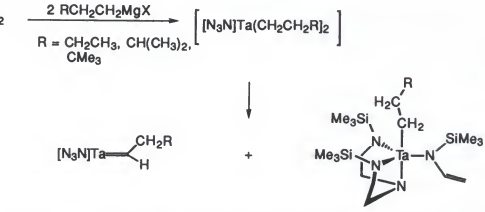

Figure 1.21 Formation of stable alkylidene complexes that contain β-hydrogens.

The stability and yield of the alkylidenes shown in **Figure 1.21** increases by increasing the size of the alkyl substituent on the α-carbon of the alkylidene. This reaction also demonstrates, however, that the tripodal ligand is sensitive to some reaction conditions and can undergo C-N cleavage (byproduct in **Figure 1.21**).

Monomeric species that contain Group VI metal-phosphorous or metal-carbon triple bonds have been synthesized with the assistance of the unique environment that the triamido [N_3N] ligand provides (**Figure 1.22**).[55b,c] The mechanism of the formation of the unusual phosphido species is not yet clear, while the formation of the methylidyne species appears to proceed in a unimolecular fashion. The authors believe that the steric protection of the pocket containing the methyl ligand cannot allow a bimolecular pathway.[55c]

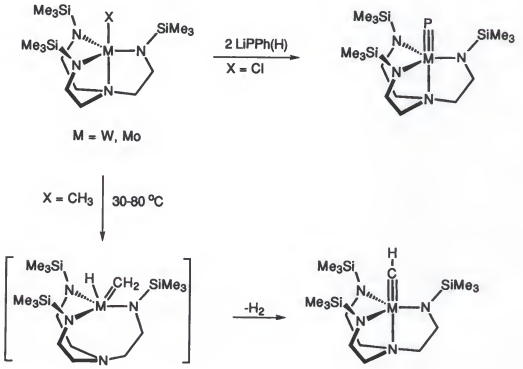

Figure 1.22 Formation of unusual methylidyne species and species containing M-P triple bonds.

The tripodal amido ligands shown in **Figure 1.19** have been used to produce various bimetallic complexes. Heterobimetallic species with unsupported M-M' bonds (usually early transition M-late transition M) are interesting because they can generate two fragments of different reactivity upon cleavage of the metal-metal bond. Such complexes have been shown to functionalize regioselectively unsaturated hydrocarbons.[59]

Although a number of such bimetallic complexes have been synthesized, many of them are too labile to characterize fully or to investigate their reactivity.[45] Some of the more stable bimetallic species have additional bridges that hold the two fragments together, but this way they probably obscure the actual reactivity role of the M-M' bond.[56]

In order to synthesize stable bimetallic complexes reduction of the high oxidation state transition metal should be prevented by a set of hard donor ligands that are efficient σ and π donors. Furthermore, the ligands of this metal fragment should reinforce thermal and kinetic stability and allow only a specific reactive site to be available where the other metal fragment can bind. All these considerations are met to the fullest by using ligands of type **B** and **C** (**Figure 1.19**).[56] Thus compounds of the type shown in **Figure 1.23** have been isolated.[39e,45,56]

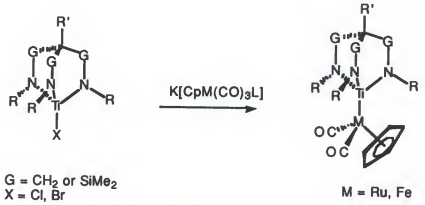

Figure 1.23 Stable heterobimetallic complexes synthesized by using a tripodal amido ligand for protection of the early transition metal center.

The examples of polydentate ligands presented throughout this chapter are but a few of the large collection of polydentate and polyanionic-polydentate ligands that are employed nowadays in the synthesis of organometallic complexes. These ligands have been shown to manipulate to a great extent the reactivity patterns of the metal complexes that contain them. They have been shown to protect certain areas of the metal complex while allowing enough surface for large substrates to coordinate. They have stabilized unusual complexes such as the heterobimetallic complexes presented earlier in the chapter. Although the chelating ligands have proven to be much more stable than their unchelated counterparts, they are not completely inert to certain reaction conditions. The advantages that they bring to a metal complex however, outweigh their shortcomings. The following chapters will present some further aspects of using chelating ligands. Chapter 2 will present the synthesis of some new tris-pyrazolyl borate tungsten alkylidyne complexes, and how the effect of the chelating ligand may dictate the reactivity of these complexes. Chapter 3 will present the synthesis of some new polydentate ligands and their reactions with Group IV and V transition metal complexes.

CHAPTER 2
SYNTHESIS, STRUCTURE AND EXAMINATION OF PROTON TRANSFER IN W(VI) ALKYLIDYNE AMIDO COMPLEXES

Introduction

The chemistry of transition-metal to ligand multiple bonds has received extensive interest, especially concerning high-oxidation state metal-carbon double and triple bonds.[4a] Many of these complexes have been shown to catalyze olefin[4,60] and acetylene metathesis reactions.[61] Transition metal alkylidynes are also known to perform metathesis-like reactions with isocyanates,[62] and Wittig-type reactions with nitriles and other carbonyl containing reagents.[63] Additionally, alkylidyne complexes have been frequently employed in the preparation of the corresponding alkylidene complexes via intra or intermolecular protonation of the metal-carbon triple bond.[64]

A number of air and moisture stable W(VI) and Mo(VI) alkylidenes and alkylidynes have been synthesized by employing chelating ligands of the hydrido(trispyrazolyl)borate family.[65,66] The stability of these complexes is attributed partially to the electronic and coordinative saturation of the metal center, and partially to the rigid geometry imposed by the Tp or Tp' ligands. Due to the saturated nature of these complexes, the observable chemistry is initated by attack of reagents at the ligands rather than at the metal center. The enhanced thermal stability of complexes such as Tp'W(O)(CHC$(CH_3)_3$)Cl or TpMo(CHC$(CH_3)_2$Ph)(NAr)(OTf) has also allowed detailed studies on the rotational isomerization of the M-C alkylidene bond.[65d,66a] The rotational isomerization of the alkylidene bond is a crucial feature of this bond given its immediate involvement in the olefin metathesis reaction.[67]

The Tp and Tp' alkylidyne chemistry has not been explored in as much depth compared to the alkylidene chemistry. Complexes such as Tp'W(CC(CH$_3$)$_3$)Cl$_2$ (**1**)[65a,d] and TpW(CC(CH$_3$)$_3$)Cl$_2$ (**2**)[65d] were used as starting materials for the synthesis of oxo containing compounds Tp'W(O)(CHC(CH$_3$)$_3$)Cl, TpW(O)(CHC(CH$_3$)$_3$)Cl and, TpW(O)$_2$(CH$_2$C(CH$_3$)$_3$) respectively. Moreover, complexes **1** and **2** were shown to be stable to protonation by trifluoromethanesulfonic acid (HOTf), hydrochloric, and tetrafluoroboric acid.[65d] This chapter will present a further study of the reactivity of chelate stabilized tungsten alkylidynes. These complexes, as their alkylidene counterparts,[65,66] have displayed ligand centered reactivity. The synthesis of amido complexes of the general formula Tp*W(NHR)$_x$(CC(CH$_3$)$_3$)Cl$_{2-x}$ (* = Tp or Tp', R = H, Ph, or aryl) will be discussed along with an unusual acid catalyzed proton transfer from the amido ligand to the alkylidyne ligand.

Attempted Ligand Removal from TpW(CC(CH$_3$)$_3$)Cl$_2$ and Tp'W(CC(CH$_3$)$_3$)Cl$_2$ and Attempted Preparation of Monoalkyl Complexes

We were initially interested to see if complexes Tp'W(CC(CH$_3$)$_3$)Cl$_2$ (**1**) and TpW(CC(CH$_3$)$_3$)Cl$_2$ (**2**) could be possible alkyne metathesis catalysts. Attempted reaction of **1** or **2** with diphenyl acetylene produces only unreacted starting materials even after refluxing in toluene. In retrospect, the lack of metal centered reactivity of the neutral alkylidyne complexes is not surprising, and is comparable to the neutral Tp and Tp' alkylidenes.[65,66] For initiation of the alkyne metathesis reaction, the incoming alkyne would be expected to bind to the metal center. In the case of **1** and **2** that would require formation of a highly congested seven coordinate species. Seven-coordinate tungsten trispyrazolyl borate complexes are known but posses comparatively small ancillary ligands.[38c] The seven-coordinate alkylidyne species W(CC(CH$_3$)$_3$)(P(CH$_3$)$_3$)$_3$Cl$_3$ has

also been isolated but again the ancillary ligands are not sterically demanding and can be accommodated in the coordination sphere.[68]

Removal of a ligand from a neutral Tp and Tp' alkylidene complexes produced species that were active towards ring opening metathesis polymerization. Addition of a Lewis acid (e.g. $AlCl_3$) to $Tp'W(O)(CHC(CH_3)_3)Cl$ produced a species that was active towards polymerization of cyclooctene. Although full characterization of this active species was impossible, it was proposed that this species could be a cationic alkylidene formed by chloride abstraction from $Tp'W(O)(CHC(CH_3)_3)Cl$ by $AlCl_3$.[65a,d] Furthermore, addition of $HBAr'_4$ ($HBAr'_4.Et_2O$, Ar' = 3,5-$C_6H_3(CF_3)_2$) to $TpMo(NAr)(CHC(CH_3)_2Ph)(CH_3)$ (Ar = 2,6-*i*-propyl-C_6H_4) resulted in the formation of a cationic alkylidene by protolysis of the methyl ligand.[66a] In light of these results, we decided to activate complexes **1** and **2** in a similar manner.

Addition of 1 equivalent of a Lewis acid ($AlCl_3$ or $GaBr_3$) to either **1** or **2** does not result in abstraction of one of the chloride ligands and isolation of a cationic species (Equation 2.1). Attempted preparation of monoalkyl alkylidyne complexes by reaction of **1** and **2** with lithium alkyls, Grignard or, other alkylating agents only produced intractable products.

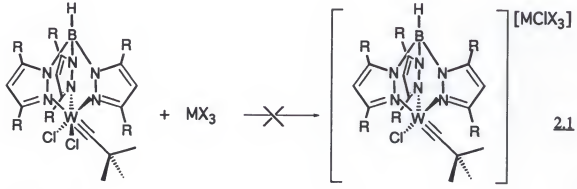

2.1

M = Al, Ga
X = Cl, Br
R = H, CH_3

Synthesis of Hydrotris(1-pyrazolyl)borate (Tp) Neopentylidyne Amido Complexes

Addition of **2** to 2.3 equivalents of Li^+NHPh^- to a -78 °C Et_2O solution of $TpW(CC(CH_3)_3)Cl_2$ (**2**) results in a slow color change from purple to dark orange. The excess anilide is essential for the reaction to proceed to any significant degree. Even so, the reaction is not complete and yields vary from 20 to 50 %. The yield is unaffected by heating the reaction mixture to 80 °C in toluene, or extending the reaction time. Repeated extraction of the reaction mixture with an Et_2O/pentane solvent mixture yield compound $TpW(CC(CH_3)_3)(NHPh)Cl$ (**3**) (Equation 2.2) as a dark orange powder. Complete separation of complex **3** from $TpW(CC(CH_3)_3)Cl_2$ is difficult due to the very similar solubilities of the two complexes.

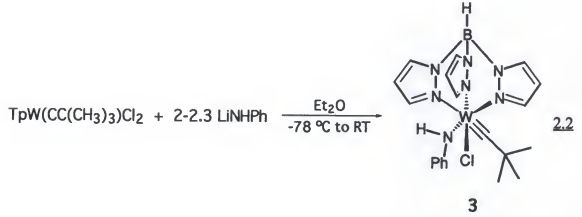

2.2

3

The ^1H NMR spectrum of **3** (**Figure 2.1**) is consistent with the formation of the phenylamido alkylidyne complex. The amido N-H proton appears as a broad singlet at δ 10.50 ppm in the room-temperature proton NMR spectrum of **3**. The lack of symmetry in the complex renders all the Tp ring protons inequivalent. The ^{15}N labeled analog **3a** was prepared in a similar manner and confirms our assigned resonance at δ 10.50 ppm as due to the N-H moiety. The $^1J_{N\text{-}H}$ coupling of 70 Hz for the ^{15}N-H proton of **3a** is in agreement with literature values.[58a]

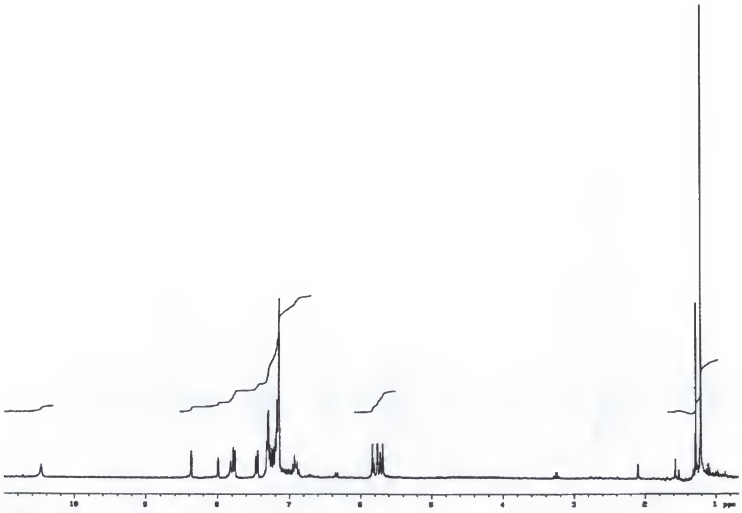

Figure 2.1 The ^{1}H NMR Spectrum of 3.

Compound $TpW(CC(CH_3)_3)(NHPh\text{-}p\text{-}Br)Cl$ (**4**) is prepared in a slightly different manner than **3**. Due to the low stability of the $(K^+)(^-NHPh\text{-}p\text{-}Br)$, the anilide is prepared *in situ* , and added without further purification to a THF solution of **2**. The reaction mixture slowly turns dark orange after 10 hours of reaction at room temperature. Removal of THF and repeated recrystallizations from an Et_2O/pentane mixture at -40 ° C afford **4** as an orange solid. As with **3**, the presence of $TpW(CC(CH_3)_3)Cl_2$ (**2**) prevents the isolation of analytically pure **4**. Compound **4** is moisture sensitive both in solution and in the solid state, decomposing to a brown oil after extended exposure to air. The ^1H NMR of $TpW(CC(CH_3)_3)(NHPh\text{-}p\text{-}Br)Cl$ (**4**) reveals the asymmetric nature of the compound with seven distinct resonances (2 others are masked by solvent) due to the Tp protons. The amide N-H proton appears as a broad singlet at δ 10.15 ppm.

The synthesis of $TpW(NHPh(3,5\text{-}(CF_3)_2))(CC(CH_3)_3)Cl$ (**5**) is achieved in the same manner as compound **4**. Compound **5** is isolated as a bright orange semicrystalline material from a -40 °C Et_2O/pentane solution. The ^1H NMR spectrum of **5** is similar to the other amido complexes discussed. The amido proton resonates at δ 9.79 ppm as a broad singlet. Complex **5** is moderately air and moisture sensitive and slowly decomposes to a dark orange solid. It is however, thermally stable in solution up to at least 90 °C. In the case of **4** and **5**, there is at times some decomposition observed in addition to unreacted $TpW(CC(CH_3)_3)Cl_2$, which may be attributed to some unreacted KH from the *in situ* prepared anilides.

The reaction of 5 equiv of $NaNH_2$ with $TpW(CC(CH_3)_3)Cl_2$ (**2**) in THF, at ambient temperature results in a color change from blue to dark yellow after stirring overnight. The solid obtained from removal of THF, can be recrystallized from an Et_2O/pentane mixture at -40 ° C affording $TpW(NH_2)(CC(CH_3)_3)Cl$ (**6**) as a pale yellow solid. In the ^1H NMR of **6** (**Figure 2.2**), broad singlets at δ 8.59 and 8.90 ppm correspond to the inequivalent protons of the NH_2- ligand due to the chirality of the metal

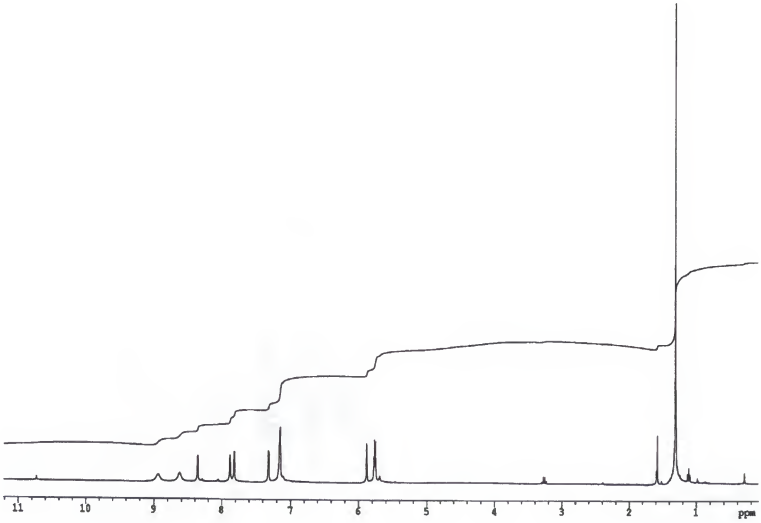

Figure 2.2 The ^{1}H NMR Spectrum of **6**.

center. The inequivalence of the two protons also indicates slow rotation about the W-N bond of the amido ligand on the NMR time scale.

When 3-4 equivalents of Li^+NHPh^- are added to a -78 °C Et_2O solution of **2**, an immediate color change from purple to bright orange occurs. After 3 hours the reaction mixture is extracted from toluene followed by recrystallization from an CH_2Cl_2/pentane solvent mixture. $TpW(NHPh)_2(CC(CH_3)_3)$ (**7**) is collected as bright orange crystals. The ^1H NMR spectrum of the crude reaction mixture also shows formation of a small amount of free aniline and of a yet unidentified compound that appears due to partial decomposition of the Tp ligand. Formation of this pyrazole decomposition product increases with increasing anilide concentrations (4 equivalents or more).

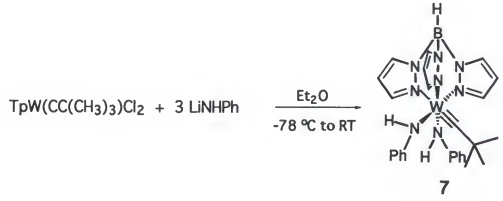

2.3

7

In the room temperature ^1H NMR spectrum of **7** (**Figure 2.3**), resonances attributable to the protons of the Tp pyrazole rings appear in a 2:1 ratio indicating existence of a plane of symmetry in the molecule. Two amido protons (relative to the Tp ligand) appear as a broad singlet at δ 7.8 ppm. Further structural information for **7** was obtained by a single-crystal X-ray diffraction study.

X-ray quality single crystals were obtained by slow diffusion of pentane into a saturated CH_2Cl_2 solution of **7** at room temperature for 1 week. A thermal ellipsoid plot of **7** is found in **Figure 2.4**. The data collection and atomic parameters are presented in **Tables A1.1-A1.5**. Selected bond distances and angles are summarized in **Table 2.I**.

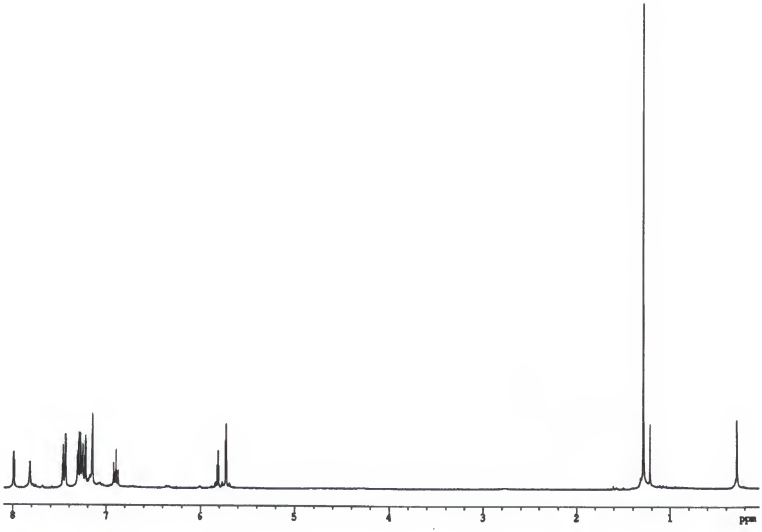

Figure 2.3 The ^{1}H NMR Spectrum of **7**.

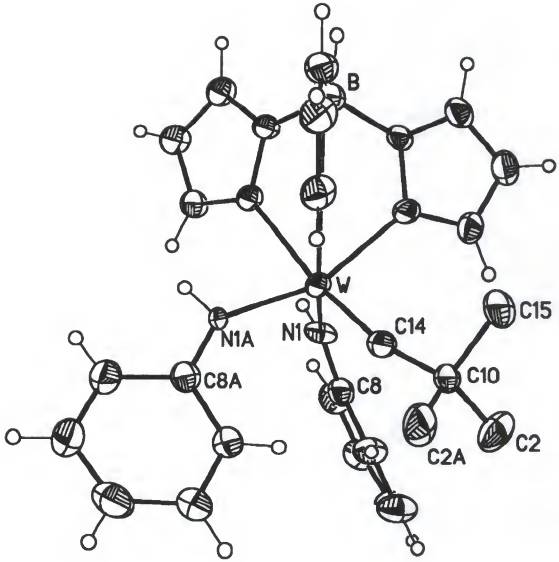

Figure 2.4 The crystal structure of complex $TpW(NHPh)_2(CC(CH_3)_3)$ (7).

The structure about the metal center is best described as a distorted octahedron with the Tp ligand bound facially to the tungsten atom. Compound **7** adopts a *syn* conformation with respect to the alkylidyne ligand with the phenyls of the two amido ligands pointing towards the neopentylidyne group. The W-C14 bond length (1.790 Å) is within the expected range for d^0 tungsten-carbon triple bonds.[4a] The W-C14-C10 angle of 166.6° is less than expected for an sp hybridized α-carbon,[4a] and can be attributed to the steric interaction between the *t*-butyl group of the neopentylidyne ligand and the two phenyl rings of the amido ligands. The N-W bond lengths of the pyrazole rings range from 2.354 to 2.237 Å and are consistent with the decreasing *trans* influence of the ligands alkylidyne > amido. The amido N-W bonds are slightly longer than similar monoamido compounds.[66] This is perhaps due to combined contributions of the two amido nitrogen lone pairs to the tungsten $d\pi$ orbital.

Table 2.I Bond Lengths (Å) and Angles (deg) for the Non-H Atoms of Compound **7**.

1	2	3	1-2	1-2-3
C1	W	N1	1.789(5)	100.66(14)
C1	W	N1A		100.66(14)
C1	W	N2		171.8(2)
C1	W	N3		93.2(2)
C1	W	N3A		93.2(2)
N1	W	N1A	2.034(3)	102.7(2)
N1	W	N2		84.39(11)
N1	W	N3		88.65(13)
N1	W	N3A		159.96(12)
N1A	W	N2	2.034(3)	84.39(11)
N1A	W	N3		159.96(12)
N1A	W	N3A		88.65(13)
N2	W	N3	2.356(4)	80.31(11)
N2	W	N3A		80.31(11)
N3	W	N3A	2.239(3)	76.1(2)
N3A	W		2.239(3)	
C5	N1	W	1.353(5)	140.5(3)
C5A	N1A	W	1.353(5)	140.5(3)
C2	C1	W	1.512(7)	166.5(4)

As an interesting note, it should be added that there was no evidence of formation of an imido/alkylidene containing species in the above reactions. Wigley *et al.*have reported that reacting 2 equivalents of an aryl amide with complex $Mo(NAr)_2(Cl)_2.THF_2$ produces the salt $[Li(THF)_4][Mo(NAr)_3Cl]$.[69] Experimental evidence supports that the mechanism of the reaction proceeds via initial formation of the intermediate $Mo(NAr)_2(NHAr)Cl$, and subsequent deprotonation of this species by excess $[NHAr]^-$ to produce $[Li(THF)_4][Mo(NAr)_3Cl]$. Moreover, Schrock *et al.* have observed that a strong base such as $Ph_3P{=}CH_2$ dehydrohalogenates $W(CC(CH_3)_3)(NHPh)L_2Cl_2$ producing the imido alkylidene complex $W(CC(CH_3)_3)(NPh)L_2Cl$.[64b] One could possibly envision a similar pattern of reactivity for our amido alkylidyne complexes in the presence of excess anilide (**Scheme 2.I**).

Scheme 2.I

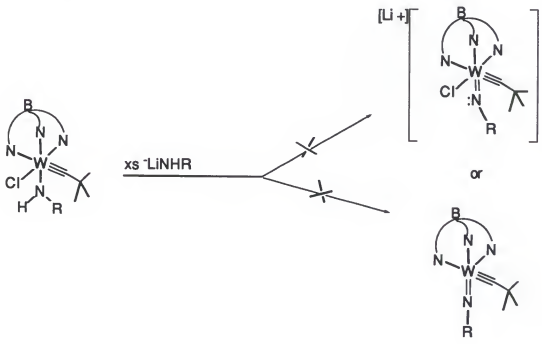

The preceding reactions suggest that the chloride ligand in $Tp'W(CC(CH_3)_3)Cl_2$ (**1**) and $TpW(CC(CH_3)_3)Cl_2$ (**2**) is only modestly labile. This may be explained by the fact that these complexes are formally 16 electron species which, if one includes π-donation from the chloride ligands can be considered electronically saturated. Thus, it could be difficult to replace the first chloride on the complex. However, if one of the chloride ligands is substituted by an amido ligand, the stronger π-donation of the N-lone pair to the metal can cause the second chloride to become more labile. The steric hindrance of the Tp ligand can only partially be used as an argument for the non-facile substitution, since the highly congested $TpW(CC(CH_3)_3)(NHPh)_2$ (**7**) has been isolated. Attempted substitution of the chlorides by $(M^+)(^-O_3SCF_3)$ (M = Ag, Tl) did not lead to the formation of readily isolable products. Finally, attempts to prepare **3** in higher yields by following a procedure analogous to the synthesis of $Tp'W(CC(CH_3)_3)(NHPh)Cl$ (**8**) gave a mixture of products in addition to a small amount of **3**.

Synthesis of a Hydrotris(3,5-dimethyl-1-pyrazolyl)borate (Tp') Neopentylidyne Amido Complex

The reaction of 1-2 equivalents of K^+NHPh^- with $Tp'W(CC(CH_3)_3)Cl_2$ in THF gives an intractable mixture of products. An alternate route was therefore chosen. As shown in Equations 2.4 and 2.5, $(CH_3)_3SiNHPh$ in THF is reacted with a -78 °C THF solution of $(DME)W(CC(CH_3)_3)Cl_3$ for approximately 30-40 minutes, followed by addition of 1 equivalent of KTp' in THF. Recrystallization from Et_2O at -40 ° C affords dark orange crystals of $Tp'W(CC(CH_3)_3)(NHPh)Cl$ (**8**). The initial product between reaction of $(CH_3)_3SiNHPh$ with $(DME)W(CC(CH_3)_3)Cl_3$ has not been isolated, but it is assumed to be the species $(DME)W(CC(CH_3)_3)Cl_2(NHPh)$ by comparison to $(DME)W(CC(CH_3)_3)Cl_2(NH(o\text{-}2,6\text{-}i\text{-}Pr_2C_6H_3))$ isolated in an analogous reaction.[64a,d,70]

The room temperature ^1H NMR spectrum of **8** (**Figure 2.5**) displays six inequivalent methyl peaks and three inequivalent pyrazole ring protons consistent with the

existence of a chiral metal center. The amide peak is identified as a broad singlet at d 10.62 ppm. Compound **8** is air and moisture stable and does not decompose when heated in solution up to 110 °C. Upon heating a C_7D_8 sample of **8** a color change from orange to yellow-orange can be observed, with no changes evident in its ^1H NMR spectrum. The color change is possibly a thermochromic phenomenon. The air and thermal stability of this compound is comparable to other W-Tp' complexes previously synthesized in our group. Clearly, methylation of the pyrazole rings dramatically increases the kinetic stability of these compounds.

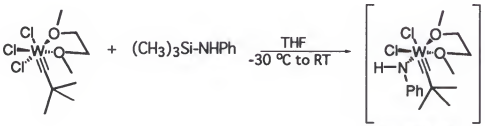

2.4

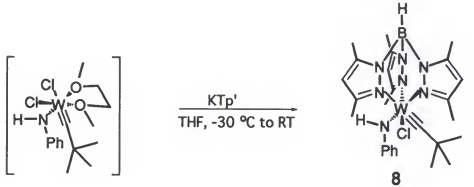

2.5

The geometry of compound **8** is further supported by a single-crystal X-ray diffraction study. X-ray quality crystals were obtained by cooling a saturated Et_2O/pentane solution of **8** for 2 weeks at -30 °C.

Information on the data collection and atomic coordinates are found in **Tables A2.1-A2.5** in Appendix A. Selected bond lengths and angles are summarized in **Table 2.II,**

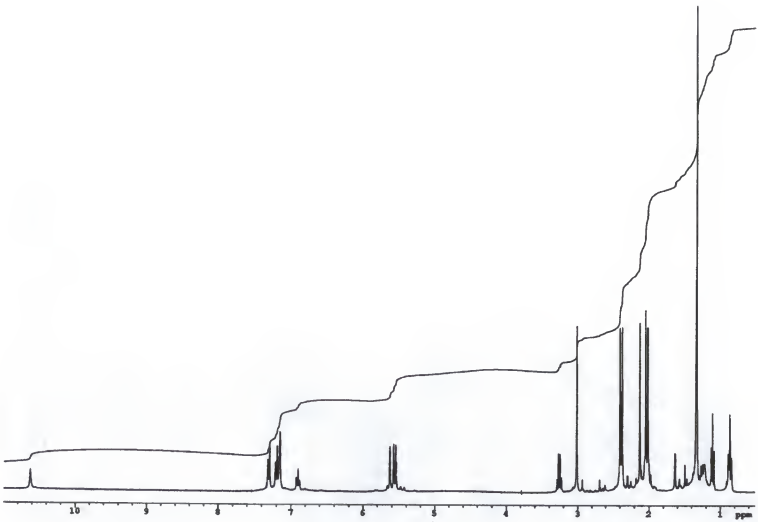

Figure 2.5 The ^{1}H NMR Spectrum of **8**.

while a thermal ellispsoid plot is shown in **Figure 2.6**. From the crystal structure, it is apparent that the geometric constraints of the Tp' ligand force the neopentylidyne, amido, and chloride groups to be mutually *cis*.[71] Complex **8** is formally a 16-electron species with the neopentylidyne ligand donating electron density to two metal d orbitals of π symmetry. The *cis* orientation of the phenylamido ligand with respect to alkylidyne achieves maximum dπ-pπ bonding and accounts for the short (1.946 Å) length of the W-N(HPh) bond. The expected *trans* influence trend is observed for **8** (alkylidyne > amide > chloride) with pyrazole nitrogen-tungsten bonds ranging from 2.392 to 2.175 Å. The sp hybridized nature of the neopentylidyne α-carbon is evident by the 1.766 Å W-C1 bond length and the nearly linear W-C1-C2 angle (174.5 °). The hindrance imposed by the size of the Tp' ligand forces the amido ligand to assume the *syn* conformation with the phenyl ring tilted towards the alkylidyne ligand.

Table 2.II. Bond Lengths (Å) and Angles (deg) for the Non-H Atoms of Compound **8**.

1	2	3	1-2	1-2-3
Cl	W	N1	2.401(3)	97.6(2)
Cl	W	N2		84.9(2)
Cl	W	N3		87.4(2)
Cl	W	N4		163.1(2)
N1	W	N2	1.943(7)	80.7(3)
N1	W	N3		161.7(3)
N1	W	N4		91.0(3)
N1	W	C1		96.5(4)
N2	W	N3	2.393(8)	82.2(3)
N2	W	N4		82.1(3)
N2	W	C1		176.6(3)
N3	W	N4	2.223(8)	80.2(3)
N3	W	C1		100.7(4)
N4	W	C1	2.169(7)	100.1(3)
C1	W	Cl	1.773(10)	93.5(3)
C2	C1	W	1.512(13)	174.7(8)
C6	N1	W	1.407(11)	139.5(6)

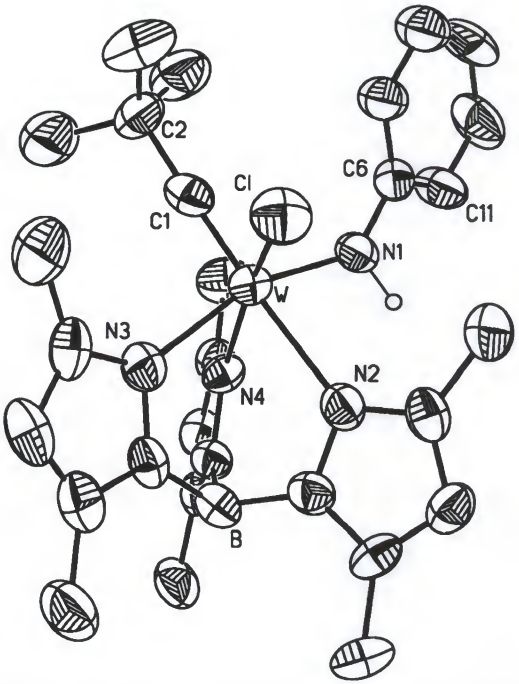

Figure 2.6 The Thermal Ellipsoid Plot of **8**.

Variable Temperature and NOe Studies for Tp Amido Complexes **3**, **6-8**

As mentioned above, the presence of two distinct amido proton resonances in the ^{1}H NMR spectrum of TpW(NH$_2$)(CC(CH$_3$)$_3$)Cl (**6**) implies hindered rotation about the W-N bond. Coalescence of the two amido protons of **6** was not achieved up to 120 °C (**6** decomposes at higher temperatures), indicating a relatively high activation barrier for rotation about the W-N bond. Since this can be true for the phenyl and aryl amides, two isomers are possible for complexes **3-5**, **7**, and **8** (with the phenyl group *syn* or *anti* with respect to the alkylidyne ligand). However, in the room temperature ^{1}H NMR spectra of all the arylamido complexes only one isomer is observed. Variable temperature ^{1}H NMR studies were performed on complexes TpW(NHPh)(CC(CH$_3$)$_3$)Cl (**3**), TpW(CC(CH$_3$)$_3$)(NHPh)$_2$ (**7**), and Tp'W(NHPh)(CC(CH$_3$)$_3$)Cl (**8**). Only one isomer was observed for each of these complexes in the temperature range -100 to 100 °C. This is can be either because the anilide group is rotating rapidly on the NMR time scale, or because it remains static and only one isomer is favored. Unfortunately, based on the variable temperature studies alone, we cannot distinguish between the two possibilities.

Further information concerning the solution orientation of the anilide groups in **3** and **7** was obtained from nOe studies.[72] Irradiation of the *t*-butyl peak in **3** produced enhancement of the ortho and meta phenyl proton signals of the phenylamido ligand, and of the two doublets at δ 7.79 and 8.37 ppm which are attributed to the Tp ligand. No enhancement of the N-H proton was evident. Alternatively, when the amido proton was irradiated, positive enhancement was measured for the ortho phenyl protons of the amido ligand and the doublet resonating at δ 7.76 ppm which is attributed to the Tp ligand. The results of the study support the *syn* conformation of **3** in solution.

For complex TpW(NHPh)$_2$(CC(CH$_3$)$_3$) (**7**), irradiation of the *t*-butyl peak of the neopentylidyne ligand enhanced the signal of the ortho protons of the phenylamido ligands and the Tp ring proton doublet at δ 8.00 ppm. When the N-H protons of the phenylamido

groups were irradiated, positive nOe was measured for the ortho protons of the phenyl ring and for the Tp doublet at δ 7.27 ppm. Conjugate experiments were also performed in order to avoid misleading assignments due to other possible mechanisms of relaxation not directly related to distance between the nuclei. The combination of the nOe and variable temperature experiments provides strong support for the existence of only the *syn* isomer of **7** in solution. Although nOe studies were not performed for the rest of the arylamido compounds, we expect that they also possess similar conformation in solution. The *syn* conformation of the phenylamido groups in both crystal structures of complexes **7** and **8** also suggest that the thermodynamically favored isomer has the amide substituent *syn* to the metal neopentylidyne bond.

We propose that in the amido alkylidyne complexes **3-5**, **7**, **8** (where R = Ph, Ar) a combination of the sterically demanding Tp and Tp' ligands and bulky substituents on the nitrogens of the amido groups together with strong N-W π donation results in a high barrier of rotation for the amido group. Similar observations due to sterics have been observed for some low-valent tungsten amido systems that contain pyrazolyl borate ligands.[73] Contrary to our observations however, the complex $TpMo(CC(CH_3)_2Ph)(NH(o\text{-}2,6i\text{-}Pr_2\text{-}C_6H_3))(OCH_3)$ appears as a mixture of two rotamers in the room temperature ^1H NMR spectrum.[66a] In this case, although the geometry of the molecule is relatively constrained, the presence of the methoxy group may compete with the N-W π interaction to effectively lower the barrier to rotation about the N-W bond.

Tautomerization Studies involving W(VI) Tp and Tp' Amido Alkylidyne Complexes

In a previous study on the alkylidene rotational isomerization of complex $TpW(NPh)(CHC(CH_3)_3)Cl$ (**9**), the coupled ^{13}C NMR spectrum of the photolytically generated minor isomer showed no C-H coupling between the alkylidene α-carbon and the alkylidene proton.[65d] In addition, the alkylidene proton signal of the minor isomer showed significant broadening. The above observations were explained in terms of a significant

amount of hydrogen bonding between the alkylidene proton of the minor isomer and the π-donating imido ligand (**Scheme 2.II** pathway **A**).

Scheme 2.II

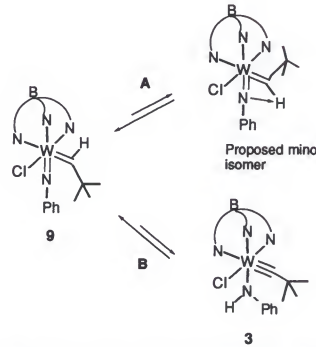

An interesting observation, however, arose from the fact that the chemical shifts of the proposed[65d] minor isomer of **9** and those of compound TpW(NHPh)(CC(CH$_3$)$_3$Cl (**3**) were completely identical (**Table 2.III**).

Table 2.III. Comparison of selected chemical shifts of the previous and present study on isomerizational behavior of TpW(NPh)(CHC(CH$_3$)$_3$Cl.

Compound (C_6D_6 as solvent)	δ (alkylidene/amido region)	δ C(CH$_3$)$_3$ region)
Syn TpW(NPh)(CHC(CH$_3$)$_3$Cl (Prepared by method of Gamble *et al.*)	10.82 (sharp singlet)	1.41 ppm
"Anti" TpW(NPh)(CHC(CH$_3$)$_3$Cl (Observed by photolysis of the syn)	10.52 ppm (broad singlet)	1.24 ppm
TpW(NHPh)(CC(CH$_3$)$_3$Cl (**3**)	10.5 ppm (broad singlet)	1.20 ppm
TpW(^{15}NHPh)(CC(CH$_3$)$_3$Cl (**3a**)	10.47 ppm $^1J_{NH}$ = 70 Hz	1.22 ppm

This unexpected result suggested that the species generated upon photolysis of **9** was not produced merely by rotation about the W-C double bond, but by proton transfer from the alkylidene to the imido ligand of **9** (**Scheme 2.II**, pathway **B**). This conclusion is in agreement with the absence of C-H coupling and the broadened peak observed for the proton of the proposed alkylidene minor isomer. Since compounds **3** and **9** are formally related by proton transfer from the alkylidene to the nitrogen of the imido ligand, we were interested in studying the tautomerization between these two species.

There are a number of examples involving intramolecular α-hydrogen transfers, in which the ultimate proton acceptor is itself another multiply bonded ligand.[4a] Such examples are proton transfers between imido/amide,[2c,58a,74] amido/alkylidyne,[64a,b,d,70a,b,c] oxo/hydroxo,[75] and oxo/alkylidene ligands.[76] These transfers are usually slow. In the tungsten and molybdenum amido/alkylidyne systems, the transfer can be thermal, it is, however, catalyzed significantly by bases.[64a,b,d,70a,b,c] Although not directly observed, a base induced proton transfer may also be operative in the synthesis of $Tp'Ta(NPh)(CH_2C(CH_3)_3)Cl$ (Equation 2.6).[77] In the $TpMo(NAr)(OCH_3)(CHC(CH_3)_2Ph)$ system, a base catalyzed proton transfer has been observed, in which the alkylidene proton is transfered to the imido ligand in the presence of excess methoxide (Equation 2.7).[66a]

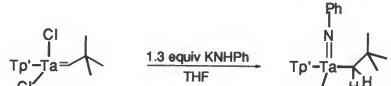

2.6

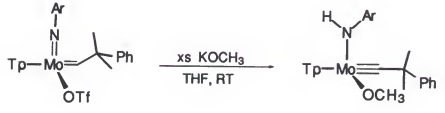

2.7

In the previous study by Blosch *et al.*, the minor isomer (which has now been identified as complex **3**) was thermally driven to TpW(NPh)(CHC(CH_3)$_3$)Cl (**9**).[65d] Kinetics studies demonstrated that the conversion was first-order. It should be noted that all kinetic runs in that study were made using aliquots from the same sample. In view of those results, we attempted the thermal conversion of **3**, independently synthesized in the present study, to **9**.

To our surprise, the thermal tautomerization of TpW(NHPh)(CC(CH_3)$_3$)Cl (**3**) to the imido/alkylidene complex TpW(NPh)(CHC(CH_3)$_3$)Cl (**9**) was not consistently reproducible. In some cases conversion of **3** to the corresponding imido alkylidene **9** was readily achieved, while in others no proton transfer was observed even upon heating a sample of **3** at 70 °C for two days. The ^{1}H NMR spectra of samples of **3** that successfully tautomerized suggested a first order dependence on metal. Unfortunately, since none of these samples were scrupulously pure, detailed kinetic studies were precluded. The other amido alylidyne complexes (**4**, **6**-**8**), except TpW(NHPh(3,5-(CF_3)$_2$))(CC(CH_3)$_3$)Cl (**5**), did not thermally transfer the amido proton to the neopentylidyne ligand either. Compound **5** showed more consistent behavior with proton transfer occurring after heating (Equation 2.8), but these samples were also impure, thus preventing a detailed kinetic study.

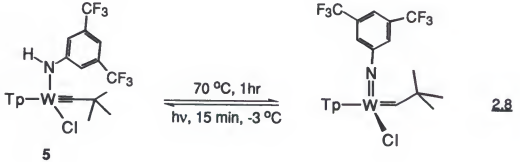

2.8

Given the fact that the thermally induced proton transfer was not consistently reproducible, it was proposed that the tautomerization may be catalyzed by an impurity. Since it has been demonstrated that proton transfer between the alkylidyne and amido ligands can be catalyzed by base, we attempted to catalyze the tautomerization by adding base to the samples of **3** that did not thermally convert to **9**.

Addition of up to 10 equivalents of NEt_3 or $PhNH_2$ to a sample of $TpW(NHPh)(CC(CH_3)_3)Cl$ (**3**) did not produce any change even after 3 hours. The choice of $PhNH_2$ was obvious based on the possibility of its presence in these samples. Compound **3** was also heated in the presence of these bases with no observable changes. Moreover, since $TpW(NPh)_2(CHC(CH_3)_3)$ (**7**) instead of $TpW(NPh)(CHC(CH_3)_3)Cl$ (**9**) is isolated by addition of 3 or more equivalents of Li^+NHPh^-, it can be concluded that in **3**, the proton transfer is not base promoted even in the presence of a base such as anilide. Similar results can be deduced for the other Tp amido complexes as well, since an excess of amide was also used in their synthesis with no observable formation of imido/alkylidene complexes. Finally, the proton transfer does not occur photolytically since extended low temperature photolysis of **3** produces no change in its ^1H NMR spectrum.

A closer examination of the ^1H NMR spectra of the samples of $TpW(NHPh)(CC(CH_3)_3)Cl$ (**3**) that underwent tautomerization, revealed the presence of trace amounts of the oxo alkylidene $TpW(O)(CHC(CH_3)_3)Cl$. Its formation suggests the presence of trace H_2O (probably from solvents). In an attempt to identify if H_2O was indeed facilitating the proton transfer, a catalytic amount of H_2O (~0.1 eq) was added to a sample of **3** that had not tautomerized upon previous heating at 80 °C for 10 hours. A slow color change from orange to yellowish-olive was observed, and ^1H NMR spectra showed the formation of imido/ alkylidene **9**. Heating of this sample accelerated the formation of **9**. It was also noted that **3** is somewhat moisture sensitive. When larger amounts of H_2O are present, hydrolysis of the amide to form $TpW(O)(CHC(CH_3)_3)Cl$ and/or $TpW(O)_2(CH_2C(CH_3)_3)$ was observed. This suggests that hydrolysis is a

competing reaction and is faster than the tautomerization to **9** (**Scheme 2.III**). Indeed, the ^1H NMR spectra of most samples of $TpW(NHPh(3,5\text{-}(CF_3)_2))(CC(CH_3)_3)Cl$ (**5**) exhibit trace amounts of $TpW(O)(CHC(CH_3)_3)Cl$ which can explain why the tautomerization of **5** was observed to be more consistent than **3**.

Scheme 2.III

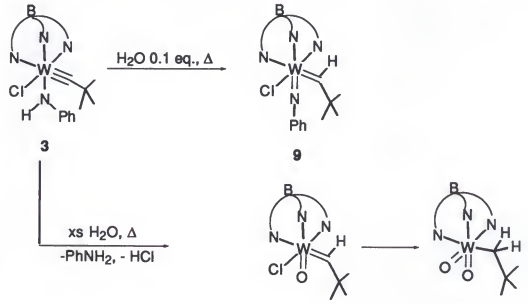

Since proton transfer in $TpW(NHPh)(CC(CH_3)_3)Cl$ (**3**) is H_2O catalyzed and not base catalyzed, it can be inferred that H_2O, in this case, acts as an acid. To further test this assumption, a trace amount of HCl (1.0 M in Et_2O) was added to a C_6D_6 solution of **3**, in which case a rapid color change from orange to olive green was observed, and the ^1H NMR spectrum showed complete conversion of **3** to **9**. Higher amounts of HCl resulted in complete protonation of the amido ligand and formation of $TpW(CC(CH_3)_3)Cl_2$ (**2**) (**Scheme 2.IV**). Complex **3** was only partially converted to **9** by addition of solid NEt_3HCl, whereas addition of NH_4Cl did not have any effect at all on **3**. These observations are presumably due to the lower solubility of these acids in C_6D_6 or C_7D_8.

Scheme 2.IV

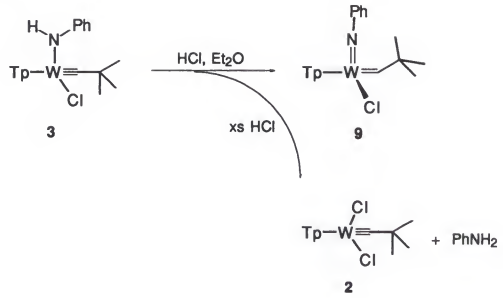

When H_2O was added to a sample of $TpW(NH_2)(CC(CH_3)_3)Cl$ (**6**), no formation of $TpW(NH)(CHC(CH_3)_3)Cl$ was detected even upon heating. Higher amounts of H_2O partially hydrolyzed **6** producing the oxo complexes $TpW(O)(CHC(CH_3)_3)Cl$ and/or $TpW(O)_2(CH_2C(CH_3)_3)$, but slower than **3**. Compounds $TpW(CC(CH_3)_3)(NHPh\text{-}p\text{-}Br)Cl$ (**4**) and $TpW(NHPh(3,5\text{-}(CF_3)_2))(CC(CH_3)_3)Cl$ (**5**) on the other hand, are much more susceptible to reaction with H_2O. Upon addition of H_2O to complex **5**, $TpW(O)(CHC(CH_3)_3)Cl$ is the major product along with $TpW(NPh(3,5\text{-}(CF_3)_2))(CHC(CH_3)_3)Cl$. After 3 days, the only evident compound in this sample is $TpW(O)(CHC(CH_3)_3)Cl$ which suggests that $TpW(NPh(3,5\text{-}(CF_3)_2))(CHC(CH_3)_3)Cl$ is also moisture sensitive. Compound **4** completely hydrolyzes to $TpW(O)(CHC(CH_3)_3)Cl$ and $TpW(O)_2(CH_2C(CH_3)_3)$. Attempts to acid catalyze the tautomerization of complexes $TpW(CC(CH_3)_3)(NH_2)Cl$ (**6**) and $TpW(CC(CH_3)_3)(NHPh)_2$ (**7**) were not successful because even trace amounts of acid quantitatively removed the amido ligands yielding the starting material $TpW(CC(CH_3)_3)Cl_2$ (**2**).

The acid catalyzed proton transfer in **3** is contrary to previous observations in other alkylidyne/amido systems.[64a,b,d,70a,b,c] It is, however, similar to the acid catalyzed proton transfer in the oxo/hydroxy species $Re(O)(^{18}OH)(RCCR)_2$.[78]

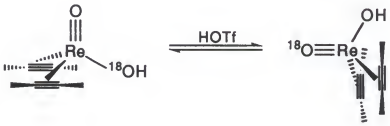

2.9

In the rhenium complex shown in Equation 2.9, proton transfer between the oxo and hydroxy ligands is slow (half-life of ~ 11h), but is rapid in the presence of trifluorometahnesulfonic acid (HOTf). The acid catalysis is believed to occur by initial protonation of the oxo ligand and formation of a symmetrical bis-hydroxide species. This claim was made because HOTf was shown to protonate the oxo ligand of the related complex $[Re(O)Et(MeCCMe)_2]$.[78]

For compound **3** two pathways could lead to **9** depending on where protonation occurs first (**Scheme 2.V**). One pathway could originate from protonation of the neopentylidyne ligand and formation of a transient cationic alkylidene/amido species. Subsequent abstraction of a proton from the amido group would lead to formation of **9**. Alternatively, protonation of the amido ligand followed by proton transfer to the alkylidyne, and finally deprotonation of the amido/alkylidene species can also be envisioned. The acid catalysis by H_2O may proceed in a similar fashion. Alternatively, production of H^+ from hydrolysis of **3** and/or **2** in the samples where H_2O was added, may also provide the acid needed for tautomerization of **3**.

Scheme 2.V

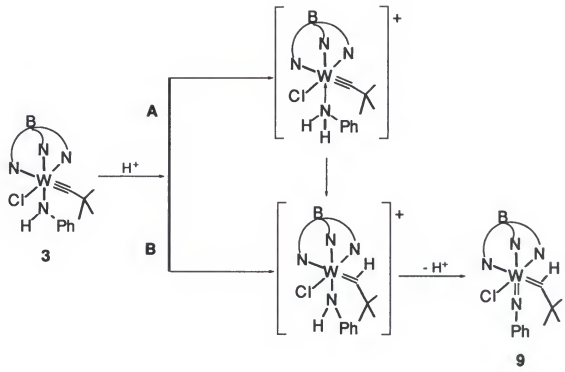

Although we cannot be certain which pathway (**A** or **B**, **Scheme 2.V**) is the most prominent one, pathway **B** may be supported more by the following reasoning. In general, alkylidynes are prone to protonation if there are no more basic ancillary ligands on the metal center.[4a,79] For example, in $W(CC(CH_3)_3)(OC(CH_3)_3)_3$ HX (2 equiv., X = Cl^-, I^-) protonates the neopentylidyne ligand together with one of the alkoxide ligands,[64c] but not in $Re(CC(CH_3)_3)(CHC(CH_3)_3)(CH_2C(CH_3)_3)_2$, in which the neopentylidene is protonated instead.[80] For $TpW(NHPh)(CC(CH_3)_3)Cl$ (**3**), it is possible that the amido ligand is more basic than the alkylidyne since the electron withdrawing nature of the phenyl group may reduce the effective donation of the nitrogen lone pair to the metal. Furthermore, the alkylidyne ligand in compounds $Tp'W(CC(CH_3)_3)Cl_2$ (**1**) and $TpW(CC(CH_3)_3)Cl_2$ (**2**) is not susceptible to protonation even by strong acids.[65d] In addition, there is direct evidence that, at least to some extent, the amido ligand is protonated

since it is possible to completely remove the amido group and reform $TpW(CC(CH_3)_3)Cl_2$ (**2**) by addition of a higher concentration of HCl to samples of **3**, **6** and **7**.

Photolysis of complex $TpW(NPh)(CHC(CH_3)_3)Cl$ (**9**), produced by acid addition to $(TpW(NHPh)(CC(CH_3)_3)Cl)$ (**3**), at -5 °C does establish a photostationary state between **9** and **3** after 15 minutes of irradiation indicating that, under these conditions a reverse proton transfer from the alkylidene to the imido ligand is possible.
To further support that this reverse proton transfer is not also acid catalyzed, NEt_3 was added to a sample of **9** prior to photolysis in order to scavenge any H^+ either originally present or generated. Addition of base, had no significant effect on the ratio of the tautomers. In any case, it would be unlikely that the proton transfer from **9** to **3** is acid catalyzed because if that were true, then addition of HCl should produce an equilibrium between **3** and **9**. Such reverse proton transfers from an alkylidene to an imido ligand have been observed before, but in most cases they have been either base[66a] or acid catalyzed.[81]

What is surprising is that in this case, the photolytically generated **3** returns readily to **9** upon heating even when an excess of triethyl amine is present. The thermal tautomerization could still be acid catalyzed, however, because any *in situ* generated NEt_3HCl may be more soluble in C_6D_6 or C_7D_8 than solid NEt_3HCl providing the system with the acidic catalyst needed for tautomerization of **3** to **9**. It also should be reminded that most of these samples were contaminated with **2** which is easily hydrolyzed in the presence of trace H_2O.

Conclusions

Due to the electronic and coordinative saturation of chelate stabilized compounds $Tp'W(CC(CH_3)_3)Cl_2$ (**1**) and $TpW(CC(CH_3)_3)Cl_2$ (**2**) their chemistry is ligand centered rather than metal centered. Attempted activation of these alkylidyne complexes towards

alkyne metathesis was not successful. Substitution of one or two chloride ligands with amido groups led to isolation of several amido alkylidyne complexes.

The arylamido alkylidyne complexes **3-8** do not tautomerize readily to the corresponding alkylidene/imido complexes. The phenyl and aryl amido ligands are *cis* to the neopentylidyne in order to avoid competition between the carbon p orbitals used for the W-C triple bond and the p orbital that contains the nitrogen lone pair. In addition, the amido ligands adopt a *syn* conformation with the larger group oriented towards the neopentylidyne moiety, and the proton towards the Tp or Tp' ligand to minimize steric interactions. NOe studies confirm that there is hindered rotation about the W-N bond of the amido group. While this conformation minimizes the steric crowding of the molecules, it disfavors intramolecular proton transfer since the proton of the amido ligand is not proximal to the alkylidyne moiety. In other examples where such proton transfers are possible, the hydrogen is either pointing towards the alkylidyne group, or the W-N bond is not rigid. For $TpW(NH_2)(CC(CH_3)_3)Cl$ (**6**), the steric argument does not hold since one of the protons is close enough to the neopentylidyne group. We believe that no tautomerization is observed in this complex due to the decreased acidity on going from $NH(Ar)$ to NH_2.

The tautomerization from the amido/alkylidyne to the imido/alkylidene complexes in the present study was shown to be acid catalyzed. We have presented evidence that protonation of the amido ligand may be the first step in this process but initial protonation of the alkylidyne ligand has not been rigorously excluded. Finally, the fact that protonation of the amido ligand is now a possibility, may provide an entry to synthesizing cationic alkylidynes by using an acid with a non-coordinating counter ion (e.g. HBF_4). This possibility has yet to be explored.

CHAPTER 3
SYNTHESIS OF BISAMIDO-CYCLOPENTADIENYL AND (BIS)SULFAMIDE CHELATING LIGANDS AND THEIR USE IN THE SYNTHESIS OF ZIRCONIUM (IV) AND TANTALUM (V) METAL COMPLEXES

Synthesis of a Trianionic Bisamido-cyclopentadienyl Ligand

A number of "constrained geometry" ligands are reported in the literature that combine a cyclopentadienyl ligand, or its substituted derivatives, and pendent groups such as amines, amides or alkoxides ("Cp-SiX" systems were X = NR, O).[8,14,24,26-31,33,34,36] The functionalized cyclopentadienyl ligands that have been synthesized so far are dianionic, and they are used mainly in the synthesis of Group III and IV transition metal complexes. These metal complexes have been shown to be active olefin polymerization catalysts.[24,26,27] There are also a few examples in which these ligands have been used in the synthesis of group V and VI metal complexes.[36]

We were interested in synthesizing similar chelating mixed cyclopentadienyl ligands that are trianionic. Our approach was to combine an *o*-phenylenediamine moiety with a cyclopentadienyl ring. In principal, such a ligand could be used in the synthesis of Group V metal complexes that are analogous to the Group IV "Cp-SiNR" systems.

Our initial attempts focused on reactions between $(C_5Me_4H)SiMe_2Cl$ and unsubstituted *o*-phenylenediamine or the monosubstituted N-trimethylsilyl-1,2-phenylenediamine. The latter diamine compound was prepared by dropwise addition of a cold Et_2O solution of Me_3SiCl to a cold solution of *o*-phenylenediamine that contained 1.5 equivalents of NEt_3. Upon addition of $(C_5Me_4H)SiMe_2Cl$ to an Et_2O solution of *o*-phenylenediamine and NEt_3, slow precipitation of an off-white solid was observed. After removal of Et_2O, the product was extracted with hexanes. Removal of hexanes afforded a

waxy off-white solid. The ^1H NMR spectrum of this solid showed the presence of at least two different new species, and a small amount of the starting material, $C_6H_4(NH_2)_2$. Higher dilution of $(C_5Me_4H)SiMe_2Cl$ and slower addition to a -78 °C solution of *o*-phenylenediamine, or the use of a large excess of NEt_3 did not reduce the number of products. The mass spectrum of this crude reaction mixture indicated that the product consisted of $C_6H_4[(C_5Me_4H)SiMe_2(NH)]_2$ together with the desired product 1,2-$C_6H_4(NH_2)[(C_5Me_4H)SiMe_2(NH)]$.

In order to avoid addition of $(C_5Me_4H)SiMe_2Cl$ to both amines of the phenylenediamine, the monosubstituted diamine N-trimethylsilyl-1,2-phenylenediamine was used instead. One equivalent of $(C_5Me_4H)SiMe_2Cl$ in Et_2O was slowly added to a -78 °C Et_2O solution of 1,2-$C_6H_4(Me_3SiNH)(NH_2)$ containing excess NEt_3. The ^1H NMR spectrum of the resulting oil again revealed the presence of multiple products. A mass spectrum of the oil showed that the product consisted $C_6H_4[(C_5Me_4H)SiMe_2(NH)]_2$ together with the desired product $C_6H_4(Me_3SiNH)[(C_5Me_4H)SiMe_2(NH)]$. The presence of the (bis)cyclopentadienyl product $C_6H_4[(C_5Me_4H)SiMe_2(NH)]_2$ suggested that cleavage of the -$SiMe_3$ group is occurring during the reaction. We believe that this may be due to ineffective removal of HCl, generated in the initial substitution, by NEt_3. Since the products from the above reactions were not readily isolable/separable, 1,2-$(PhNH)C_6H_4(NH_2)$, which contains a robust N-C bond, was used as the starting material

The reaction between 1,2-$(PhNH)C_6H_4(NH_2)$ and $(C_5Me_4H)SiMe_2Cl$ in Et_2O proceeded smoothly (Equation 3.1). The reaction mixture slowly turned pink as it warmed to room temperature. After addition of NEt_3, a color change from pink to dark yellow was observed with concomitant precipitation of more solids. It should be noted that the addition of $(PhNH)C_6H_4(NH_2)$ to $(C_5Me_4H)SiMe_2Cl$ instead of the other way around gave a cleaner product of 1,2-$(NHPh)C_6H_4((C_5Me_4H)SiMe_2NH)$ (**10**). In addition, a large excess of NEt_3 was still necessary to obtain good yields of **10**. An alternate synthesis of **10** was achieved by first lithiating 1,2-$(PhNH)(NH_2)C_6H_4$ with one equivalent of *n*-BuLi

and then reacting the resulting solid with $(C_5Me_4H)Si(CH_3)_2Cl$. This route compromises however, the yield and purity of **10**. In the ^1H NMR spectrum of compound **10** (**Figure 3.1**), the two secondary amine protons appear as broad singlets at δ 4.10 and δ 4.38 ppm, whereas the tetramethylcyclopentadienyl methine proton peak is observed at δ 2.91 ppm. Although other cyclopentadienyl isomers are possible via proton or silicon sigmatropic shifts,[82] only one isomer with the silicon and the proton at the 5 positions is observed for **10**. Compound **10** is stable in hydrocarbon solutions but relatively unstable in chlorinated solvents such as $CHCl_3$, CH_2Cl_2. We believe that cleavage of the Si-N bond in chlorinated solvents is a likely decomposition pathway.

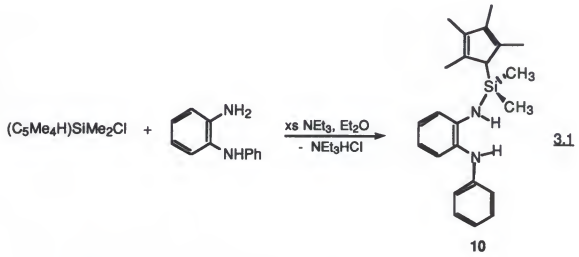

3.1

10

Reactions of **10** with Various Metal Complexes

The usual synthetic approach to transition metal complexes that contain cyclopentadienyl amido ligands utilizes the metathetical reaction of the lithio salts of these ligands with the appropriate metal halides.[24,26,27] Therefore, lithiation of **10** was thought

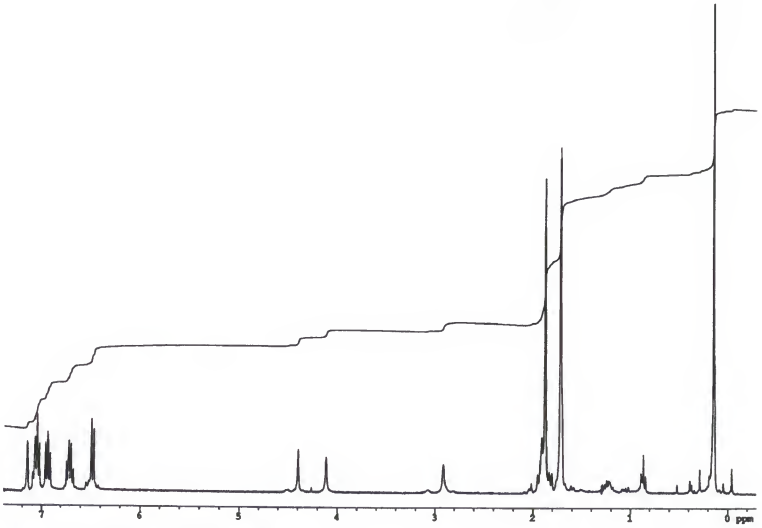

Figure 3.1 The ^{1}H NMR Spectrum of **10**.

to be an important step in order to prepare a variety of metal complexes. In principle, 1,2-(NHPh)C_6H_4($(C_5Me_4H)SiMe_2NH$) (**10**) should be susceptible to deprotonation, with the amine protons abstracted first, followed by the sterically hindered cyclopentadienyl methine proton. Attempts to lithiate **10**, however, have been unsuccessful so far. Addition of a slight excess of MeLi, n-BuLi, or $LiN(CH_3)_2$ in either hexanes, toluene, or Et_2O usually gave a green reaction mixture upon warming to room temperature, and attempted isolation of these products failed. Since other deprotonated phenylenediamine compounds have also shown to be quite unstable when isolated,[49,53] we attempted *in situ* deprotonation of **10** and its subsequent addition to a number of metal halide complexes such as $ZrCl_4$ and $TaCl_5$. The ^1H NMR spectra of these reaction mixtures showed the formation of a number of compounds but their separation and purification was impossible even after repeated recrystallizations. The steric bulk of the ligand may simply be blocking access to the amine and cyclopentadienyl methine protons by bases.

An alternative strategy is offered by ligand metathesis of amido or alkyl ancillary ligands of a metal complex by the cyclopentadienyl-phenylenediamido ligand, with subsequent elimination of amine or alkane. This synthetic route has proven quite successful in numerous cases.[28,36,43b] Efforts were therefore undertaken to investigate the utility of such reactions with **10**.

The reaction of **10** with $Zr(NMe_2)_4$ (**11**) was used as a model reaction in order to investigate if amine elimination was a viable route for the addition of **10** to metal complexes. Dropwise addition of an Et_2O or hexanes solution of **10** to a room temperature solution of **11** resulted in immediate color change from yellow to orange and precipitation of a dark yellow solid. The reaction mixture was vented through a bubbler to remove the amine byproduct. The isolated solid was washed with hexanes and recrystallized from a toluene/pentane mixture to afford **12** in low yield. The isolation of **12** was not trivial because in most cases compound **13** (discussed later in the chapter) was also formed and was not readily separated. The ^1H NMR spectrum (**Figure 3.2**) of **12** reveals four

inequivalent methyls (δ 1.61, 1.77, 2.07, 2.14 ppm) of the cyclopentadienyl ligand and two inequivalent methyls on the silyl group (δ 0.79, 0.86 ppm). The methyl groups of the NMe_2 ligand appear as a sharp singlet at δ 2.71 ppm. The amine proton of the coordinated NMe_2H was not located, in the room temperature ^1H NMR spectrum of **12**. Finally, NMe_2H could not be liberated from the metal complex even when the reaction was heated under a continuous flow of nitrogen.

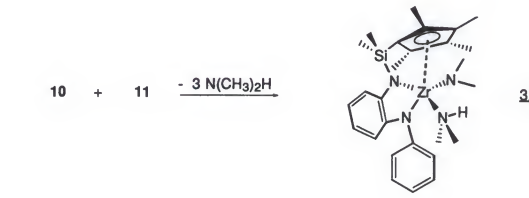

An X-ray diffraction analysis was performed on a single crystal of **12** in order to elucidate the structural details of the complex. Dark yellow, X-ray quality crystals of **12** precipitated from a room temperature C_6D_6 solution of **12** in a resealable NMR tube after approximately 1 week. Selected bond lengths and angles for **12** are given in **Table 3.I** whereas additional information for the structural parameters of the molecule are presented in **Tables 3.1-3.5** of Appendix A. A thermal ellipsoid plot of **12** is depicted in **Figure 3.3**.

The geometry around the metal center can best be described as a distorted square pyramid with the dimethylamido ligand occupying the axial position. The dimethylamine, the centroid of the cyclopentadienyl ligand (Cp(c)), and the two amido groups of the phenylenediamine occupy the equatorial plane.

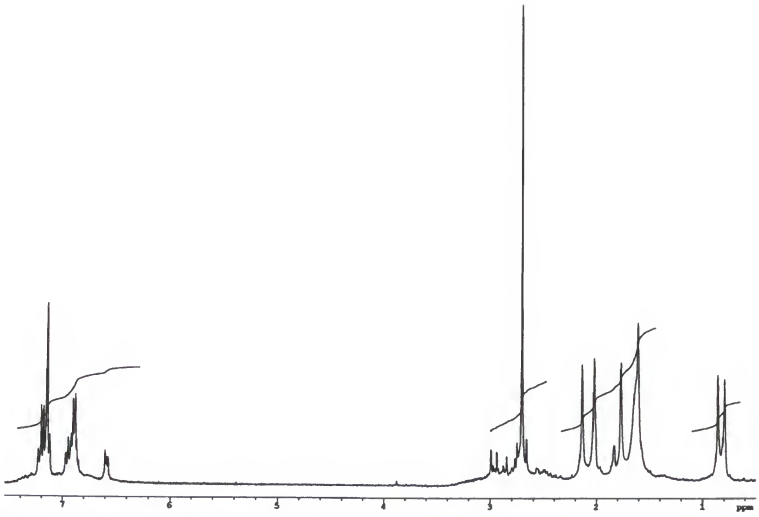

Figure 3.2 The ^{1}H NMR Spectrum of **12**.

Table 3.I Selected bond distances (Å) and angles (°) for **12**. Cp(c) denotes the centroid of the cyclopentadienyl ring.

1	2	3	1-2	1-2-3
Zr	N1	N2	2.1451(12)	71.34(4)
Zr	N1	N3		102.88(5)
Zr	N1	N4		145.90(5)
Zr	N1	Cp(c)		97.4(5)
Zr	N2	N3	2.2513(12)	96.47(5)
Zr	N2	N4		77.72(5)
Zr	N2	Cp(c)		153.0
Zr	N3	N4	2.0599(13)	94.38(5)
Zr	N3	Cp(c)		109.6
Zr	N4	Cp(c)	2.4005(13)	104.3
Zr	Cp(c)		2.332(2)	
Si	N1	Zr	1.7173(13)	107.25(6)
Si	N1	C1		92.86(6)
C8	N1	Zr	1.385(2)	121.87(9)
C8	N1	Si		130.64(10)
C20	N3	Zr	1,462(2)	117.44(11)
C21	N3	Zr	1.452(2)	132.83(12)

The Zr atom is situated slightly above the equatorial plane of the square pyramid, as indicated by the angles between the trans ligands which are less than 180 °. The distances between zirconium and the cyclopentadienyl carbons range from 2.474 to 2.769 Å. This indicates that the cyclopentadienyl ring is severely tilted which is reasonable given the constraints imposed from the rest of the chelating ligand. The Zr-Cp(c) distance (where Cp(c) is the centroid of the cyclopentadienyl ring) is comparable to values reported in the literature.

The presence of the -$SiMe_2$ bridge leads to substantial reduction of the Cp(c)-Zr-N1 angle compared to similar complexes with unlinked cyclopentadienyl and amido ligands. It is also slightly smaller than values reported for other bridging "Cp-SiNR" zirconium complexes. The constrained geometry imposed by the ligand is also characterized by the substantial displacement of the Si atom from the plane of the cyclopentadienyl ring (Cp(c)-C1-Si = 159.4 °), and results in the internal C1-Si-N1 and Si-N-Zr angles lying between 92.86 and 107.25 °.

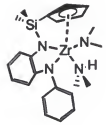

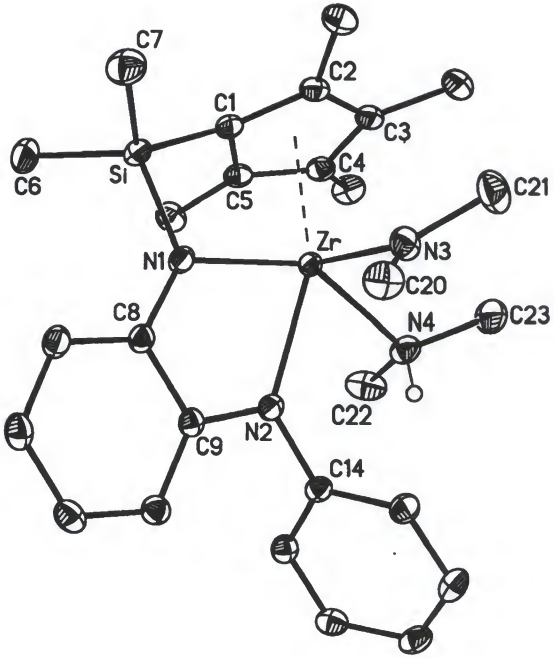

Figure 3.3 The Thermal Ellipsoid Plot of **12**.

The bite angle of the phenylenediamido fragment is 71.34 °, which is comparable to those reported for other phenylenediamido metal complexes.[47-49] The sums of the angles around either of the nitrogens of the chelating ligand is approximately 360 °, indicating an sp^2 hybridized geometry. The NMe_2 ligand also exhibits trigonal planar geometry at the nitrogen center. The Zr-N amido bond lengths are comparable to those reported for other zirconium amido complexes.[39-47]

As mentioned above, the ^1H NMR spectra of crude reaction mixtures of **12**, also indicated formation of second complex containing ligand **10**. This complex appeared to be symmetric because the silyl methyl protons appeared equivalent and the methyl groups of the -C_5Me_4 ring appeared as two singlets integrating to six protons each. We found that dropwise addition of a hexanes solution of **11** to approximately 2 equivalents of 1,2-(NHPh)((C$_5$Me$_4$H)SiMe$_2$NH)C$_6$H$_4$ (**10**) resulted in an immediate color change from yellow to dark orange and in the precipitation of a dark orange solid. After the addition was complete, the orange solution was decanted, and the solid was washed with copious amounts of pentane in order to remove the excess ligand **10**. The complex was identified by ^1H NMR and by an X-ray study to be the monochloride *o*-C$_6$H$_4${N(C$_6$H$_5$)N'[Si(CH$_3$)$_2$(C$_5$(CH$_3$)$_4$)]}Zr(Cl)(NH(CH$_3$)$_2$)$_2$ (**13**) (Equation 3.3). This unexpected result suggested presence of chloride in **10**, and was also supported by a positive chloride test. Attempts to completely remove the HCl generated during the synthesis of **10**, in order to prevent formation of **13**, have not been successful. This suggests that an adduct between **10** and HCl is formed, which cannot be converted completely to **10** even in the presence of a large excess of NEt3. Also this **10**.HCl adduct seems to be very soluble in non-polar solvents making its separation from **10** impossible. Smaller amines may be more effective in removing the residual HCl, and such investigations are underway.

The ^1H NMR spectrum of **13** (**Figure 3.4**) reveals its symmetric nature. The methyls of the silyl group resonate as a sharp singlet at δ 0.70 ppm, whereas the C_5Me_4

methyls appear as two singlets at δ 1.88 and 1.93 ppm (6H each). The N-H protons of NMe_2H can be located in this case, and resonate as a very broad singlet at δ 3.29 ppm.

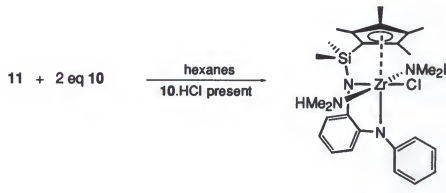

3.3

13

Orange crystals suitable for an X-ray diffraction study were isolated from a C_7D_8 solution of **13** after 4 days at room temperature. **Table 3.II** illustrates selected bond lengths and angles for complex **13**. A thermal ellipsoid plot of the structure is shown in **Figure 3.5**. Further information on the structural parameters of **13** are include in **Tables 4.1-4.5** in Appendix A. The structure of *o*-$C_6H_4\{N(C_6H_5)N'[Si(CH_3)_2(C_5(CH_3)_4)]\}Zr(Cl)(NH(CH_3)_2)_2$ (**13**) can best be described as a distorted octahedron with the center of the cyclopentadienyl ring and one of the nitrogens of the phenylenediamido ligand occupying the axial positions. The distortion is generated due to the chelated ligand, and results in a slight displacement of the zirconium from the equatorial plane of the octahedron. The sums of the angles around the nitrogens of the phenylenedamido fragment of the chelating ligand are approximately 360 °. The Zr-Cp(c) distance is shorter in **13** than in **12**, probably because of the presence of the chloride ligand. The silicon atom is displaced from the cyclopentadienyl plane as indicated by the Cp(c)-C1-Si = 156.5 ° due to the constraints imposed by the chelating ligand. The Zr-N

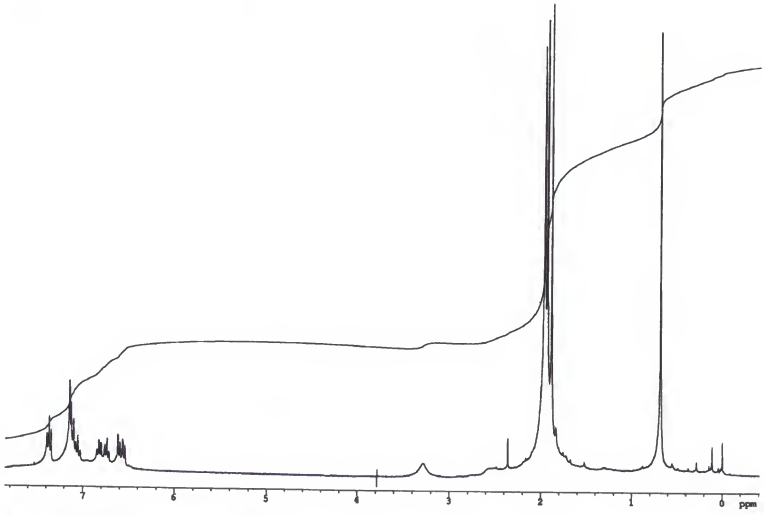

Figure 3.4 The ^{1}H NMR Spectrum of **13**.

distances of the phenylenediamido ligands are within the average values observed for other d^0 transition metal amido complexes.

Table 3.II Selected bond distances (Å) and angles (°) for **13**. Cp(c) denotes the centroid of the cyclopentadienyl ring.

1	2	3	1-2	1-2-3
Zr	N1	N2	2.1245(12)	71.84(5)
Zr	N1	N3		92.33(5)
Zr	N1	N4		97.92(5)
Zr	N1	Cl		158.74(4)
Zr	N1	Cp(c)		97.1
Zr	N2	N3	2.3024(13)	74.95(5)
Zr	N2	N4		74.19(5)
Zr	N2	Cl		87.13(3)
Zr	N2	Cp(c)		168.9
Zr	N3	N4	2.4511(14)	142.42(5)
Zr	N3	Cl		78.82(4)
Zr	N3	Cp(c)		107.1
Zr	N4	Cl	2.4190(13)	78.73(4)
Zr	N4	Cp(c)		107.4
Zr	Cl	Cp(c)	2.5376(4)	104.0
Zr	Cp(c)		2.300(2)	
N1	Si	C1	1.7296(14)	92.64(7)

The isolation of complexes **12** and **13** supported the viability of the synthesis of metal complexes via the amine elimination route. Therefore, various Group V and VI amido, imido, and alkyl complexes were reacted with **10** (**Figure 3.6**). These reactions however, either did not proceed, or isolation of characterizable products was not possible. When $W(CCMe_3)(CH_2CMe_3)_3$ was added to a C_6D_6 solution of **10**, evolution of neopentane was not observed by ^{1}NMR even when the reaction mixture was heated to 90 °C for 2 days. Similar results were observed when **10** was reacted with $Mo(NPh)_2(CH_2CMe_3)_2$. Addition of **10** to a hexanes solution of $Ta(NMe_2)_5$ (**16**) produced a slow color change from yellow to orange, but the ^{1}H NMR spectrum revealed a complicated reaction mixture.

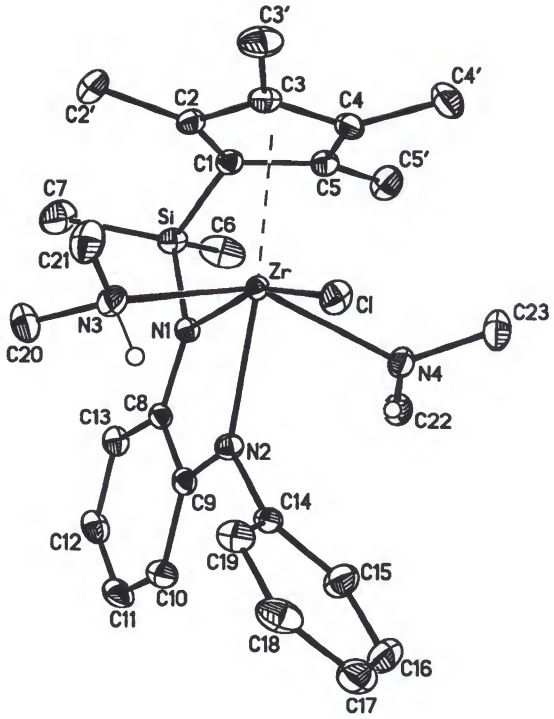

Figure 3.5 The Thermal Ellipsoid Plot of **13**.

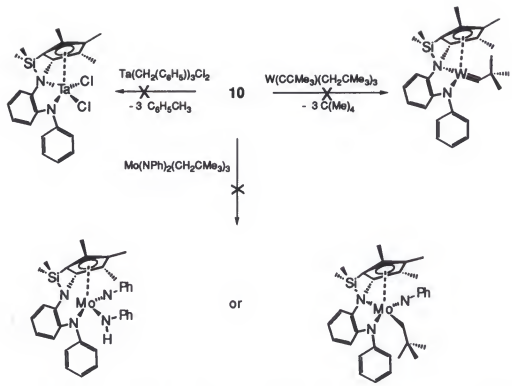

Figure 3.6 Attempted reactions of **10** with various Group V and VI metal complexes.

(Bis)sulfamides as Ligands

As was discussed in Chapter 1, polydentate amido ligands have received a great deal of attention recently.[39,41,43-45] Among the several advantages these ligands offer over more classical polydentate and monodentate ligands is the synthesis of high oxidation state early transition metal complexes with lower coordination numbers. This results in lower electron density at the metal center, and easy "tuning" of the coordination environment around the metal by changing the substituents on the nitrogen. In view of these observations, we decided to synthesize new diamido ligands from parent diamine compounds with the general formula $O_2S(NH(R))_2$.

We believe these compounds are good candidates for use as chelating ligands in the synthesis of d^0 early transition metal complexes. Their synthesis is easy and proceeds in nearly quantitative yields.[83] A general synthetic route is shown in Equation 3.4.

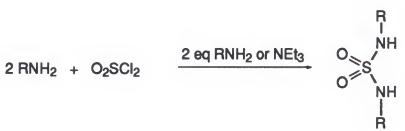

3.4

The yields and purity of the products depends somewhat on the size of the alkyl substituents on the nitrogen. For smaller alkyls (e.g. CH_3, C_2H_5), formation of by-products such as the one shown in Equation 3.5 is a potential problem, but running the reactions at much lower temperatures usually improves the product selectivity.[83a] These compounds could also be used as potential ligands, however.

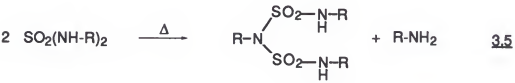

3.5

Equation 3.4 also exhibits the versatility of (bis)sulfamide ligands since they can have any amido substituents on the SO_2 backbone. In fact, the easy access to a number of symmetrically or unsymmetrically substituted sulfamides can produce ligands that vary in steric, electronic properties, and symmetry, thus allowing facile tailoring of the ligand. In

addition, the SO_2 backbone is electron withdrawing which in turn can render the metal centers even more electron deficient.

Considering the potential of the (bis)sulfamide compounds, it is surprising that there are only a few previous examples of these compounds as bidentate ligands. Most of them include complexation of (bis)sulfamides with main group elements and late transition metals (Equations 3.6, 3.7).[84] Also, as shown in the Equation 3.8, the chiral (C_2 symmetry) (bis)sulfamide (*S,S*)-*N,N'* -Bis(α-methylbenzyl)sulfamide was used as a bidentate ligand for asymmetric $LiAlH_4$ reductions of ketones.[83c]

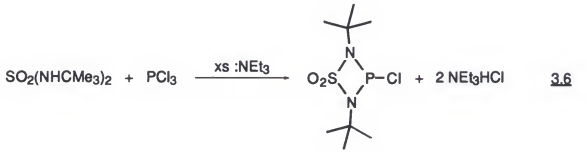

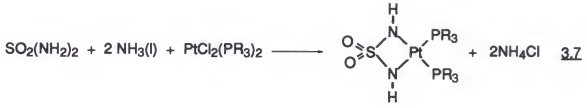

For the work described below, two (bis)sulfamide compounds were synthesized, $SO_2[NHCMe_3]_2$ (**14**) and $SO_2[NH(CHMePh)]_2$ (**15**). They were prepared in high yield

and purity, and various synthetic routes were examined in order to incorporate them into the coordination sphere of various metal complexes.

Attempted Deprotonation of $SO_2(NHR)_2$ (R = t-butyl (**14**), CHMePh (**15**))

Since halide displacement by the metal salt of a ligand (usually Li, K, Na, or Mg salts of the ligand) is one of the easiest routes to introduce a ligand to a transition metal complex, attempts to deprotonate $SO_2(NHR)_2$ (**14**, **15**) and prepare $(M^+)_2(SO_2(NR)_2)^{-2}$ salts were undertaken. The (bis)sulfamide ligand is analogous to H_2SO_4 ($SO_2(OH)_2$), except that the two hydroxyl groups are substituted by amido groups. As shown in Equation 3.6, compound **14** has been shown to react with PCl_3 in the presence of excess NEt_3 to give the (bis)sulfamide complex $PCl[SO_2(NCMe_3)_2]$.[84d] In this reaction, it is suggested that the ligand is either deprotonated prior to or after adduct formation PCl_3. Furthermore, when $SO_2(NH)_2$ is to reacted with $PtCl_2(PPh_2Me)_2$ in liquid ammonia, it forms the (bis)sulfamide containing complex $Pt[(HN)_2SO_2](PPh_2Me)_2$ (Equation 3.7).[84c] The formation of this complex is proposed to occur via initial deprotonation of the (bis)sulfamide **14** by ammonia.

In view of the observations described above, excess NEt_3 was added to a solution of **14**, and stirred for 20 minutes. $W(NPh)Cl_4.Et_2O$ was slowly added to give a dark brown product (Equation 3.9).

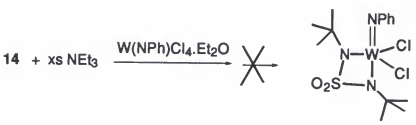

3.9

The ^1H NMR spectrum of the recrystallized dark brown product showed the formation of multiple complexes that could not be identified individually. Therefore, it is not certain if any of these compounds is the desired $W(NPh)Cl_2[SO_2(NCMe_3)_2]$ (Equation 3.9). Similar results were obtained when **15** was allowed to react with $W(NPh)Cl_4.Et_2O$ in the presence of NEt_3. Attempted reactions of $TaCl_5$ and $ZrCl_4$ with **14** or **15** also have not shown promise. Allowing $SO_2(NHR)_2$ (R = *t*-butyl (**14**), CHMePh (**15**)) to react longer with NEt_3 prior to addition of the metal halides did not change the outcome of the reactions.

Since, deprotonation of $SO_2[NHC(CH_3)_3]_2$ (**14**) and $SO_2[NH(CHMePh)]_2$ (**15**) by NEt_3 did not produce promising results, deprotonation of the (bis)sulfamide compounds (**14**) and (**15**) with stronger bases was attempted. Reaction of **14** or **15** with 2 equivalents of *n*-BuLi, $LiNMe_2$, KH, and $(n\text{-}Bu)_2Mg$ in various solvents (e.g. Et_2O, C_7H_8, THF) gave gummy solids that could be triturated with pentane to produce off-white powders that were semi-soluble in C_6D_6. Their ^1H NMR spectra showed that the N-H amido protons were absent but also that other decomposition reacions were occurring.

Addition of 14 and 15 to Various Group IV-VI Alkyl, Imido, and Amido Metal Complexes

Due to the fact that lithiation of $SO_2[NHC(CH_3)_3]_2$ (**14**) and $SO_2[NH(CHMePh)]_2$ (**15**) proved non-trivial, other synthetic routes were pursued, in order to incorporate **14** and **15** into the metal sphere of a complex. Reactions of **14** and **15** with various alkyl, amido, and imido complexes were examined next.

The synthesis of tantalum complexes containing (bis)sulfamide ligands was investigated first. Such complexes would be interesting due to the fact that, that depending on the rest of the other ancillary ligands, they could potentially act as either Ziegler-Natta olefin polymerization or olefin metathesis catalysts (**Figure 3.7**).

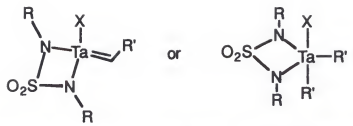

Figure 3.7 Potential formation of (bis)sulfamide Ta alkylidene or alkyl complexes depending on the size of the ancillary ligands.

$Ta(NMe_2)_5$ was reacted with one equivalent of **14** at room temperature for 12 hours. The reaction mixture was periodically evacuated to remove the dimethyl amine by-product (Equation 3.10).

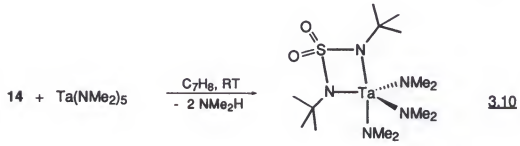

The reaction proceeds in nearly quantitative yield. Complex $Ta(NMe_2)_3[SO_2(NCMe_3)_2]$ (**17**) is isolated as a light beige solid and can be recrystallized from a toluene-pentane mixture. The room temperature ^1H NMR spectrum of **17** shows only two singlets each integrating to 18 protons. The δ 1.46 ppm (18H) peak, assigned to the t-butyl groups on the sulfamido ligand, is much sharper than the peak corresponding to the methyls of the dimethylamido ligands (δ 3.12 ppm, 18H).

Compound **17** is pentacoordinate, and thus it can have either a square pyramidal or a trigonal bipyramidal structure.[11b] The fact that the three NMe_2 ligands appear to be equivalent in the room temperature ^1H NMR spectrum of **17** implies that a fluxional process is taking place, equilibrating the axial and equatorial NMe_2 ligands on the NMR time scale. A variable temperature ^1H NMR study was performed on **17** in order to elucidate this fluxional process. A sample of $Ta(NMe_2)_3[SO_2(NCMe_3)_2]$ (**17**) was dissolved in C_7D_8 and the temperature in the NMR probe was lowered to -60 °C. **Figure 3.8** shows the ^1H NMR spectra of **17** at different temperatures. At -60 °C, the ^1H NMR spectrum of **17** displays inequivalent *t*-butyl sulfamide peaks each integrating to 9 protons (δ 1.50, 1.56 ppm) and three dimethylamido peaks each integrating to 6 (δ 2.95, 2.98, 3.19 ppm). The two dimethylamido peaks (from the dimethyl amido ligands) at δ 2.95 and 2.98 coalesce at -35 °C (δ 2.93 ppm). The two *t*-butyl peaks of the (bis)sulfamide ligand coalesce at -30 °C whereas, the dimethyl amido peaks at δ 2.93 and 3.19 ppm coalesce at -9 °C. These spectroscopic features are best fit by structure **A** shown in **Figure 3.9**.

At low temparature, the two *t*-butyl groups of the sulfamido ligand are inequivalent; one is axial and the other equatorial. The resolution of the dimethylamido peaks to three peaks instead of two, suggests that at very low temperatures, rotation about the Ta-N bond of the amido ligands is also very slow (**Figure 3.9**). Otherwise two peaks would be observed at low temperature in a 2:1 ratio (equatorial:axial NMe_2). Slow rotation renders each methyl on the equatorial amido ligands inequivalent with respect to the other but related to the adjacent amide by a mirror plane. The activation energy $\Delta G^{\ddagger}$ for the coalescence of the peaks at δ 2.95, 2.98 ppm was estimated by the equally populated two-site exchange approximation[85] to be 12.3 kcal/mol. The activation energy of the coalescence of the two *t*-butyl peaks at δ 1.50 and 1.56 ppm was estimated by the equally polulated two-site exchange approximation to be 12.3 kcal/mol. Finally, the activation energy $\Delta G^{\ddagger}$ for the coalescence of the dimthylamido peaks at δ 2.93 and 3.19 ppm (2:1 ratio) was estimated by the unequally populated two-site exchange[85] to be 12.8 kcal/mol.

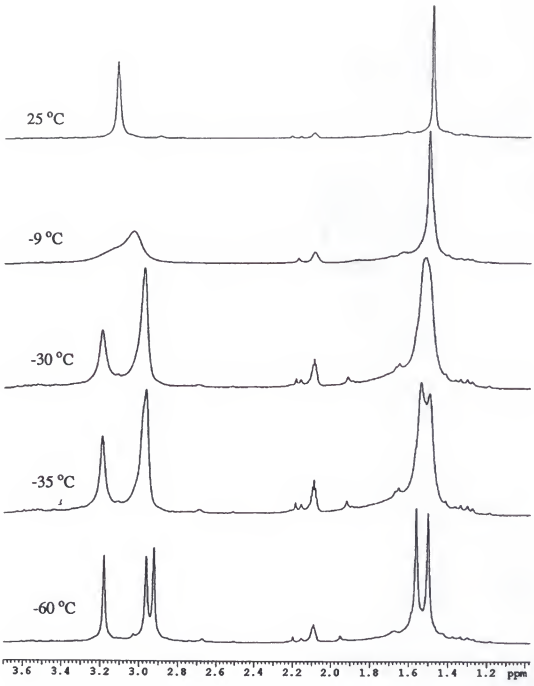

Figure 3.8 Variable Temperature ^{1}H NMR Spectrum of **17**.

The activation energy values that were calculated for the coalescence of the axial-equatorial dimethylamido groups (1:2 ratio) and for the axial-equatorial *t*-butyl groups were expected to be the same (~ 12 kcal/mol within experimental error) because it is the same fluxional process that equilibrates them. This fluxional process is suggested to follow the Berry pseudorotation mechanism.[11b] The activation energy for the overall fluxional process is also similar to the activation energy needed to equilibrate the inequivalent methyls of the two equatorial NMe_2 ligands (Me_a and Me_b **Figure 3.9**). There are two possibilities for this observation. One is that the coalescence of the peaks at δ 2.95, 2.98 ppm is only due to rotation of the dimethyl amido groups, with exchange between the dimethylamidos in the axial and equatorial positions still not taking place at -35 °C.

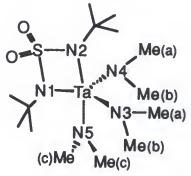

A

Figure 3.9 A possible structure that gives rise to the low temperature ^1H NMR spectrum observed for **17**.

If that is the case, then the energy of rotation around the Ta-N bond happens to coincide with the energy of the overall fluxional process. The other possibility is that at temperatures higher than -60 °C there is only one process with activation energy of ~12 kcal/mol responsible for all the experimental observations.

The trigonal bipyramidal configuration of **17** at low temperatures is also consistent with an X-ray diffraction study on a single crystal of **17**. Singles crystals were grown by

slow diffusion of pentane in a saturated toluene solution of **17**. **Figure 3.10** shows a thermal ellipsoid plot of **17** whereas **Table 3.III** summarizes important bond distances and angles. Complete structural parameters are included in **Tables 5.1-5.5** of Appendix A. The structure of **17** can best be described as a distorted trigonal bipyramid with the bidentate ligand occupying one axial and one equatorial position. The bite angle of the ligand is 67.54 ° which is much smaller than other bidentate amido complexes reported in the literature due to the four-membered chelate ring.

Table 3.III Selected bond distances (Å) and angles (°) for **17**

1	2	3	1-2	1-2-3
N1	Ta	N2	2.074(3)	67.54(12)
N1	Ta	N3		120.90(14)
N1	Ta	N4		121.45(14)
N1	Ta	N5		98.78(14)
N2	Ta	N3	2.145(3)	94.94(14)
N2	Ta	N4		94.65(14)
N2	Ta	N5		166.32(14)
N3	Ta	N4	1.961(4)	115.7(2)
N3	Ta	N5		92.4(2)
N4	Ta	N5	1.965(3)	92.5(2)
N5	Ta		1.996(4)	

The Ta-N1 and Ta-N2 bond lengths of the (bis)sulfamide ligand are longer than those Ta-N bonds of the dimethylamido ligands. The angles around N1 and N2, however, suggest that these nitrogens are trigonal planar indicating significant π-back bonding interaction from the nitrogens of the (bis)sulfamide ligand to the Ta center.

The synthesis of complex $Ta(NMe_2)_3[SO_2(NCHMe(C_6H_5)]_2$ (**18**) (Equation 3.11) was analogous to that of **17** and proceeds nearly quantitavely. In the ^1H NMR spectrum of **18** (**Figure 3.11**), the methyl groups of the (bis)sulfamide appear as a doublet at δ 1.76 ppm while the NMe_2 protons appear as a sharp singlet at

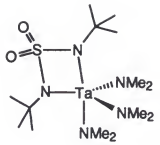

17

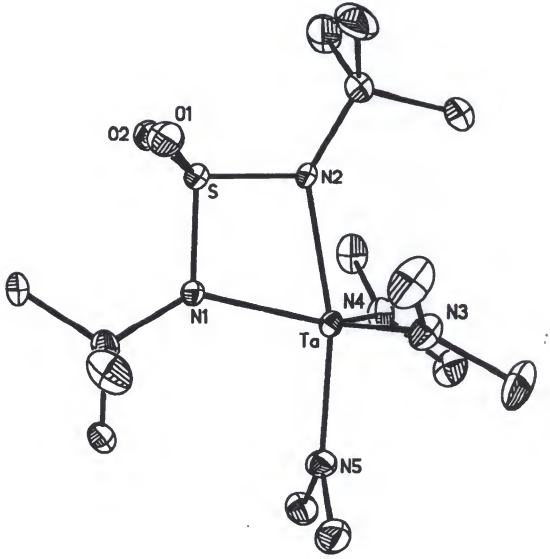

Figure 3.10 The Thermal Ellipsoid Plot of **17**.

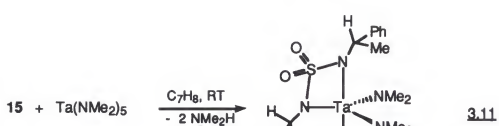

3.11

18

δ 2.75 ppm. The benzyl methine proton of the (bis)sulfamide ligand resonates as a quartet at δ 5.56 ppm. A variable temperature study on **18** showed no significant broadening of the peaks down -90 °C. The difference between the dynamic behavior of **17** and **18** may be attributed to the smaller alkyl substituents on the (bis)sulfamide **18**.

In order to produce a (bis)sulfamide tantalum complex via alkane elimination, the reaction between **14** and $Ta(CH_2Ph)_3Cl_2$ was attempted (Equation 3.12).

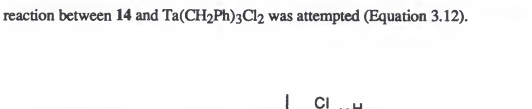

3.12

No reaction was observed after 2 days at room temperature or upon heating the reaction mixture to 40 °C for 5 hours. The thermal instability of $Ta(CH_2Ph)_3Cl_2$ precluded heating the reaction mixture to higher temperatures.

In view of the successful synthesis of (bis)sulfamide tantalum amido complexes via amine elimination, an analogous reaction was attempted by addition of **14** and **15** to

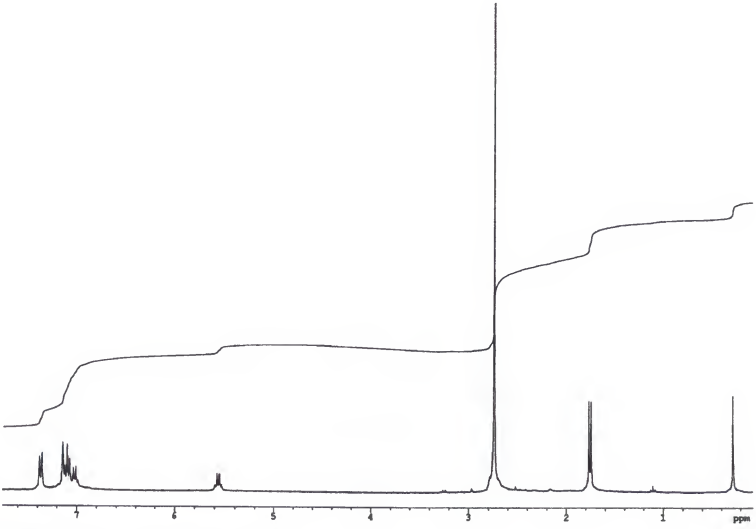

Figure 3.11 The ^{1}H NMR Spectrum of **18**.

$Zr(NMe_2)_4$ (**11**). These reactions were initially run under conditions similar to those used for the synthesis of **17** and **18**. After slow addition of **14** to **11**, elimination of amine was observed, and the reaction mixture was left to stir overnight. A very pale yellow semi-crystalline solid was isolated upon removal of solvent, and was recrystallized from a mixture of toluene and hexanes. The ^1H NMR spectrum of this compound exhibited two very broad peaks which, however, did not integrate to the expected $Zr(NMe_2)_2(SO_2(NH(CMe_3)_2)$. Attempts to recrystallize the product of this reaction have so far failed. In an attempt to identify if the disubstituted $Zr(SO_2(NH(CMe_3)_2)_2$ had formed, a solution of **11** was added to two equivalents of **14**. Again, however, a single product was not isolated and repeated recrystallizations failed to purify the mixture further.

The isolation of $((NSiMe_3)_2C_6H_4)Mo(NPh)Cl_2$ by reaction of $Mo(NPh)_2Cl_2$.DME with $((NHSiMe_3)_2)C_6H_4$ suggested[49c] that it may possible to synthesize molybdenum containing (bis)sulfamide ligands by an analogous reaction of $Mo(NPh)_2Cl_2$.DME with $SO_2(NHR)_2$ (R = t-butyl (**14**), CHMePh (**15**)). No reaction was, however, observed, and only starting materials were recovered from reaction mixtures of $Mo(NPh)_2Cl_2$.DME with **14** and **15**.

Attempted Conversion of **17** and **18** to their Halide and Alkyl Derivatives

In order to further explore the reactivity of the disulfamido containing complexes **17** and **18**, removal of the dimethyl amido ligands was attempted. Complex $Ta(NMe_2)_3[SO_2(NC(CH_3)_3)_2]$ (**17**) did react with 3 equivalents of NEt_3HCl but did not produce the expected $TaCl_3[SO_2(NC(CH_3)_3)_2]$. The ^1H NMR spectrum of the reaction mixture in C_7D_8 was complicated. After 4 days, the presence of **14** in the ^1H NMR spectrum of the reaction mixture indicated that protonation of the (bis)sulfamide ligand had

taken place. Comparing the basicities of the NMe_2 and $SO_2(NHC(CH_3)_3)_2$ groups, one would expect that the dimethylamido ligands should be more easily protonated.

Addition of $SiMe_3Cl$ is often used to replace -NMe_2 with Cl^-.[19f,86] In the case of reaction of **17** with $SiMe_3Cl$, clean abstraction of the dimethylamido ligands did not occur. Reaction between the silyl chloride and **17** is evident since the color of the reaction slowly turns from pale yellow to orange, but a single product could not be isolated. It is possible that $SiMe_3Cl$ may be reacting with the oxygens of the SO_2 backbone leading to decomposition of the ligand. Addition of MeI to Ti amido complexes has been shown to remove selectively an amido ligand.[87] To the same end, however, addition of 36 equivalents of MeI to a sample of **17** also failed to generate the Ta-I complex.

Reaction of several zirconium *ansa*-metallocene amido complexes with $AlMe_3$ has led to isolation of their dimethyl analogs.[86a,b] A similar reaction was used in an attempt to produce a methyl derivative of **17**. The reaction mixture of 6 or more equivalents of $AlMe_3$ with **17** at room temperature slowly changed colors from pale yellow to dark orange. Washing the solid, isolated upon removal of solvent, with hexanes and reextraction with toluene produced a pure light beige compound. According to its ^1H NMR, spectrum **19** has the general formula $Ta(NMe_2)_3[SO_2(NCMe_3)_2](AlMe_3)_2$ (Equation 3.13). In the ^1H NMR spectrum of **19** there are three singlets each integrating to 18 protons each, which are assigned to the two $AlMe_3$ groups, the *t*-butyl peaks of the sulfamide ligand, and the dimethyl amido ligands. The $AlMe_3$ chemical shift of **19** at δ -0.10 ppm is 0.25 ppm downfield from that of free $AlMe_3$. The *t*-butyl and dimethylamido peaks in **18** are shifted slightly upfield compared to $Ta(NMe_2)_3[SO_2(NCMe_3)_2]$ (**17**). From the spectrum, it is clear that $AlMe_3$ does not remove the amido groups but rather it forms an adduct with **17**. Reaction of **17** with $AlEt_3$ gives the analogous complex $Ta(NMe_2)_3[SO_2(NCMe_3)_2](AlEt_3)_2$ (**20**). Both **19** and **20** slowly decompose in solution to form a black insoluble solid.

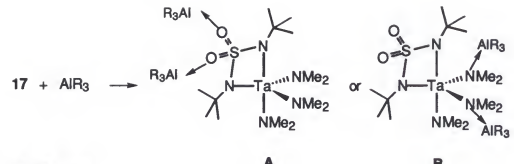

3.13

R = Me, **19**
R = Et, **20**

At this point we are not certain whether the AlR_3 groups are coordinated to the oxygens of the (bis)sulfamide ligand or to the nitrogens of the amido ligands (Structure **A** or **B**, Equation 3.13). The stronger Al-O bonds compared to Al-N[37] bonds would support structure **A** of Equation 3.13. Moreover, the lone pairs on the oxygens of the SO_2 backbone should be more available for formation of the O-Al dative bond, since the nitrogens of the amido groups in **17** are involved in nitrogen-to-metal lone pair donation. On the other hand, the ^1H NMR spectrum of **19** and **20** are temperature independent to -90 ^oC, contrary to the temperature dependence of the ^1H NMR spectrum of **17**. This observation suggests possible interaction of AlR_3 with any of the amido ligands of **17**, which in turn would weaken the Ta-N bonds and lower the activation barrier of the fluxional process. Similar results have been observed in the case of $Yb[N(SiMe_3)_2]_2[AlMe_3]_2$.[88]

The IR spectra of **17**, **19**, and **20** were quite complicated and were not very helpful in identifying changes in the S-O stretches of the SO_2 backbone. A crystal structure would be very useful in this case, however it has not yet been possible to isolate good quality single crystals of either **19** or **20**. The structure of complexes such as **19** and **20** would be of interest because of their possible utility in Ziegler-Natta polymerization reactions.

Conclusions and Future Work

A new trianionic cyclopentadienyl-phenylenediamido ligand, o-$C_6H_4\{NH(C_6H_5)N'H[Si(CH_3)_2(C_5(CH_3)_4H)]\}$ (**10**), was synthesized and was employed in the synthesis of the zirconium complexes o-$C_6H_4\{N(C_6H_5)N'[Si(CH_3)_2(C_5(CH_3)_4)]\}Zr(N(CH_3)_2)(NH(CH_3)_2)$ (**12**) and o-$C_6H_4\{N(C_6H_5)N'[Si(CH_3)_2(C_5(CH_3)_4)]\}Zr(Cl)(NH(CH_3)_2)_2$ (**13**). The formation of the chloride containing complex **13** was attributed to ineffective removal of HCl during the synthesis of ligand *o*-$C_6H_4\{NH(C_6H_5)N'H[Si(CH_3)_2(C_5(CH_3)_4H)]\}$ (**10**). Compound **13** usually forms in addition to **12** and their separation is difficult. The reactivity of these compounds has not yet been tested. Due to the trianionic ligand they contain, complexes **12** and **13** cannot form cationic alkyl species needed for metal complexes involved in Ziegler-Natta type catalysis. These compounds could possibly, however, be used as building blocks of heterobimetallic complexes similar to those presented in Chapter 1.

The crystal structures of **12** and **13** and the coordination of up to two NMe_2H to the zirconium complexes show that the coordination sphere of the cyclopentadienyl-diamido ligand is not very sterically demanding, and also renders the metal center very electron deficient. This in turn suggests that if a Group V complexes containing this ligand were synthesized, they could possibly be analogous to the highly electrophilic Group IV "Cp-SiNR" metal complexes and may exhibit similar reactivities.

Unfortunately, we have not yet had success in coordinating $C_6H_4\{NH(C_6H_5)N'H[Si(CH_3)_2(C_5(CH_3)_4H)]\}$ (**10**) to $Ta(NMe_2)_5$ and $Ta(CH_2Ph)_3Cl_2$. The problem in the synthesis of these complexes may lie in the steric bulk of the rest of the ancillary ligands. Therefore, reaction of **10** with tantalum complexes that contain smaller ligands may assist the coordination of the cyclopentadienyl-diamido ligand **10** to the tantalum center. If for example, homoleptic tantalum amides were synthesized, in which the amido ligands have smaller cone angles than NMe_2, then the amine elimination reaction may proceed more easily. Such dependence of amine elimination on the size of the amido

ligands has been observed in other cases.[86d] Moreover, the deprotonation of **10** and formation of M^+-**10** salts (M = Li, K, etc) should be further investigated, since in that case, the halide displacement route could be used in order to synthesize a wider variety of metal complexes.

(Bis)sulfamide compounds were also successfully employed as chelating amido ligands in the synthesis of tantalum amido complexes $Ta[N(CH_3)_2]_3[SO_2(NC(CH_3)_3)_2]$ (**17**) and $Ta[N(CH_3)_2]_3\{SO_2[N[CH(CH_3)(C_6H_5)]]_2\}$ (**18**) via the amine elimination method. Attempts to remove the NMe_2 ancillary ligands from **17** by use of NEt_3HCl, $SiMe_3Cl$ or AlR_3 (R = Me, C_2H_5) were not successful. In the case of AlR_3 however, the AlR_3 adducts $Ta[N(CH_3)_2]_3[SO_2(NC(CH_3)_3)_2][Al(CH_3)_3]_2$ (**19**) and $Ta[N(CH_3)_2]_3[SO_2(NC(CH_3)_3)_2][Al(CH_2CH_3)_3]_2$ (**20**) were isolated. A crystal structure is needed to elucidate the exact nature of these adducts.

The synthesis of other metal complexes containing the (bis)sulfamide ligands **14** and **15** is still under investigation. Attempts to synthesize zirconium complexes containing (bis)sulfamide ligands by the amine elimination route have not yet proven successful. The use of other Group IV metal complexes such as $M(CH_2Ph)_4$ (M = Ti, Zr) may prove more suitable for reaction with **14** and **15**.

The deprotonation of **14** and **15** has not been trivial. Use of non-nucleophilc strong bases such as *t*-BuLi or LDA may allow deprotonation of the amine protons without leading to decomposition of the ligand. Other ways of removing the protons such as use of proton sponge are still underway. Another possibility is to lithiate **14** and **15** in the presence of $MgBr_2$ in order to produce the magnesium salts of the ligands. This may allow for easier isolation of the salts of **14** and **15**, and possibly reduce any side reactions that are occurring. This method has been successfully used in the synthesis and isolation of other diamide salts.[41c]

CHAPTER 4
EXPERIMENTAL PROCEDURES

Materials and Methods

All procedures were performed using standard Schlenk techniques or in a N_2-filled dry box. Diethyl ether (Et_2O), tetrahydrofuran (THF), pentane, and hexanes were distilled from sodium benzophenone ketyl; toluene was previously deolefinated by washing twice with cold H_2SO_4 followed by water and bicarbonate, and was then distilled from potassium metal; dichloromethane (CH_2Cl_2) was distilled from CaH_2. After collection, all solvents were stored under argon and over molecular sieves. Glassware was oven dried before use. Compounds (DME)W($CC(CH_3)_3$)Cl_3,[79] potassium hydrotirs(1-pyrazolyl)borate (KTp),[38] potassium hydrotris-(3,5-dimethyl-1-pyrazolyl)borate (KTp'),[38] TpW($C(CH_3)_3Cl_2$ **(2)**,[65d] Tp'W($C(CH_3)_3Cl_2$ **(1)**,[65a,d] $C_5(CH_3)_4HSi(CH_3)_2Cl$,[24a] $SO_2[NH(C(CH_3)_3)]_2$ **(14)**,[83] and $SO_2\{NH[CH(CH_3)(C_6H_5)]\}_2$ **(15)**[83] were synthesized according to published procedures. The homoleptic amides $Zr(N(CH_3)_2)_4$ **(11)** and $Ta(N(CH_3)_2)_5$ **(16)** were synthesized according to an improved procedure reported by Jordan *et al.*[86a] All NMR solvents were degassed and stored over molecular sieves in the dry box prior to use.

^1H and ^{13}C spectra were measured either on a General Electric QE 300 or a Varian VXR-300 (300 MHz) spectrometer. Chemical shifts were referenced relative to residual protons in the deuterated solvents and are reported relative to tetramethylsilane. Elemental analyses were performed either by the University of Florida Analytical Services or by

Atlantic Microlabs, Norcross, Ga. Mass spectrometry was performed by the UF Department of Chemistry Analytical Services. IR spectra were recorded on a Perkins Elmer 1200 series FTIR from Nujol mulls that were prepared in the dry box.

Photolyses

All photolyses were performed on solutions of the compounds in resealable NMR tubes. A 275 W tungsten lamp was used as irradiation source and the sample was cooled to -10 °C in an ice/$CaCl_2$ bath that was refreshed every 5 minutes to maintain temperature.

TpW(NHPh)(CC(CH_3)$_3$)Cl (3)

Complex TpW($C(CH_3)_3Cl_2$ (**2**) (0.15 g, 0.27 mmol) was dissolved in 20 mL Et_2O giving a purple solution and cooled to -78 °C. To this solution an Et_2O solution of LiNHPh (0.05 g, 0.54 mmol, 2 equiv.) was slowly added. A slow color change from purple to green was observed. The reaction mixture was left to warm to room temperature and stir for 12 hours, yielding finally a dark orange solution. Removal of solvent under reduced pressure, and recrystallization from a minimum of Et_2O/pentane at -78 °C yielded **3** as an orange powder (yield: 0.09 g, 45 %). Repeated recrystallizations did not successfully remove unreacted **2**. ^1H NMR (25 °C in C_6D_6): δ 1.2 (s, 9H $C(CH_3)_3$), 5.69,5.78,5.82 (t, 1H each, Tp ring H's, 4-position), 6.9 (t, 1H, p-Ph), 7.32, 7.35,7.76,7.79,8.40 (d,1H each, five out of six H's of Tp, 3,5-position, one overlaps with solvent), 7.20 (t, 2H, m-Ph, other phenyl H's overlap with solvent), 10.5 (broad s, 1H, N-H). TpW(^{15}NHPh)(CC(CH_3)$_3$)Cl (**3a**) was prepared in a similar manner using K^{15}NHPh: ^1H (C_6D_6): δ 10.50 (d, 1H) N-H, $^1J_{NH}$ = 70 Hz).

TpW(NHPh-p-Br)(CC(CH_3)$_3$)Cl (4)

A solution of p-bromoaniline (0.09g, 0.75 mmol) in 10 mL THF was cooled to -78 °C and added slowly to a -78 °C THF suspension of KH (0.03 g, 0.75 mmol). The reaction mixture was left to warm to room temperature and was stirred until evolution of H_2 stopped. At this time, the solution was cooled again to -78 °C and was added slowly to a -78 °C solution of **2** (0.26 g, 0.5 mmol) in 20 mL THF, producing an immediate color change from blue to green. After 10 hours, the reaction mixture had finally become orange. Recrystallization from minimum Et_2O/pentane at -40 °C yielded **4** as an orange solid (yield: 0.15 g, 40 %). Repeated recrystallizations could not remove completely unreacted **2**. ^1H NMR (25 °C, C_6D_6): δ 1.19 (s, 9H, C(CH_3)$_3$), 5.70, 5.75, 5.86 (t, 1H each, Tp H's 4-position), 6.98, 7.32 (d, 2H each, phenyl ring H's), 7.2, 7.5, 7.79, 8.35 (d, 1H each, four out six of Tp H's 3,5-positions, the other two are masked by the solvent), 10.15 (broad s, 1H, N-H).

TpW(NHPh-3,5(CF_3)$_2$)(CC(CH_3)$_3$)Cl (5)

Complex **5** was synthesized in a manner analogous to that of **4**. Immediate color change of the reaction mixture from blue to brown was observed which became lighter as the reaction mixture was warmed to room temperature and left to stir for 10 hours. Recrystallization from minimum Et_2O/pentane at -40 °C yielded **5** as an orange crystalline material (yield: 0.2 g, 51 %). Repeated recrystallizations could not successfully remove unreacted **2**. ^1H NMR (25 °C, C_6D_6): δ 1.19 (s, 9H, C(CH_3)$_3$), 5.65, 5.67, 5.9 (t, 1H each, Tp H's 4-position), 7.1, 7.3, 7.56, 7.6, 7.79, 8.2 (d, 2H each, Tp H's 3,5-positions), 7.5 (s 2H, o-phenyl H's, p-H overlaps with solvent), 9.79 (broad s, 1H, N-H).

TpW(NH_2)($CC(CH_3)_3$)Cl (6)

TpW($CC(CH_3)_3$)Cl_2 (2) (0.15 g, 0.3 mmol) was dissolved in 20 mL THF and a THF suspension of $NaNH_2$ (0.035 g, 1.5 mmol, 5 equiv) was added dropwise. No immediate color change was observed. The reaction mixture was warmed to room temperature and stirred overnight. At this point the reaction mixture had turned light green and upon solvent removal, a pale yellow solid was recovered. The solid was recrystallized from minimum Et_2O/pentane at -40 °C giving TpW(NH_2)($CC(CH_3)_3$)Cl (6) as a yellow semicrystalline material (yield 0.11 g, 60%). Repeated recrystallizations could not completely remove unreacted 2. ^1H NMR (25 °C, C_6D_6): δ 1.30 (s, 9H, $C(CH_3)_3$), 5.7, 5.75, 5.80 (t, 1H each, Tp H's 4-position), 7.29,7.7.8, 7.86 [d, 1H each, 3 out 6 of the Tp H's at 3,5-position, (others overlap with solvent)], 8.60, 8.90 (broad s, 1H each, NH_2 protons). ^{13}C NMR (25°C, C_6D_6): δ 31.53 ($C(CH_3)_3$), 49.13 ($C(CH_3)_3$), 106.18, 106.37, 134.42, 134.61, 135.28, 142.02, 144.95, 147.14, 147.80 (Tp C's), 303.53 ($CC(CH_3)_3$.

TpW($NHPh)_2$($CC(CH_3)_3$) (7)

To a cold Et_2O solution of 2 (0.2g, 0.77 mmol) 3.3 equiv of LiNHPh (0.25 g, 2.54 mmol) in Et_2O was slowly added. Upon warming to room temperature, the reaction mixture immediately changed color from blue to bright orange. After stirring for 3 hours, Et_2O was removed under reduced pressure and the orange solid was extracted once with toluene and once with CH_2Cl_2. It was recrystallized from a RT CH_2Cl_2/pentane mixture to afford TpW($NHPh)_2$($CC(CH_3)_3$) (7) as an orange crystalline solid (yield: 0.19 g, 70%). X-ray quality crystals were obtained by slow diffusion of pentane to a saturated CH_2Cl_2 solution of 7 at room temperature. ^1H NMR (25 °C, C_6D_6): δ 1.29 (s, 9H, $C(CH_3)_3$),

5.73 (t, 2H, Tp H's 4-position), 5.82 (t, 1H, Tp H, 4-position), 6.90 (t, 2H, p-Ph), 7.23 (d, 2H, Tp H, 3,5 position), 7.26 (t, 4H, m-Ph), 7.28 (d, 1H, Tp proton, 3,5 position), 7.31 (d, 1H, Tp proton 3,5, position), 7.45 (d, 4H, o-Ph), 7.82 (s, 2H, N-H), 7.99 (d, 2H, Tp H's 3,5 positions). ^{13}C NMR (25 °C, C_6D_6): δ 32.47 ($C(CH_3)_3$), 50.71 ($C(CH_3)_3$), 105.88, 106.68, 120.61, 121.43, 128.76, 134.74, 135.31, 140.72, 144.96, 157.08 (Tp, Ph), 295.37 ($CC(CH_3)_3$).

Tp'W(NHPh)(CC(CH$_3$)$_3$)Cl (8)

$(CH_3)_3Si$-N(H)Ph (0.19 mL, 1.1 mmol) in 10 mL THF was added to a THF solution of (DME)W($CC(CH_3)_3$)Cl_3 (0.5 g, 1.1 mmol) at -78 °C. An immediate color change from purple to green was observed. The reaction mixture slowly became brown-orange as it warmed to room temperature. After 30 minutes, the reaction mixture was cooled to -78 °C and a THF solution of KTp' (0.37 g, 1.1 mmol) was slowly added. The reaction mixture slowly turned bright orange. After stirring for 2 more hours at room temperature, the solvent was removed under reduced pressure. Recrystallization from minimum Et_2O at -40 °C gave bright orange X-ray quality crystals of 8 (yield: 0.5 g, 75%). ^1H NMR (25 °C, C_6D_6): δ 1.38 (s, 9H, $C(CH_3)_3$), 2.00, 2.12, 2.17, 2.28, 2.40, 3.10 (s, 3H each, Tp' CH_3, 3,5-positions), 5.57, 5.59, 6.10 (t, 1H each, Tp' H's, 4-position), 6.90 (t, 1H, p-Ph), 7.20 (t, 2H, m-Ph), 7.30 (d, 2H, o-Ph), 10.62 (broad s, 1H, N-H). ^{13}C NMR (25°C, C_6D_6): δ 12.09, 12.81, 13.47, 18.48, 18.77 (Tp' CH_3's, overlapping), 32.62 ($CC(CH_3)_3$), 49.66 ($CC(CH_3)_3$), 107.31, 107.65, 143.06, 144.78, 145.44, 152.46, 153.18, 153.84, 157.29 (Tp' ring C's), 123.94, 124.55, 128.47 (Ph C's). 310.17 ($CC(CH_3)_3$). Anal. Calcd for $C_{26}H_{37}ClN_7W$: C, 46.82; H, 5.55; N, 14.71. Found: C, 46.51; H, 5.46; N, 14.45.

Addition of H_2O to **3**, **4**, **5**, and **6**

In a typical experiment approximately 0.1 to 2 equivalents of H_2O, either neat or as a THF solution, was added to solutions of **3**, **4**, **5** or **6**.

Addition of a) $NHCl_4$, b) NEt_3HCl, c)HCl to solutions of **3** that did not tautomerize to $TpW(NPh)(CHC(CH_3)_3)Cl$ (**9**)

a) To a C_6D_6 or C_7D_8 solution of **3** (0.050 g , 0.084 mmol) solid NH_4Cl (0.001 g, 0.018 mmol) was added. No color change was observed and no formation of **9** was detected by ^1H NMR even after heating overnight at ~80 °C. Prolonged heating (48 hrs) showed only a trace of **9** present in the solution. Addition of more NH_4Cl did not significantly increase formation of **9**.

b) To a C_6D_6 or C_7D_8 solution of **3** (0.05 g, 0.084 mmol) ground NEt_3HCl (0.0022 g, 0.016 mmol) was added with no observable color change. No immediate formation of **9** was observed, but upon heating overnight slow formation of **9** could be detected by ^1H NMR. The proton transfer however, was not complete even after 2 days at 80 °C.

c) HCl (0.1mL, 0.01 mmol, 0.1M in Et_2O) was added to a sample of **3** (0.06 g, 0.10 mmol) in C_6D_6 or C_7D_8. An immediate color change was observed from orange to olive-yellow. The sample was then dried under vacuum in order to remove the Et_2O and was redissolved in deuterated solvent. The ^1H NMR spectrum showed complete conversion to the imido alkylidene **9**. Higher concentrations of HCl led to a color change from orange to green-blue and the ^1H NMR of the product showed formation of mostly **2** and unreacted **9**. Similar reactant ratios were used in the attempted tautomerizations of **6** and **7**.

1,2-(NH(C_6H_5)(N'H((($C_5H(CH_3)_4$)Si(CH_3)$_2$)C_6H_4 (**10**)

To a -78 °C Et_2O solution of ($C_5(CH_3)_4H$)Si(CH_3)$_3$Cl (1.17 g, 5.44 mmol) one equivalent of N-phenyl-*o*-phenylenediamine (1.03 g, 5.59 mmol) in Et_2O was slowly added. The reaction mixture was warmed to room temperature and stirred for ~ 6 h. At this time the reaction mixture was light pink in color and a pink solid had precipitated. An excess of Et_3N (3 ml, 40.9 mmol) was then added at room temperature, and the reaction mixture changed from pink to pale orange, and was stirred for an additional hour. Upon removal of Et_2O under reduced pressure, a sticky pale orange solid was obtained. Extraction of the solids with 4 portions of cold pentane followed by removal of solvent gave **10** as a pale orange thick oil (yield: 1.6 g, 82%). ^{1}H NMR (25 °C, C_6D_6): δ 0.14 (s, 6H, Si(CH_3)$_2$), 1.72, 1.87 (s, 6H each, $C_5(CH_3)_4$H), 2.91 (s, 1H, $C_5(CH_3)_4$*H*), 4.10, 4.38 (broad s, 1H each, N-*H*), 6.49-7.09 (phenyl region, 9H). ^{13}C NMR (25 °C, C_6D_6): δ 11.25 14.38 (C_5(*C*H$_3$)$_4$)H), 54.88 (*C*H$C_4(CH_3)_4$), 115.09, 115.98, 118.31, 119.30 (CH*C*$_4(CH_3)_4$), 126.98, 127.47, 129.38, 130.04, 132.45, 136.48, 144.84, 146.80 (aromatic C's).

Alternate synthesis of o-C_6H_4{NH(C_6H_5)N'H[Si(CH_3)$_2$($C_5(CH_3)_4$H)]} (**10**)

To a -78 °C Et_2O solution of N-phenyl-o-phenylenediamine (0.5 g, 2.71 mmol) 1 equivalent of n-BuLi (1.2 ml, 2.72 mmol, 2.5M in hexanes) was slowly added. The reaction mixture was warmed to room temperature and stirred for 3.5 h. The solvent was removed in *vacuo*, and the remaining solid was washed 3 times with hexanes. The solid was then redissolved in Et_2O and cooled in an ice-bath. To this solution, an Et_2O solution of ($C_5(CH_3)_4$H)Si(CH_3)$_3$Cl (0.58 g, 2.72 mmol) was slowly added. After 3 hrs, some solid had precipitated from the reaction mixture. Removal of Et_2O and extraction of the solid with pentane gave a pale orange solution. A thick oil was isolated upon removal of

pentane. A ^{1}H NMR of the oil showed formation of **10** but also a significant amount of $(C_5(CH_3)_4H)Si(CH_3)_3Cl$ still present that could not be successfully removed due to its similar solubility with the product **10**.

o-C_6H_4{N(C_6H_5)N'[Si(CH_3)$_2$($C_5(CH_3)_4$)]}Zr(N(CH_3)$_2$)(NH(CH_3)$_2$) (**12**)

To a stirring room temperature hexanes solution of $Zr(N(CH_3)_2)_4$ (**11**) (0.126 g, 0.47 mmol) a solution of **10** (0.18 g, 0.48 mmol) in hexanes was added dropwise. The solution immediately became light orange and when approximately half of the ligand had been added, compound **12** began precipitating as a yellow solid. After addition of **10** was completed the reaction mixture was left to stir for an additional 6 hrs. The precipitate was left to settle, the supernatant was removed, and the remaining solid was washed with pentane until the solution was clear. Compound **12** was recrystallized from a toluene/ pentane mixture. The ^{1}H NMR of the first crop isolated from the toluene/pentane mixture contained c.a. 60 % of **12** with the remaining 40 % being complex **13** (overall yield of **12**: 0.07 g, 25%). Repeated recrystallizations helped remove most of **13**. Similar results were observed when the reaction was run in Et_2O. X-ray quality crystals precipitated from a C_6D_6 room temperature solution of **12**. ^{1}H NMR (25 °C, C_6D_6): δ 0.79, 0.86 (s, 6H each, Si(CH_3)$_2$), 1.61, 1.77, 2.07, 2.14 (s, 3H each, C5(CH_3)$_4$), 1.61 (6H, N(CH_3)$_2$H), 2.71 (s, 6H, -N(CH_3)$_2$), 6.88-7.21 (multiplets, 9H, aromatic H). The N(CH_3)$_2H$ is hidden in the baseline.

o-C_6H_4{N(C_6H_5)N'[Si(CH_3)$_2$($C_5(CH_3)_4$)]}Zr(Cl)(NH(CH_3)$_2$)$_2$ (**13**)

To a room temperature hexanes solution of **10** (0.14 g, 0.39 mmol, 2.1 eq), a hexanes solution of $Zr(N(CH_3)_2)_4$ (0.05 g, 0.18 mmol) was added dropwise. An

immediate color change to orange and precipitation of a yellow-orange solid was observed. The reaction mixture was stirred for an additional 15 min and was left to settle. The supernatant was removed and the solid was washed twice with pentane to remove the excess ligand (yield: 0.03 g, 28%). X-ray quality crystals were obtained within 4 days from a room temperature C_7D_8 solution of **13**. The presence of chloride is most likely due to presence of small amounts of **10**·HCl adduct that cannot be successfully removed even after addition of excess NEt_3 or repeated extractions of **10** with pentane. ^1H NMR (25 °C, C_6D_6): δ 0.70 (s, 6H, -Si(CH_3)$_2$), 1.88, 1.93 (s, 6H each, $C_5(CH_3)_4$)H), 2.00 (broad s, 12H, NH(CH_3)$_2$), (very broad s, 2H, NH(CH_3)$_2$), 6.57-7.41 (multiplets, 9H, aromatic protons). ^{13}C NMR (25 °C, C_6D_6): δ 3.46 (-Si(CH_3)$_2$), 12.21, 14.05 ($C_5(CH_3)_4$)H), 40.40 (NH(CH_3)$_2$), 112.58, 115.12, 115.92, 121.10, 123.62, 126.24, 127.31, 129.51, 143.51, 155.09 ($C_5(CH_3)_4$)H and aromatic C's).

Ta[N(CH_3)$_2$]$_3$[SO_2(NC(CH_3)$_3$)$_2$] (**17**)

A toluene solution of SO_2[NH(C(CH_3)$_3$)]$_2$ (0.155 g, 0.75 mmol) was added dropwise to a room temperature toluene solution of Ta(N(CH_3)$_2$)$_5$ (0.30 g, 0.75 mmol). No color change was observed. The reaction mixture was left to stir for 12 hrs. Periodic vacuum was applied to remove the (CH_3)$_2$NH produced from the reaction. The solvent was removed under reduced pressure, yielding **17** as a pale beige solid which was washed twice with pentane (yield: 0.4 g, 95%). X-ray quality pale yellow crystals were obtained from a saturated toluene solution of **17** by slow diffusion of pentane at -30 °C for 5 days. ^1H NMR (25 °C, C_6D_6): δ 1.51 (s, 18H, SO_2(NC(CH_3)$_3$)$_2$), 3.09 (broad S, 18H, N(CH_3)$_2$). ^{13}C NMR (25 °C, C_6D_6): δ 32.83 (SO_2(NC(CH_3)$_3$)$_2$), 45.16 (N(CH_3)$_2$).

Ta[N(CH$_3$)$_2$]$_3$[SO$_2$[N[CH(CH$_3$)(C$_6$H$_5$)]]$_2$] (**18**)

Compound **18** was synthesized with the same procedure that was followed for the preparation of **17**. Compound **18** was isolated as a light yellow solid (yield: 0.4 g, 94%). ^{1}H NMR (25 °C, C_6D_6): δ 1.76 (d, 6H, SO$_2$[N[CH(C*H*$_3$)(C$_6$H$_5$)]]$_2$), 2.75 (s, 18H, N(C*H*$_3$)$_2$), 5.56 (q, 2H, SO$_2$[N[C*H*(CH$_3$)(C$_6$H$_5$)]]$_2$), 7.01 (t, 2H, p-C$_6$H$_5$), 7.09 (t, 4H, m-C$_6$H$_5$), 7.27 (d, 4H, o-C$_6$H$_5$). ^{13}C NMR (25 °C, C_6D_6): δ 24.43 (SO$_2$[N[CH(*C*H$_3$)(C$_6$H$_5$)]]$_2$), 43.92 (SO$_2$[N[*C*H(CH$_3$)(C$_6$H$_5$)]]$_2$), 55.85 (N(*C*H$_3$)$_2$), 126.60, 128.13, 146.50 (aromatic C's).

Ta[N(CH$_3$)$_2$]$_3$[SO$_2$(NC(CH$_3$)$_3$)$_2$][Al(CH$_3$)$_3$]$_2$ (**19**)

A solution of Al(CH$_3$)$_3$ (0.22 ml, 2.30 mmol) in hexanes was added dropwise to a 0 °C toluene solution of **17** (0.2 g, 0.38 mmol) over a period of 15 minutes. No immediate color change was observed. The reaction mixture was stirred at room temperature for 3 hrs and slowly changed to a dark yellow-brown color. The solvent was removed under reduced pressure and the remaining solid was washed with two aliquots of pentane. Removal of pentane gave **19** as a dark beige powder (yield: 0.23, 94%). ^{1}H NMR (25 °C, C_6D_6): δ -0.10 (s, 18H, Al(C*H*$_3$)$_3$), 1.34 (s, 18H, SO$_2$(NC(C*H*$_3$)$_3$)$_2$), 2.94 (s, 18H, N(C*H*$_3$)$_2$). ^{13}C NMR (25 °C, C_7D_8): δ -5.23 (Al(*C*H$_3$)$_3$), 32.34 (SO$_2$(NC(*C*H$_3$)$_3$)$_2$), 45.06 (N(*C*H$_3$)$_2$), 59.86 (SO$_2$(N*C*(CH$_3$)$_3$)$_2$).

No change in the outcome of the reaction was observed even when 10 equivalents of Al(CH$_3$)$_3$ are used. Compound **19** is thermally unstable in solution and decomposes to a black insoluble oil over time.

$Ta[N(CH_3)_2]_3[SO_2(NC(CH_3)_3)_2][Al(CH_2CH_3)_3]_2$ (**20**)

The same procedure was used as in the synthesis of **19**. The reaction mixture changed color from pale yellow to light orange over time. Removal of toluene under reduced pressure and repeated washes with pentane, yielded **20** as a beige waxy solid (yield: 0.26 g, 92%). ^1H NMR (25 °C, C_6D_6): δ 0.50 (q, 12H, $Al(CH_2CH_3)_3$), 1.29 (s, 18H, $SO_2(NC(CH_3)_3)_2$), 1.65 (t, 18H, $Al(CH_2CH_3)_3$), 2.98 (s, 18H, $N(CH_3)_2$). ^{13}C NMR (25 °C, C_6D_6): δ 2.48 ($Al(CH_2CH_3)_3$), 10.75 ($Al(CH_2CH_3)_3$), 32.15 ($SO_2(NC(CH_3)_3)_2$), 44.84 ($N(CH_3)_2$). Compound **20** is thermally unstable in solution and decomposes to a black insoluble oil over time.

Crystallographic Studies

X-ray data collection and structure refinement for compounds 7 and 8

Compound **7**: Data were collected at 173 K on a Siemens CCD SMART PLATFORM equipped with a CCD area detector and a graphite monochromator utilizing MoK_α radiation (λ = 0.71073 Å). Cell parameters were refined using the entire data set. A hemisphere of data (1381 frames) was collected using the ω-scan method (0.3° frame width). The first 50 frames were remeasured at the end of data collection to monitor instrument and crystal stability (maximum correction on I was < 1 %). Ψ-scan absorption corrections were applied based on the entire data set. Compound **8**: Data were collected at room temperature on a Siemens P3m/V diffractometer equipped with a graphite monochromator utilizing MoK_α radiation (λ = 0.71073 Å). 32 reflections with $20.0° \leq 2q \leq 22.0°$ were used to refine the cell parameters. The w-scan method was used for data collection. Four

reflections were measured every 96 reflections to monitor instrument and crystal stability (maximum correction on I was < 1%).

Both structures were solved by the Direct Method in *SHELXTL5*,[89] and refined using full-matrix least squares on F^2. The non-H atoms were refined with anisotropic thermal parameters. The H atoms of **8** were all refined in a riding mode on their parent atoms except that bonded to Boron which was refined without constraint. The structure also contains a disordered half ether molecule. It was refined with isotropic thermal parameters in three parts with site occupation factors of 0.25, 0.15 and 0.10, respectively. Compound **7** had all H riding on their parent atoms except the one on Boron. For compound **8**, 411 parameters were refined in the final cycle of refinement using 4274 reflections with $I > 2\sigma(I)$ to yield R_1 and wR_2 of 5.53 and 11.16, respectively. For compound **7**, 179 parameters were refined in the final cycle of refinement using 2978 reflections with $I > 2\sigma(I)$ to yield R_1 and wR_2 of 3.04 and 7.56, respectively. Refinement was done using F^2. The final atomic coordinates for the non-hydrogen atoms of **7** and **8** are given in **Tables A1.1-A2.5** of Appendix A.

X-ray data collection and structure refinement for compounds **12** and **13**

Data for both compounds were collected at 173 K on a Siemens CCD SMART PLATFORM equipped with a CCD area detector and a graphite monochromator utilizing MoK_α radiation ($\lambda = 0.71073$ Å). Cell parameters were refined using 8192 reflections from each data set. A hemisphere of data (1381 frames) was collected using the ω-scan method (0.3° frame width). The first 50 frames were remeasured at the end of data collection to monitor instrument and crystal stability (maximum correction on I was < 1 %). Absorption corrections were applied based on the ψ scan using the entire data sets.

Both structures were solved by the Direct Methods in *SHELXTL*,[89] and were refined using full-matrix least squares on F^2. The non-H atoms were refined with anisotropic thermal parameters. All of the H atoms were refined without any constraints. Compound **15** also has disordered benzene molecules located on centers of inversion. They were refined as two dependent parts and their site occupation factors refined to 0.56(3) and 0.44(3) respectively. The benzene H atoms were included in the final cycle of refinement in a riding mode on their parent atoms. For compound **12**, 514 parameters were refined in the final cycle of refinement using 6040 reflections with $I > 2\sigma(I)$ to yield R_1 and wR_2 of 2.38 and 5.92, respectively. For compound **13**, 472 parameters were refined in the final cycle of refinement using 5484 reflections with $I > 2\sigma(I)$ to yield R_1 and wR_2 of 2.37 and 5.79, respectively. Refinement was done using F^2. The final atomic coordinates for compounds **12** and **13** are presented in **Tables A3.1-A4.5** of Appendix A.

X-ray data collection and structure refinement for compound (**17**)

Data were collected at 173 K on a Siemens SMART PLATFORM equipped with a CCD area detector and a graphite monochromator utilizing MoK_α radiation ($\lambda = 0.71073$ Å). Cell parameters were refined using up to 6753 reflections. A hemisphere of data (1381 frames) was collected using the w-scan method (0.3° frame width). The first 50 frames were remeasured at the end of data collection to monitor instrument and crystal stability (maximum correction on I was < 1 %). Ψ scan absorption corrections were applied based on the entire data set.

The structure was solved by the Direct Methods in *SHELXTL5*,[89] and refined using full-matrix least squares. The non-H atoms were treated anisotropically, whereas the hydrogen atoms were calculated in ideal positions and were riding on their respective

carbon atoms. 209 parameters were refined in the final cycle of refinement using 4356 reflections with $I > 2\sigma(I)$ to yield R_1 3.04% and wR_2 of 7.70% , respectively. Refinement was done using F^2. The final atomic coordinates for compound **17** are presented in **Tables A5.1-A5.5** of Appendix A.

APPENDIX A
TABLES OF CRYSTALLOGRAPHIC DATA

Crystallographic Data for $TpW(NHPh)_2(CC(CH_3)_3)$ (7)

Table A1.1: Crystallographic Data

A. Crystal Parameters	**7**
Empirical Formula	$C_{26}H_{31}BN_8W$
Formula wt	650.25
Cryst syst	Monoclinic
Space group	P2(1)/m
a, Å	7.6125(2)
b, Å	16.3776(4)
c, Å	10.5398(2)
β, deg	98.705(1)
V, Å^3	1298.91(5)
Z	2
Crystal size (mm^3)	0.24 x 0.16 x 0.14
d_{calc}, g cm^{-3}	1.663
Temp, K	173(2)
F(000), electrons	644
B. Data collection	
Radiation, λ, (Å)	Mo-K_α, 071073
Mode	ω-scan
Scan width & rate	0.3 deg/frame & 30 sec. /frame
2θ range, deg	1.95 - 27.50
Range of *hkl*	$-6 \le h \le 10$ $-18 \le k \le 22$ $-14 \le l \le 14$
tot. reflcns measd	9523
unique reflcns	3087
abs coeff, μ(Mo Kα), mm^{-1}	4.478
min, max transm	0.411, 0.543
C. Structure Refinement	
Refinement method	Full-matrix leat-squares on F^2
S, Goodness-of-fit	1.111
No. of variables	179
R_1/Reflections	****
ωR_2/Reflections	****
Rint (%)	3.38
Max. shift/esd	0.001
min. peak in diff. four. map (e Å^{-3})	-2.44
max. peak in diff. four. map (e Å^{-3})	1.387

$R_1 = \sum(||F_o| - |F_c||) / \sum|F_o|$

$wR_2 = [\sum[w(F_o^2 - F_c^2)^2] / \sum[w(F_o^2)^2]]^{1/2}$

$S = [\sum[w(F_o^2 - F_c^2)^2] / (n-p)]^{1/2}$

$w = 1/[s^2(F_o^2)+(0.0370*p)^2+0.31*p]$, $p = [\max(F_o^2,0)+ 2* F_c^2]/3$

Table A1.2. Atomic coordinates (x 10^4) and equivalent isotropic displacement parameters (A^2 x 10^3) for 7. U(eq) is defined as one third of the trace of the orthogonalized Uij tensor.

Atom	x	y	z	U(eq)
W2	402(1)	7500	4860(1)	24(1)
N1	3872(4)	6530(2)	4428(3)	25(1)
N2	4350(6)	7500	6823(4)	26(1)
N2'	3733(6)	7500	7970(4)	28(1)
N3	922(4)	6657(2)	5995(3)	27(1)
N3'	880(4)	6743(2)	7281(3)	27(1)
B1	715(8)	7500	8004(6)	28(1)
C1	672(7)	7500	3507(5)	27(1)
C2	-1072(7)	7500	2604(5)	27(1)
C3	-2560(7)	7500	3459(7)	44(2)
C4	-1302(6)	6731(3)	1766(5)	45(1)
C5	4079(5)	6038(3)	3430(4)	30(1)
C6	3110(6)	6152(3)	2208(4)	37(1)
C7	3181(6)	5589(4)	1218(4)	45(1)
C8	4280(7)	4899(3)	1441(5)	46(1)
C9	5369(6)	4802(3)	2586(5)	43(1)
C10	5279(6)	5374(3)	3587(4)	38(1)
C11	6133(7)	7500	7100(6)	31(1)
C12	6661(7)	7500	8424(6)	39(2)
C13	5090(7)	7500	8943(6)	34(1)
C14	-13(4)	5988(2)	5624(3)	33(1)
C15	-663(4)	5630(2)	6638(3)	38(1)
C16	-71(5)	6128(3)	7670(4)	34(1)

Table A1.3. Bond lengths (Å) and angles [°] for **7**.

W-C1	1.789(5)
W-N1	2.034(3)
W-N(1)#1	2.034(3)
W-N(3)#1	2.239(3)
W-N3	2.239(3)
W-N2	2.356(4)
N1-C5	1.353(5)
N1-H1A	0.86
N2-C11	1.344(7)
N2-N2'	1.361(6)
N2'-C13	1.342(7)
N2'-B	1.542(7)
N3-C14	1.332(5)
N3-N3'	1.368(4)
N3'-C16	1.341(5)
N3'-B	1.541(5)
B-N(3')#1	1.541(5)
B-H	1.12(7)
C1-C2	1.512(7)
C2-C(4)#1	1.533(6)
C2-C4	1.533(6)
C2-C3	1.551(8)
C3-H3A	0.88
C3-H3B	0.93
C4-H4A	0.96
C4-H4B	0.96
C4-H4C	0.96
C5-C6	1.396(6)
C5-C10	1.414(6)
C6-C7	1.400(7)
C6-H6A	0.93
C7-C8	1.404(7)
C7-H7A	0.93
C8-C9	1.366(7)
C8-H8A	0.93
C9-C10	1.420(7)
C9-H9A	0.93
C10-H10A	0.93
C11-C12	1.393(8)
C11-H11A	0.93
C12-C13	1.388(8)
C12-H12A	0.93
C13-H13A	0.93
C14-C15	1.38
C14-H14A	0.93
C15-C16	1.380(6)
C15-H15A	0.93
C16-H16A	0.93
C1-W-N1	100.66(14)
C1-W-N(1)#1	100.66(14)
N1-W-N(1)#1	102.7(2)

C1-W-N(3)#1	93.2(2)
N1-W-N(3)#1	159.96(12)
N(1)#1-W-N(3)#1	88.65(13)
C1-W-N3	93.2(2)
N1-W-N3	88.65(13)
N(1)#1-W-N3	159.96(12)
N(3)#1-W-N3	76.1(2)
C1-W-N2	171.8(2)
N1-W-N2	84.39(11)
N(1)#1-W-N2	84.39(11)
N(3)#1-W-N2	80.31(11)
N3-W-N2	80.31(11)
C5-N1-W	140.5(3)
C5-N1-H1A	109.7(2)
W-N1-H1A	109.74(8)
C11-N2-N2'	106.3(4)
C11-N2-W	132.1(4)
N2'-N2-W	121.6(3)
C13-N2'-N2	110.5(4)
C13-N2'-B	129.5(5)
N2-N2'-B	120.0(4)
C14-N3-N3'	106.5(3)
C14-N3-W	129.8(2)
N3'-N3-W	123.7(3)
C16-N3'-N3	108.7(3)
C16-N3'-B	130.9(4)
N3-N3'-B	120.2(4)
N(3')#1-B-N3'	107.1(4)
N(3')#1-B-N2'	109.0(3)
N3'-B-N2'	109.0(3)
N(3')#1-B-H	112(2)
N3'-B-H	112(2)
N2'-B-H	108(4)
C2-C1-W	166.5(4)
C1-C2-C(4)#1	112.0(3)
C1-C2-C4	112.0(3)
C(4)#1-C2-C4	110.6(5)
C1-C2-C3	106.4(5)
C(4)#1-C2-C3	107.8(3)
C4-C2-C3	107.8(3)
C2-C3-H3A	104.9(3)
C2-C3-H3B	108.8(2)
H3A-C3-H3B	120.3
C2-C4-H4A	109.5(2)
C2-C4-H4B	109.5(3)
H4A-C4-H4B	109.5
C2-C4-H4C	109.5(3)
H4A-C4-H4C	109.5
H4B-C4-H4C	109.5
N1-C5-C6	122.0(4)
N1-C5-C10	121.1(4)
C6-C5-C10	116.9(4)
C5-C6-C7	121.6(4)
C5-C6-H6A	119.2(3)

C7-C6-H6A	119.2(3)
C6-C7-C8	119.7(4)
C6-C7-H7A	120.2(3)
C8-C7-H7A	120.2(3)
C9-C8-C7	120.5(5)
C9-C8-H8A	119.7(3)
C7-C8-H8A	119.7(3)
C8-C9-C10	119.2(4)
C8-C9-H9A	120.4(3)
C10-C9-H9A	120.4(3)
C5-C10-C9	121.5(4)
C5-C10-H10A	119.2(3)
C9-C10-H10A	119.2(3)
N2-C11-C12	110.3(5)
N2-C11-H11A	124.9(3)
C12-C11-H11A	124.9(3)
C13-C12-C11	105.1(5)
C13-C12-H12A	127.5(3)
C11-C12-H12A	127.5(3)
N2'-C13-C12	108.0(5)
N2'-C13-H13A	126.0(3)
C12-C13-H13A	126.0(3)
N3-C14-C15	111.2(2)
N3-C14-H14A	124.4(2)
C15-C14-H14A	124.4
C14-C15-C16	104.3(2)
C14-C15-H15A	127.8
C16-C15-H15A	127.8(2)
N3'-C16-C15	109.2(3)
N3'-C16-H16A	125.4(2)
C15-C16-H(6A	125.4(2)

Symmetry transformations used to generate equivalent atoms: #1 x,-y+3/2, z

Table A1.4. Anisotropic displacement parameters ($A^2 \times 10^3$) for **7**. The anisotropic displacement factor exponent takes the form: $-2\pi^2 [h^2 a^{*2} U11 + ... + 2 h k a^* b^* U12]$

Atom	U11	U22	U33	U23	U13	U12
W	15(1)	37(1)	19(1)	0	-2(1)	0
N1	18(1)	41(2)	17(1)	8(1)	7(1)	15(1)
N2	15(2)	44(3)	18(2)	0	-2(2)	0
N2'	15(2)	47(3)	20(2)	0	1(2)	0
N3	21(1)	39(2)	21(1)	1(1)	1(1)	0(1)
N3'	15(1)	44(2)	22(2)	3(1)	3(1)	0(1)
B	14(2)	47(4)	24(3)	0	2(2)	0
C1	24(2)	37(3)	21(2)	0	5(2)	0
C2	16(2)	39(3)	25(2)	0	2(2)	0
C3	15(2)	69(5)	47(4)	0	6(2)	0
C4	31(2)	57(3)	41(2)	-12(2)	-9(2)	8(2)
C5	19(2)	42(2)	30(2)	1(2)	6(1)	-1(2)
C6	31(2)	51(3)	29(2)	2(2)	6(2)	8(2)
C7	43(2)	65(3)	30(2)	1(2)	13(2)	15(2)
C8	54(3)	50(3)	38(2)	-6(2)	20(2)	1(2)
C9	42(2)	43(3)	44(3)	10(2)	7(2)	10(2)
C10	32(2)	45(3)	38(2)	7(2)	5(2)	6(2)
C11	16(2)	51(4)	27(3)	0	2(2)	0
C12	16(2)	71(5)	27(3)	0	-6(2)	0
C13	22(3)	54(4)	23(3)	0	-4(2)	0
C14	25(2)	41(2)	32(2)	1(2)	-2(2)	-6(2)
C15	27(2)	44(3)	40(2)	6(2)	3(2)	-7(2)
C16	22(2)	51(3)	31(2)	6(2)	5(2)	-1(2)

Table A1.5. Hydrogen coordinates (x 10^4) and isotropic displacement parameters (A^2 x 10^3) for **7**.

	x	y	z	U(eq)
H1A	4597(4)	6386(2)	5097(3)	30
H	1512(90)	7500	9040(67)	37(19)
H3A	-3557(7)	7500	2917(7)	65
H3B	-2326(7)	7087	4072(7)	65
H4A	-2421(6)	6754(3)	1209(5)	67
H4B	-1273(6)	6257(3)	2305(5)	67
H4C	-355(6)	6700(3)	1261(5)	67
H6A	2401(6)	6614(3)	2047(4)	44
H7A	2504(6)	5671(4)	417(4)	54
H8A	4267(6)	4505(3)	804(5)	55
H9A	6160(6)	4366(3)	2709(5)	51
H10A	6027(6)	5310(3)	4364(4)	46
H11A	6903(7)	7500	6494(6)	38
H12A	7816(7)	7500	8865(6)	47
H13A	4996(7)	7500	9813(6)	41
H14A	-202(4)	5790(2)	4788(3)	40
H15A	-1346(4)	5159(2)	6630(3)	45
H16A	-297(5)	6049(3)	8504(4)	41

Crystallographic Data for Tp'W(NHPh)(CC(CH$_3$)$_3$)Cl **8**

Table A2.1. Crystallographic Data

A. Crystal Parameters	**8**
Empirical Formula	$C_{26}H_{37}N_7W.1/2[C_4H_{10}O]$
Formula wt	714.80
Cryst syst	Monoclinic
Space group	P2(1)/c
a, Å	11.731(2)
b, Å	17.315(3)
c, Å	17.754(4)
b, deg	108.56(2)
V, Å^3	3418.7(11)
Z	4
Crystal size (mm^3)	0.24 x 0.25 x 0.20
d_{calc}, g cm^{-3}	1.389
Temp, K	293(2)
F(000), electrons	1436
B. Data collection	
Radiation, λ, (Å)	Mo-K$_\alpha$, 071073
Mode	ω-scan
Scan width & rate	0.3 deg/frame & 30 sec. /frame
2θ range, deg	1.69 - 25.00
Range of *hkl*	$0 \le h \le 13$ $0 \le k \le 20$ $-21 \le l \le 20$
tot. reflcns measd	6215
unique reflcns	5911
abs coeff, μ(Mo Kα), mm^{-1}	3.485
min, max transm	0.410 - 0.550
C. Structure Refinement	
Refinement method	Full-matrix least-squares on F^2
S, Goodness-of-fit	1.152
No. of variables	411
R_1/Reflections	***
ωR_2/Reflections	***
Rint (%)	4.19
Max. shift/esd	0.001
min. peak in diff. Four. map (e Å^{-3})	-0.77
max. peak in diff. Four. map (e Å^{-3})	0.97

$R_1 = \hat{A}(|F_o| - |F_c|) / \hat{A}|F_o|$

$wR_2 = [\hat{A}[w(F_o^2 - F_c^2)^2] / \hat{A}[w(F_o^2)^2]]^{1/2}$

$S = [\hat{A}[w(F_o^2 - F_c^2)^2] / (n-p)]^{1/2}$

$w = 1/[s^2(F_o^2)+(0.0370*p)^2+0.31*p]$, $p = [\max(F_o^2,0)+ 2* F_c^2]/3$

Table A2.2. Atomic coordinates (x 10^4) and equivalent isotropic displacement parameters (A^2 x 10^3) for **8**. U(eq) is defined as one third of the trace of the orthogonalized Uij tensor.

Atom	x	y	z	U(eq)
W	1814(1)	1443(1)	3298(1)	43(1)
Cl	379(2)	1518(2)	1988(2)	67(1)
N1	1042(6)	2172(4)	3812(4)	46(2)
N2	384(7)	597(4)	3575(4)	49(2)
N3	453(7)	345(5)	2921(4)	51(2)
N4	2946(6)	1021(4)	4441(4)	42(2)
N5	786(7)	-90(4)	3936(5)	51(2)
N6	2389(7)	-339(5)	3303(4)	50(2)
N7	2944(6)	256(4)	4652(4)	43(2)
B	2109(10)	-332(7)	4101(7)	52(3)
C1	2808(9)	2114(5)	3080(5)	52(2)
C2	3582(10)	2682(7)	2816(7)	66(3)
C3	3757(13)	3419(7)	3295(9)	98(4)
C4	2905(13)	2891(8)	1939(7)	103(5)
C5	4810(11)	2340(8)	2888(9)	102(5)
C6	880(8)	2974(5)	3858(6)	46(2)
C7	731(10)	3419(6)	3195(7)	61(3)
C8	509(11)	4209(7)	3215(9)	75(3)
C9	446(12)	4537(7)	3887(9)	79(4)
C10	591(13)	4096(8)	4548(9)	84(4)
C11	827(11)	3312(6)	4537(7)	67(3)
C12	-800(9)	625(6)	3464(6)	53(2)
C13	-1572(9)	1303(6)	3087(8)	76(3)
C14	-1151(10)	-34(6)	3757(6)	55(3)
C15	-150(9)	-486(6)	4055(5)	53(2)
C16	-5(10)	-1252(6)	4442(7)	69(3)
C17	2747(9)	127(7)	2272(6)	63(3)
C18	2881(12)	715(9)	1679(7)	94(4)
C19	2881(13)	-654(9)	2272(9)	75(5)
C20	2648(9)	-932(6)	2911(7)	58(3)
C21	2594(11)	-1760(6)	3145(8)	82(4)
C22	3747(8)	1371(6)	5063(5)	49(2)
C23	3988(10)	2224(6)	5062(7)	71(3)
C24	4255(9)	852(6)	5654(6)	53(2)
C25	3739(8)	148(5)	5386(5)	45(2)
C26	3999(10)	-613(6)	5786(6)	70(3)
O	6737(15)	3648(12)	5454(13)	91(6)
C27	7820(34)	2977(19)	4746(25)	67(10)
C28	7473(36)	3605(20)	5003(24)	74(9)
C29	6512(38)	4306(19)	5793(29)	100(11)
C30	5807(40)	4372(29)	6221(29)	96(12)
C27"	7732(59)	2795(33)	4837(41)	64(12)
C28"	7235(72)	3451(27)	4891(36)	75(11)
C29"	6444(50)	4380(16)	5589(41)	93(12)
C30"	5716(24)	4577(16)	5971(19)	92(14)
O'	6944(24)	3842(16)	5093(19)	93(19)

C27'	7681(24)	2809(16)	4515(19)	41(15)
C28'	7814(31)	3355(31)	5034(33)	57(19)
C29'	6792(55)	4054(53)	5787(26)	113(37)
C30'	5784(67)	4248(71)	5887(50)	110(34)

Table A2.3. Bond lengths [Å] and angles [°] for **8**.

W-C1	1.773(10)
W-N1	1.943(7)
W-N4	2.169(7)
W-N3	2.223(8)
W-N2	2.393(8)
W-Cl	2.401(3)
N1-C6	1.407(11)
N1-H1A	0.86
N2-C12	1.341(11)
N2-N5	1.362(10)
N3-C17	1.358(12)
N3-N6	1.380(10)
N4-C22	1.344(11)
N4-N7	1.377(9)
N5-C15	1.368(11)
N5-B	1.543(13)
N6-C20	1.329(12)
N6-B	1.552(13)
N7-C25	1.353(11)
N7-B	1.531(13)
B-H	1.11(8)
C1-C2	1.512(13)
C2-C3	1.51(2)
C2-C5	1.52(2)
C2-C4	1.55(2)
C3-H3A	0.96
C3-H3B	0.96
C3-H3C	0.96
C4-H4A	0.96
C4-H4B	0.96
C4-H4C	0.96
C5-H5A	0.96
C5-H5B	0.96
C5-H5C	0.96
C6-C11	1.359(14)
C6-C7	1.370(13)
C7-C8	1.40(2)
C7-H7A	0.82(10)
C8-C9	1.34(2)
C8-H8A	0.88(10)
C9-C10	1.36(2)
C9-H9A	0.84(11)
C10-C11	1.39(2)
C10-H10A	0.82(10)
C11-H11A	1.02(9)
C12-C14	1.370(13)
C12-C13	1.503(13)
C13-H13A	0.96
C13-H13B	0.96
C13-H13C	0.96
C14-C15	1.370(14)

C14-H14A	0.94(10)
C15-C16	1.478(13)
C16-H16A	0.96
C16-H16B	0.96
C16-H16C	0.96
C17-C19	1.36(2)
C17-C18	1.51(2)
C18-H18A	0.96
C18-H18B	0.96
C18-H18C	0.96
C19-C20	1.34(2)
C19-H19A	0.57(10)
C20-C21	1.50(2)
C21-H21A	0.96
C21-H21B	0.96
C21-H21C	0.96
C22-C24	1.367(13)
C22-C23	1.504(13)
C23-H23A	0.96
C23-H23B	0.96
C23-H23C	0.96
C24-C25	1.376(13)
C24-H24A	1.05(9)
C25-C26	1.482(13)
C26-H26A	0.96
C26-H26B	0.96
C26-H26C	0.96
O-C28	1.35(2)
O-C29	1.35(2)
O-C28"	1.35(2)
O-C29"	1.35(2)
C27-C28	1.29(2)
C27-H27D	0.96
C27-H27E	0.96
C27-H27F	0.96
C28-H28C	0.97
C28-H28D	0.97
C29-C30	1.29(2)
C29-H29C	0.97
C29-H29D	0.97
C30-H30D	0.96
C30-H30E	0.96
C30-H30F	0.96
C27"-C28"	1.29(2)
C27"-H27G	0.96
C27"-H27H	0.96
C27"-H27I	0.96
C29"-C30"	1.29(2)
C29"-H29E	0.96
C29"-H29F	0.96
O'-C28'	1.35(2)
O'-C29'	1.35(2)
C27'-C28'	1.29(2)
C27'-H27A	0.96

C27'-H27B	0.96
C27'-H27C	0.96
C28'-H28A	0.97
C28'-H28B	0.97
C29'-C30'	1.29(2)
C29'-H29A	0.97
C29'-H29B	0.97
C30'-H30A	0.96
C30'-H30B	0.96
C30'-H30C	0.96
C1-W-N1	96.5(4)
C1-W-N4	100.1(3)
N1-W-N4	91.0(3)
C1-W-N3	100.7(4)
N1-W-N3	161.7(3)
N4-W-N3	80.2(3)
C1-W-N2	176.6(3)
N1-W-N2	80.7(3)
N4-W-N2	82.1(3)
N3-W-N2	82.2(3)
C1-W-Cl	93.5(3)
N1-W-Cl	97.6(2)
N4-W-Cl	163.1(2)
N3-W-Cl	87.4(2)
N2-W-Cl	84.9(2)
C6-N1-W	139.5(6)
C6-N1-H1A	110.3(5)
W-N1-H1A	110.3(2)
C12-N2-N5	106.8(8)
C12-N2-W	135.1(7)
N5-N2-W	118.1(6)
C17-N3-N6	104.3(8)
C17-N3-W	134.0(7)
N6-N3-W	120.6(5)
C22-N4-N7	105.8(7)
C22-N4-W	132.6(6)
N7-N4-W	121.6(5)
N2-N5-C15	109.6(8)
N2-N5-B	120.2(8)
C15-N5-B	130.1(8)
C20-N6-N3	110.4(8)
C20-N6-B	129.3(9)
N3-N6-B	120.2(7)
C25-N7-N4	109.5(7)
C25-N7-B	128.9(8)
N4-N7-B	121.6(7)
N7-B-N5	109.9(8)
N7-B-N6	108.1(8)
N5-B-N6	108.8(8)
N7-B-H	105(4)
N5-B-H	117(4)
N6-B-H	108(4)
C2-C1-W	174.7(8)
C3-C2-C1	111.3(9)

C3-C2-C5	109.0(11)
C1-C2-C5	111.5(9)
C3-C2-C4	107.7(10)
C1-C2-C4	107.3(9)
C5-C2-C4	110.1(10)
C2-C3-H3A	109.5(6)
C2-C3-H3B	109.5(7)
H3A-C3-H3B	109.5
C2-C3-H3C	109.5(7)
H3A-C3-H3C	109.5
H3B-C3-H3C	109.5
C2-C4-H4A	109.5(7)
C2-C4-H4B	109.5(6)
H4A-C4-H4B	109.5
C2-C4-H4C	109.5(7)
H4A-C4-H4C	109.5
H4B-C4-H4C	109.5
C2-C5-H5A	109.5(7)
C2-C5-H5B	109.5(7)
H5A-C5-H5B	109.5
C2-C5-H5C	109.5(6)
H5A-C5-H5C	109.5
H5B-C5-H5C	109.5
C11-C6-C7	119.4(10)
C11-C6-N1	121.4(9)
C7-C6-N1	119.1(9)
C6-C7-C8	120.2(12)
C6-C7-H7A	119(8)
C8-C7-H7A	121(8)
C9-C8-C7	120.0(12)
C9-C8-H8A	123(7)
C7-C8-H8A	116(7)
C8-C9-C10	120.0(12)
C8-C9-H9A	115(8)
C10-C9-H9A	125(8)
C9-C10-C11	120.4(12)
C9-C10-H10A	130(8)
C11-C10-H10A	108(8)
C6-C11-C10	120.0(11)
C6-C11-H11A	117(5)
C10-C11-H11A	121(5)
N2-C12-C14	109.7(9)
N2-C12-C13	122.9(9)
C14-C12-C13	127.4(9)
C12-C13-H13A	109.5(6)
C12-C13-H13B	109.5(6)
H13A-C13-H13B	109.5
C12-C13-H13C	109.5(6)
H13A-C13-H13C	109.5
H13B-C13-H13C	109.5
C15-C14-C12	107.4(9)
C15-C14-H14A	128(6)
C12-C14-H14A	125(6)
N5-C15-C14	106.5(8)

N5-C15-C16	122.8(9)
C14-C15-C16	130.6(9)
C15-C16-H16A	109.5(6)
C15-C16-H16B	109.5(6)
H16A-C16-H16B	109.5
C15-C16-H16C	109.5(6)
H16A-C16-H16C	109.5
H16B-C16-H16C	109.5
N3-C17-C19	109.7(11)
N3-C17-C18	121.1(10)
C19-C17-C18	129.2(11)
C17-C18-H18A	109.5(6)
C17-C18-H18B	109.5(7)
H18A-C18-H18B	109.5
C17-C18-H18C	109.5(6)
H18A-C18-H18C	109.5
H18B-C18-H18C	109.5
C20-C19-C17	107.6(12)
C20-C19-H19A	120(10)
C17-C19-H19A	133(10)
N6-C20-C19	108.0(11)
N6-C20-C21	123.8(10)
C19-C20-C21	128.1(11)
C20-C21-H21A	109.5(6)
C20-C21-H21B	109.5(6)
H21A-C21-H21B	109.5
C20-C21-H21C	109.5(6)
H21A-C21-H21C	109.5
H21B-C21-H21C	109.5
N4-C22-C24	110.8(9)
N4-C22-C23	121.6(9)
C24-C22-C23	127.6(9)
C22-C23-H23A	109.5(6)
C22-C23-H23B	109.5(6)
H23A-C23-H23B	109.5
C22-C23-H23C	109.5(6)
H23A-C23-H23C	109.5
H23B-C23-H23C	109.5
C22-C24-C25	106.3(9)
C22-C24-H24A	135(5)
C25-C24-H24A	118(5)
N7-C25-C24	107.7(8)
N7-C25-C26	124.0(9)
C24-C25-C26	128.3(9)
C25-C26-H26A	109.5(6)
C25-C26-H26B	109.5(5)
H26A-C26-H26B	109.5
C25-C26-H26C	109.5(5)
H26A-C26-H26C	109.5
H26B-C26-H26C	109.5
C28"-O-C29"	124(3)
C28-O-C29	124(3)
C27-C28-O	126(2)
C30-C29-O	126(2)

C27"-C28"-O	126(2)
C30"-C29"-O	126(2)
C28'-O'-C29'	124(3)
C27'-C28'-O'	126(2)
C30'-C29'-O'	126(2)

Table A2.4. Anisotropic displacement parameters ($A^2 \times 10^3$) for **8**. The anisotropic displacement factor exponent takes the form: $-2\pi^2 [h^2 a^{*2} U11 + ... + 2 h k a^* b^* U12]$

Atom	U11	U22	U33	U23	U13	U12
W	44(1)	42(1)	43(1)	2(1)	14(1)	-2(1)
Cl	65(2)	74(2)	52(1)	4(1)	5(1)	-1(2)
N1	46(4)	39(4)	53(5)	3(4)	14(4)	4(4)
N2	51(5)	42(4)	56(5)	-2(4)	18(4)	4(4)
N3	53(5)	50(5)	51(5)	-3(4)	17(4)	0(4)
N4	39(4)	47(4)	40(4)	3(3)	11(3)	-6(3)
N5	54(5)	40(4)	59(5)	-3(4)	18(4)	-4(4)
N6	50(5)	48(5)	55(5)	-12(4)	22(4)	2(4)
N7	46(4)	40(4)	42(4)	-1(3)	14(4)	3(3)
B	56(7)	41(6)	55(7)	6(5)	12(6)	9(5)
C1	59(6)	44(5)	48(5)	3(4)	11(5)	10(5)
C2	67(7)	68(7)	71(7)	14(6)	33(6)	-9(6)
C3	98(10)	77(9)	125(12)	21(8)	45(9)	-19(8)
C4	132(12)	103(11)	78(9)	26(8)	40(9)	-20(9)
C5	70(8)	98(10)	148(13)	31(10)	48(9)	-4(8)
C6	47(5)	42(5)	53(6)	2(5)	19(5)	1(4)
C7	71(7)	56(7)	56(7)	7(6)	18(6)	8(6)
C8	74(8)	60(8)	87(10)	19(7)	22(7)	10(6)
C9	85(9)	31(6)	107(11)	-4(7)	10(8)	15(6)
C10	101(10)	74(9)	76(9)	-11(8)	29(8)	30(8)
C11	91(9)	46(6)	69(8)	10(5)	32(7)	13(6)
C12	50(6)	52(6)	56(6)	-11(5)	17(5)	6(5)
C13	49(6)	69(8)	110(9)	12(7)	25(6)	8(6)
C14	48(6)	57(6)	62(6)	-2(5)	20(5)	-12(5)
C15	57(6)	53(6)	51(6)	-1(5)	21(5)	-20(5)
C16	77(8)	59(7)	73(7)	15(5)	26(6)	-18(6)
C17	58(7)	81(8)	58(7)	-14(6)	30(5)	5(6)
C18	114(11)	121(11)	65(7)	1(8)	54(8)	10(9)
C19	70(8)	79(10)	68(9)	-27(8)	12(7)	23(7)
C20	45(6)	64(7)	60(7)	-7(6)	12(5)	7(5)
C21	86(9)	53(6)	109(10)	-14(7)	31(8)	12(6)
C22	46(5)	52(6)	51(5)	-10(5)	18(4)	-5(5)
C23	76(7)	59(7)	71(7)	-4(6)	14(6)	-14(6)
C24	47(6)	67(7)	45(6)	5(5)	15(5)	1(5)
C25	33(5)	53(6)	54(6)	12(5)	19(4)	13(4)
C26	69(7)	72(7)	67(7)	15(6)	20(6)	23(6)

Table A2.5. Hydrogen coordinates (x 10^4) and isotropic displacement parameters (A^4 x 10^4) for **8**.

Atom	x	y	z	U(eq)
H1A	691(6)	1931(4)	4100(4)	56
H	2380(67)	-902(45)	4394(44)	40(22)
H3A	4251(13)	3769(7)	3115(9)	146
H3B	4142(13)	3303(7)	3847(9)	146
H3C	2989(13)	3654(7)	3228(9)	146
H4A	2781(13)	2432(8)	1620(7)	154
H4B	3373(13)	3253(8)	1752(7)	154
H4C	2142(13)	3116(8)	1902(7)	154
H5A	4707(11)	1872(8)	2585(9)	153
H5B	5235(11)	2231(8)	3436(9)	153
H5C	5263(11)	2703(8)	2689(9)	153
H7A	700(95)	3203(62)	2778(63)	73(39)
H8A	536(87)	4475(59)	2802(58)	65(34)
H9A	295(95)	5009(65)	3857(62)	72(35)
H10A	719(94)	4230(63)	5013(61)	68(36)
H11A	719(78)	2958(53)	4964(55)	60(28)
H13A	-1089(9)	1683(6)	2937(8)	114
H13B	-1917(9)	1526(6)	3461(8)	114
H13C	-2203(9)	1134(6)	2625(8)	114
H14A	-1954(93)	-164(57)	3698(58)	73(33)
H16A	821(10)	-1410(6)	4582(7)	104
H16B	-503(10)	-1622(6)	4082(7)	104
H16C	-239(10)	-1223(6)	4912(7)	104
H18A	2730(12)	1222(9)	1844(7)	141
H18B	2316(12)	604(9)	1166(7)	141
H18C	3684(12)	692(9)	1649(7)	141
H19A	2963(105)	-864(65)	2046(66)	49(40)
H21A	2409(11)	-1784(6)	3634(8)	124
H21B	3357(11)	-2002(6)	3216(8)	124
H21C	1982(11)	-2024(6)	2736(8)	124
H23A	3503(10)	2444(6)	4568(7)	106
H23B	822(10)	2308(6)	5126(7)	106
H23C	3793(10)	2465(6)	5493(7)	106
H24A	4943(82)	870(52)	6202(55)	60(27)
H26A	3498(10)	-1000(6)	5454(6)	105
H26B	3840(10)	-589(6)	6284(6)	105
H26C	4829(10)	-742(6)	5880(6)	105
H27D	8343(34)	3099(19)	4442(25)	100
H27E	7119(34)	2715(19)	4413(25)	100
H27F	8236(34)	2650(19)	5183(25)	100
H28C	7120(36)	3930(20)	4543(24)	89
H28D	8212(36)	3857(20)	5313(24)	89
H29C	7290(38)	4504(19)	6110(29)	120
H29D	6202(38)	4667(19)	5357(29)	120
H30D	5816(40)	4896(29)	6398(29)	143
H30E	6090(40)	4036(29)	6673(29)	143
H30F	5001(40)	4230(29)	5916(29)	143

H27G	8272(59)	2367(33)	4888(41)	96
H27H	6932(59)	2638(33)	4535(41)	96
H27I	7981(59)	3213(33)	4570(41)	96
H28E	6963(72)	3055(27)	5172(36)	90
H28F	8014(72)	3631(27)	5207(36)	90
H29E	6575(50)	4861(16)	5360(41)	112
H29F	7120(50)	4332(16)	6064(41)	112
H30G	5980(24)	5019(16)	6307(19)	138
H30H	4994(24)	4703(16)	5549(19)	138
H30I	5558(24)	4157(16)	6277(19)	138
H27A	8464(24)	2617(16)	4551(19)	61
H27B	7301(24)	3015(16)	3993(19)	61
H27C	7201(24)	2395(16)	4613(19)	61
H28A	8476(31)	3673(31)	5001(33)	69
H28B	8101(31)	3094(31)	5543(33)	69
H29A	7224(55)	3698(53)	6201(26)	136
H29B	7241(55)	4534(53)	5897(26)	136
H30A	5961(67)	4400(71)	6433(50)	166
H30B	5290(67)	3793(71)	5789(50)	166
H30C	5364(67)	4658(71)	5548(50)	166

Table A3.1. Crystal data and structure refinement for o-$C_6H_4\{N(C_6H_5)N'[Si(CH_3)_2(C_5(CH_3)_4)]\}Zr(N(CH_3)_2)(NH(CH_3)_2)$ **12.**

Empirical formula	C27 H40 N4 Si Zr . 1/2 [C6 H6]
Formula weight	578.99
Temperature	173(2) K
Wavelength	0.71073 A
Crystal system	Triclinic
Space group	P-1
Unit cell dimensions	a = 10.9864(1) A α = 77.310(1) deg.
	b = 11.8841(2) A β = 70.304(1) deg.
	c = 12.3633(1) A γ = 77.732(1) deg.
Volume	1465.68(3) A^3,
Z	2
Density (calculated)	1.312 Mg/m^3
Absorption coefficient	0.441 mm^{-1}
F(000)	610
Crystal size	0.34 x 0.26 x 0.11 mm
θ range for data collection	1.77 to 27.50 deg.
Limiting indices	$-14 \le h \le 14, -13 \le k \le 15, -13 \le l \le 15$
Reflections collected	9603
Independent reflections	6353 [R(int) = 0.0225]
Absorption correction	Integration
Max. and min. transmission	0.9534 and 0.8753
Refinement method	Full-matrix least-squares on F^2
Data / restraints / parameters	6298 / 6 / 514
Goodness-of-fit on F^2	1.092
Final R indices [$I>2\sigma(I)$]	R1 = 0.0238, wR2 = 0.0592 [6040]
R indices (all data)	R1 = 0.0261, wR2 = 0.0647
Extinction coefficient	0.0038(5)
Largest diff. peak and hole	0.347 and -0.342 $e.A^{-3}$

Table A3.2. Atomic coordinates (x 10^4) and equivalent isotropic displacement parameters (A^2 x 10^3) for **12**. U(eq) is defined as one third of the trace of the orthogonalized Uij tensor.

Atom	x	y	z	U(eq)
Zr	7974(1)	-7233(1)	2430(1)	17(1)
Si	0850(1)	-7198(1)	2306(1)	20(1)
N1	9334(1)	-6376(1)	2733(1)	21(1)
N2	6995(1)	-5426(1)	2778(1)	18(1)
N3	7105(1)	-8096(1)	4062(1)	26(1)
N4	6087(1)	-6985(1)	1787(1)	27(1)
C1	10261(1)	-8150(1)	1623(1)	20(1)
C2	9655(2)	-9171(1)	2200(1)	23(1)
C2'	9915(2)	-10001(2)	3237(2)	32(1)
C3	8849(2)	-9326(1)	1578(1)	24(1)
C3'	8198(2)	-10375(2)	1751(2)	34(1)
C4	8959(2)	-8421(1)	594(1)	23(1)
C4'	8500(2)	-8442(2)	-423(2)	32(1)
C5	9811(1)	-7694(1)	613(1)	21(1)
C5'	10245(2)	-6682(2)	-321(2)	30(1)
C6	12147(2)	-6345(2)	1269(2)	32(1)
C7	11509(2)	-7983(2)	3527(2)	34(1)
C8	8961(1)	-5304(1)	3110(1)	19(1)
C9	7677(1)	-4759(1)	3112(1)	18(1)
C10	7214(2)	-3666(1)	3471(1)	22(1)
C11	7995(2)	-3129(1)	3829(1)	25(1)
C12	9248(2)	-3664(1)	3828(1)	26(1)
C13	9726(2)	-4750(1)	3468(1)	24(1)
C14	5689(1)	-4880(1)	2820(1)	19(1)
C15	5451(2)	-3904(1)	2003(1)	23(1)
C16	4182(2)	-3423(1)	2003(1)	26(1)
C17	3121(2)	-3909(2)	2809(2)	28(1)
C18	3336(2)	-4859(2)	3638(1)	26(1)
C19	4613(2)	-5334(1)	3653(1)	23(1)
C20	6964(2)	-7556(2)	5060(2)	33(1)
C21	6674(2)	-9231(2)	4470(2)	42(1)
C22	6151(2)	-6236(2)	651(2)	38(1)
C23	5449(2)	-8006(2)	1945(2)	40(1)
C24	14582(25)	-10441(16)	1190(18)	101(9)
C25	13728(16)	-9612(15)	727(18)	70(5)
C26	14244(24)	-9227(14)	-447(17)	82(8)
C24'	14167(13)	-10196(14)	1042(10)	70(4)
C25'	13741(11)	-9445(12)	177(14)	75(5)
C26'	14565(21)	-9234(15)	-944(15)	81(4)

Table A3.3. Bond lengths [Å] and angles [°] for **12**.

Zr-N3	2.0599(13)
Zr-N1	2.1451(12)
Zr-N2	2.2513(12)
Zr-N4	2.4005(13)
Zr-C1	2.4740(14)
Zr-C5	2.5359(14)
Zr-C2	2.6309(14)
Zr-C4	2.723(2)
Zr-C3	2.769(2)
Zr-Si	3.1201(4)
Si-N1	1.7173(13)
Si-C7	1.873(2)
Si-C6	1.874(2)
Si-C1	1.874(2)
N1-C8	1.385(2)
N2-C9	1.401(2)
N2-C14	1.432(2)
N3-C21	1.452(2)
N3-C20	1.462(2)
N4-C23	1.472(2)
N4-C22	1.477(2)
N4-H4	0.88(2)
C1-C2	1.439(2)
C1-C5	1.450(2)
C2-C3	1.414(2)
C2-C2'	1.506(2)
C2'-H2'A	0.95(3)
C2'-H2'B	0.95(3)
C2'-H2'C	0.95(3)
C3-C4	1.425(2)
C3-C3'	1.507(2)
C3'-H3'A	0.96(3)
C3'-H3'A	0.94(3)
C3'-H3'C	1.03(3)
C4-C5	1.411(2)
C4-C4'	1.510(2)
C4'-H4'A	0.97(2)
C4'-H4'B	0.98(2)
C4'-H4'C	0.94(2)
C5-C5'	1.506(2)
C5'-H5'A	0.98(3)
C5'-H5'B	0.94(3)
C5'-H5'C	0.91(3)
C6-H6A	0.93(3)
C6-H6B	0.94(3)
C6-H6C	0.91(3)
C7-H7A	0.98(3)
C7-H7B	0.96(2)
C7-H7C	0.97(3)
C8-C13	1.397(2)
C8-C9	1.421(2)

C9-C10	1.401(2)
C10-C11	1.398(2)
C10-H10	0.94(2)
C11-C12	1.387(2)
C11-H11	0.95(2)
C12-C13	1.395(2)
C12-H12	0.94(2)
C13-H13	0.96(2)
C14-C19	1.398(2)
C14-C15	1.403(2)
C15-C16	1.390(2)
C15-H15	0.95(2)
C16-C17	1.391(2)
C16-H16	0.92(2)
C17-C18	1.386(2)
C17-H17	0.95(2)
C18-C19	1.400(2)
C18-H18	0.96(2)
C19-H19	0.94(2)
C20-H20A	0.99(2)
C20-H20B	1.02(2)
C20-H20C	0.95(2)
C21-H21A	0.97(2)
C21-H21B	1.03(2)
C21-H21C	1.01(3)
C22-H22A	0.98(3)
C22-H22B	0.99(2)
C22-H22C	1.00(3)
C23-H23A	0.97(3)
C23-H23B	1.00(3)
C23-H23C	0.98(3)
C24-C(26)#1	1.34(3)
C24-C25	1.378(6)
C24-H24	0.93
C25-C26	1.378(6)
C25-H25	0.93
C26-C(24)#1	1.34(3)
C26-H26	0.93
C24'-C25'	1.378(6)
C24'-C(26')#1	1.39(3)
C24'-H24'	0.93
C25'-C26'	1.378(6)
C25'-H25'	0.93
C26'-C(24')#1	1.39(3)
C26'-H26'	0.93
N3-Zr-N1	102.88(5)
N3-Zr-N2	96.47(5)
N1-Zr-N2	71.34(4)
N3-Zr-N4	94.38(5)
N1-Zr-N4	145.90(5)
N2-Zr-N4	77.72(5)
N3-Zr-C1	111.30(5)
N1-Zr-C1	68.20(5)
N2-Zr-C1	134.79(5)

N4-Zr-C1	131.71(5)
N3-Zr-C5	137.78(5)
N1-Zr-C5	85.21(5)
N2-Zr-C5	124.95(5)
N4-Zr-C5	101.50(5)
C1-Zr-C5	33.62(5)
N3-Zr-C2	84.92(5)
N1-Zr-C2	91.91(5)
N2-Zr-C2	163.11(5)
N4-Zr-C2	119.03(5)
C1-Zr-C2	32.55(5)
C5-Zr-C2	53.16(5)
N3-Zr-C4	119.51(5)
N1-Zr-C4	115.51(5)
N2-Zr-C4	138.34(4)
N4-Zr-C4	79.18(5)
C1-Zr-C4	52.70(5)
C5-Zr-C4	30.86(5)
C2-Zr-C4	50.79(5)
N3-Zr-C3	90.71(5)
N1-Zr-C3	119.46(5)
N2-Zr-C3	165.37(5)
N4-Zr-C3	89.07(5)
C1-Zr-C3	52.12(5)
C5-Zr-C3	51.23(5)
C2-Zr-C3	30.22(5)
C4-Zr-C3	30.07(5)
N3-Zr-Si	106.42(4)
N1-Zr-Si	31.71(3)
N2-Zr-Si	102.30(3)
N4-Zr-Si	158.99(4)
C1-Zr-Si	36.90(4)
C5-Zr-Si	60.90(3)
C2-Zr-Si	61.41(4)
C4-Zr-Si	87.83(3)
C3-Zr-Si	87.77(3)
N1-Si-C7	114.68(8)
N1-Si-C6	114.01(8)
C7-Si-C6	105.95(9)
N1-Si-C1	92.86(6)
C7-Si-C1	114.75(8)
C6-Si-C1	114.64(8)
N1-Si-Zr	41.04(4)
C7-Si-Zr	121.03(7)
C6-Si-Zr	132.52(6)
C1-Si-Zr	52.45(4)
C8-N1-Si	130.64(10)
C8-N1-Zr	121.87(9)
Si-N1-Zr	107.25(6)
C9-N2-C14	113.35(11)
C9-N2-Zr	117.62(9)
C14-N2-Zr	128.71(9)
C21-N3-C20	109.49(14)
C21-N3-Zr	132.83(12)

C20-N3-Zr	117.44(11)
C23-N4-C22	111.7(2)
C23-N4-Zr	118.86(11)
C22-N4-Zr	116.15(12)
C23-N4-H4	105.0(14)
C22-N4-H4	104.7(14)
Zr-N4-H4	97.5(14)
C2-C1-C5	106.41(13)
C2-C1-Si	126.69(11)
C5-C1-Si	121.71(11)
C2-C1-Zr	79.73(8)
C5-C1-Zr	75.53(8)
Si-C1-Zr	90.64(6)
C3-C2-C1	108.74(13)
C3-C2-C2'	125.2(2)
C1-C2-C2'	125.93(14)
C3-C2-Zr	80.31(9)
C1-C2-Zr	67.71(8)
C2'-C2-Zr	121.86(11)
C2-C2'-H2'A	111(2)
C2-C2'-H2'B	115(2)
H2'A-C2'-H2'B	103(2)
C2-C2'-H2'C	114(2)
H2'A-C2'-H2'C	108(2)
H'B-C2'-H2'C	106(2)
C2-C3-C4	108.04(13)
C2-C3-C3'	127.0(2)
C4-C3-C3'	123.9(2)
C2-C3-Zr	69.48(8)
C4-C3-Zr	73.18(8)
C3'-C3-Zr	132.24(11)
C3-C3'-H3'A	109(2)
C3-C3'-H3'A	112(2)
H3'A-C3'-H3'A	107(2)
C3-C3'-H3'C	114(2)
H3'A-C3'-H3'C	106(2)
H3'A-C3'-H3'C	108(2)
C5-C4-C3	108.60(13)
C5-C4-C('	126.2(2)
C3-C4-C4'	123.6(2)
C5-C4-Zr	67.22(8)
C3-C4-Zr	76.75(9)
C4'-C4-Zr	133.24(11)
C4-C4'-H4'A	109.7(13)
C4-C4'-H4'B	113.4(13)
H4'A-C4'-H4'B	106(2)
C4-C4'-H(4'C	110.2(14)
H4'A-C4'-H4'C	107(2)
H('B-C4'-H4'C	110(2)
C4-C5-C1	108.20(13)
C4-C5-C5'	124.78(14)
C1-C5-C5'	126.85(14)
C4-C(-Zr	81.92(9)
C1-C5-Zr	70.85(8)

C5'-C5-Zr	117.39(10)
C5-C5'-H5'A	113(2)
C5-C5'-H5'B	113(2)
H5'A-C5'-H5'B	114(2)
C5-C5'-H5'C	114(2)
H5'A-C5'-H5'C	104(2)
H5'B-C5'-H5'C	99(2)
Si-C6-H6A	112(2)
Si-C6-H6B	110(2)
H6A-C6-H6B	108(2)
Si-C6-H6C	113(2)
H6A-C6-H6C	107(2)
H6B-C6-H6C	107(2)
Si-C7-H7A	107.8(14)
Si-C7-H7B	112.0(14)
H7A-C7-H7B	109(2)
Si-C7-H7C	111.7(14)
H7A-C7-H7C	110(2)
H7B-C7-H7C	106(2)
N1-C8-C13	125.89(13)
N1-C8-C9	114.31(12)
C13-C8-C9	119.80(14)
C10-C9-N2	127.27(13)
C10-C9-C8	118.57(13)
N2-C9-C8	114.13(12)
C11-C10-C9	120.65(14)
C11-C10-H10	120.7(12)
C9-C10-H10	118.6(12)
C12-C11-C10	120.6(2)
C12-C11-H11	120.3(12)
C10-C11-H11	119.1(12)
C11-C12-C13	119.4(2)
C11-C12-H12	120.0(12)
C13-C12-H12	120.5(12)
C12-C13-C8	120.89(14)
C12-C13-H13	120.4(12)
C8-C13-H13	118.7(12)
C19-C14-C15	118.12(13)
C19-C14-N2	120.73(13)
C15-C14-N2	121.10(13)
C16-C15-C14	120.86(14)
C16-C15-H15	119.7(12)
C14-C15-H15	119.4(12)
C15-C16-C17	120.4(2)
C15-C16-H16	118.4(13)
C17-C16-H16	121.1(13)
C18-C17-C16	119.46(14)
C18-C17-H17	120.8(13)
C16-C17-H17	119.7(13)
C17-C18-C19	120.2(2)
C17-C18-H18	121.6(12)
C19-C18-H18	118.2(12)
C14-C19-C18	120.84(14)
C14-C19-H19	118.0(12)

C18-C19-H19	121.1(12)
N3-C20-H20A	112.1(14)
N3-C20-H20B	111.0(13)
H20A-C20-H20B	108(2)
N3-C20-H20C	114.3(13)
H20A-C20-H20C	106(2)
H20B-C20-H20C	105(2)
N3-C21-H21A	110.8(14)
N3-C21-H21B	113.9(13)
H21A-C21-H21B	109(2)
N3-C21-H21C	113(2)
H21A-C21-H21C	105(2)
H21B-C21-H21C	105(2)
N4-C22-H22A	111(2)
N4-C22-H22B	108.4(13)
H22A-C22-H22B	110(2)
N4-C22-H22C	107(2)
H22A-C22-H22C	110(2)
H22B-C22-H22C	111(2)
N4-C23-H23A	111(2)
N4-C23-H23B	111(2)
H23A-C23-H23B	114(2)
N4-C23-H23C	107(2)
H23A-C23-H23C	104(2)
H23B-C23-H23C	111(2)
C(26)#1-C24-C25	116.6(14)
C(26)#1-C24-H24	121.7(10)
C25-C24-H24	121.7(14)
C26-C25-C24	113(2)
C26-C25-H25	123.3(13)
C24-(25-H25	123.3(14)
C(24)#1-C26-C25	129.9(13)
C(24)#1-C26-H26	115.1(10)
C25-C26-H26	115.0(13)
C25'-C24'-C(26')#1	126.6(10)
C25'-C24'-H24'	116.7(7)
C(26')#1-C24'-H24'	116.7(11)
C26'-C25'-C24'	121.4(13)
C26'-C25'-H25'	119.3(11)
C24'-C(5'-H25'	119.3(7)
C25'-C26'-C(24')#1	112(2)
C25'-C26'-H26'	124.0(11)
C(24')#1-C26'-H26'	124.1(11)

Symmetry transformations used to generate equivalent atoms: #1 -x+3,-y-2,-z

Table A3.4. Anisotropic displacement parameters ($A^2 \times 10^3$) for **12**.
The anisotropic displacement factor exponent takes the form: $-2\pi^2 [h^2 a^{*2} U11 + ... + 2 h k a^* b^* U12]$

Atom	U11	U22	U33	U23	U13	U12
Zr	15(1)	17(1)	18(1)	-4(1)	-4(1)	-2(1)
Si	15(1)	23(1)	22(1)	-6(1)	-6(1)	0(1)
N1	16(1)	23(1)	26(1)	-9(1)	-6(1)	-2(1)
N2	16(1)	19(1)	21(1)	-5(1)	-6(1)	-2(1)
N3	28(1)	26(1)	21(1)	-2(1)	-2(1)	-6(1)
N4	22(1)	30(1)	33(1)	-13(1)	-11(1)	0(1)
C1	17(1)	21(1)	19(1)	-5(1)	-4(1)	1(1)
C2	22(1)	19(1)	24(1)	-4(1)	-6(1)	2(1)
C2'	36(1)	25(1)	33(1)	3(1)	-14(1)	-2(1)
C3	23(1)	19(1)	29(1)	-7(1)	-8(1)	0(1)
C3'	36(1)	22(1)	44(1)	-8(1)	-13(1)	-5(1)
C4	22(1)	23(1)	23(1)	-9(1)	-7(1)	1(1)
C4'	33(1)	37(1)	30(1)	-14(1)	-13(1)	0(1)
C5	21(1)	22(1)	19(1)	-6(1)	-4(1)	2(1)
C5'	35(1)	28(1)	25(1)	0(1)	-8(1)	-6(1)
C6	22(1)	36(1)	36(1)	-6(1)	-5(1)	-8(1)
C7	35(1)	36(1)	35(1)	-6(1)	-19(1)	0(1)
C8	17(1)	22(1)	19(1)	-5(1)	-2(1)	-4(1)
C9	18(1)	20(1)	15(1)	-2(1)	-3(1)	-4(1)
C10	22(1)	21(1)	21(1)	-4(1)	-5(1)	-3(1)
C11	32(1)	21(1)	24(1)	-7(1)	-6(1)	-6(1)
C12	28(1)	29(1)	27(1)	-8(1)	-8(1)	-10(1)
C13	20(1)	28(1)	27(1)	-7(1)	-7(1)	-6(1)
C14	18(1)	21(1)	19(1)	-7(1)	-6(1)	-1(1)
C15	23(1)	24(1)	20(1)	-4(1)	-5(1)	-4(1)
C16	29(1)	24(1)	26(1)	-5(1)	-14(1)	1(1)
C17	20(1)	35(1)	32(1)	-12(1)	-12(1)	2(1)
C18	18(1)	36(1)	25(1)	-9(1)	-3(1)	-4(1)
C19	21(1)	25(1)	20(1)	-4(1)	-6(1)	-2(1)
C20	38(1)	37(1)	20(1)	-5(1)	-5(1)	-2(1)
C21	48(1)	35(1)	36(1)	2(1)	-2(1)	-18(1)
C22	50(1)	34(1)	40(1)	-13(1)	-28(1)	7(1)
C23	30(1)	36(1)	63(1)	-16(1)	-20(1)	-6(1)
C24	154(25)	65(11)	132(12)	7(9)	-89(16)	- 66(1)
C25	36(5)	56(7)	129(13)	-71(9)	-1(8)	-10(5)
C26	84(16)	41(6)	159(23)	-39(11)	-83(18)	10(8)
C24'	41(5)	72(8)	109(8)	-56(7)	-5(5)	-20(5)
C25'	28(4)	73(6)	142(14)	-79(9)	-15(7)	-1(3)
C26'	90(10)	51(5)	131(10)	-27(6)	-53(10)	-31(5)

Table A3.5. Hydrogen coordinates (x 10^4) and isotropic displacement parameters (A^2 x 10^3) for **12**.

Atom	x	y	z	U(eq)
H4	5551(21)	-6562(19)	2301(19)	35(5)
H2'A	10823(25)	-10265(22)	3095(21)	53(7)
H2'B	9689(26)	-9672(24)	3923(24)	61(8)
H2'C	9483(26)	-10665(24)	3450(23)	60(7)
H3'A	8470(27)	-10675(24)	1030(25)	64(8)
H3'A	8435(26)	-10985(24)	2308(24)	60(7)
H3'C	7196(27)	-10193(23)	1989(22)	60(7)
H4'A	8999(23)	-9097(21)	-812(20)	46(6)
H4'B	7576(23)	-8537(19)	-195(19)	41(6)
H4'C	8653(22)	-7764(21)	-973(20)	44(6)
H5'A	11170(31)	-6826(26)	-758(26)	77(9)
H5'B	9694(26)	-6420(23)	-798(22)	57(7)
H5'C	10167(28)	-6011(26)	-51(25)	68(8)
H6A	12507(25)	-5981(23)	1657(22)	57(7)
H6B	12824(24)	-6849(22)	834(21)	49(6)
H6C	11849(25)	-5778(23)	756(23)	56(7)
H7A	11840(24)	-7416(22)	3781(21)	51(7)
H7B	10849(24)	-8327(21)	4175(21)	48(6)
H7C	12203(24)	-8623(22)	3289(21)	50(7)
H10	6363(21)	-3313(18)	3486(17)	32(5)
H11	7647(20)	-2408(18)	4100(18)	33(5)
H12	9765(20)	-3297(17)	4077(17)	31(5)
H13	10575(20)	-5145(17)	3494(17)	29(5)
H15	6167(20)	-3559(17)	1454(18)	31(5)
H16	4062(20)	-2767(19)	1464(18)	35(5)
H17	2261(21)	-3571(19)	2803(18)	38(5)
H18	2622(20)	-5210(17)	4217(17)	30(5)
H19	4773(18)	-5979(17)	4212(17)	26(5)
H20A	6047(24)	-7462(21)	5580(21)	49(6)
H20B	7542(22)	-8042(20)	5544(19)	42(6)
H20C	7219(21)	-6804(20)	4860(18)	36(5)
H21A	5761(24)	-9155(21)	4940(21)	49(6)
H21B	6801(23)	-9686(21)	3814(21)	48(6)
H21C	7162(26)	-9767(24)	4998(23)	60(7)
H22A	5286(28)	-6016(24)	542(23)	65(8)
H22B	6503(21)	-5526(20)	622(19)	39(6)
H22C	6748(25)	-6698(23)	39(23)	58(7)
H23A	4586(27)	-7763(22)	1855(22)	58(7)
H23B	6024(26)	-8568(24)	1418(23)	62(8)
H23C	5274(24)	-8369(22)	2766(23)	53(7)
H24	14357(25)	-10755(16)	1977(18)	121
H25	12886(16)	-9339(15)	1163(18)	84
H26	13696(24)	-8650(14)	-775(17)	99
H24'	13544(13)	-10337(14)	1764(10)	84
H25'	12880(11)	-9072(12)	354(14)	90
H26'	14304(21)	-8766(15)	-1560(15)	97

Table A4.1. Crystal data and structure refinement for o-$C_6H_4\{N(C_6H_5)N'[Si(CH_3)_2(C_5(CH_3)_4)]\}Zr(Cl)(NH(CH_3)_2)_2$ **13**.

Empirical formula	C27 H41 Cl N4 Si Zr
Formula weight	576.40
Temperature	173(2) K
Wavelength	0.71073 A
Crystal system	Monoclinic
Space group	P2(1)/c
Unit cell dimensions	a = 12.1925(2) A $\alpha = 90^\circ$
	b = 18.9677(4) A $\beta = 91.407(1)^\circ$
	c = 12.2218(2) A $\gamma = 90^\circ$
Volume	2825.61(9) $Å^3$
Z	4
Density (calculated)	1.355 Mg/m^3
Absorption coefficient	0.548 mm^{-1}
F(000)	1208
Crystal size	0.34 x 0.26 x 0.13 mm
θ range for data collection	1.98 to 27.50 deg.
Limiting indices	$-14 \le h \le 16$
	$-24 \le k \le 21$
	$-15 \le l \le 16$
Reflections collected	18666
Independent reflections	6387 [R(int) = 0.0250]
Absorption correction	ψ Scan
Max. and min. transmission	0.949 and 0.845
Refinement method	Full-matrix least-squares on F^2
Data / restraints / parameters	6381 / 0 / 472
Goodness-of-fit on F^2	1.022
Final R indices [$I>2\sigma(I)$]	R1 = 0.0237, wR2 = 0.0579 [5484]
R indices (all data)	R1 = 0.0310, wR2 = 0.0614
Extinction coefficient	0.0013(2)
Largest diff. peak and hole	0.398 and -0.422 $e.A^{-3}$

Table A4.2. Atomic coordinates (x 10^4) and equivalent isotropic displacement parameters (A^2 x 10^3) for **13**. U(eq) is defined as one third of the trace of the orthogonalized Uij tensor.

Atom	x	y	z	U(eq)
Zr	7580(1)	782(1)	2290(1)	15(1)
Cl	7912(1)	1986(1)	3142(1)	23(1)
Si	6696(1)	-628(1)	1242(1)	22(1)
N1	7855(1)	-294(1)	1900(1)	18(1)
N2	9312(1)	481(1)	2922(1)	18(1)
N3	7370(1)	516(1)	4236(1)	22(1)
N4	8836(1)	1297(1)	1013(1)	24(1)
C1	5964(1)	239(1)	1298(1)	19(1)
C2	5487(1)	526(1)	2268(1)	20(1)
C2'	4848(2)	118(1)	3093(2)	28(1)
C3	5521(1)	1269(1)	2207(1)	22(1)
C3'	5027(2)	1791(1)	2980(2)	34(1)
C4	5989(1)	1461(1)	1197(1)	24(1)
C4'	6010(2)	2208(1)	780(2)	37(1)
C5	6260(1)	832(1)	632(1)	22(1)
C5'	6624(2)	790(1)	-538(2)	34(1)
C6	6922(2)	-968(1)	-175(2)	43(1)
C7	6051(2)	-1372(1)	2008(3)	44(1)
C8	8829(1)	-645(1)	2192(1)	18(1)
C9	9637(1)	-213(1)	2717(1)	18(1)
C10	10658(1)	-525(1)	2992(1)	25(1)
C11	10854(2)	-1236(1)	2778(2)	29(1)
C12	10043(2)	-1659(1)	2301(2)	27(1)
C13	9034(1)	-1359(1)	2010(1)	23(1)
C14	10173(1)	936(1)	3313(1)	20(1)
C15	11057(2)	1106(1)	2650(2)	31(1)
C16	11887(2)	1557(1)	3012(2)	40(1)
C17	11860(2)	1849(1)	4046(2)	37(1)
C18	11000(2)	1687(1)	4719(2)	33(1)
C19	10167(1)	1235(1)	4356(1)	26(1)
C20	7366(2)	-236(1)	4548(2)	31(1)
C21	6720(2)	938(1)	5001(2)	31(1)
C22	9423(2)	783(1)	318(2)	28(1)
C23	8707(2)	1975(1)	429(2)	35(1)

Table A4.3. Bond lengths [Å] and angles [deg] for **13**.

Zr-N1	2.1245(12)
Zr-N2	2.3024(13)
Zr-N4	2.4190(13)
Zr-N3	2.4511(14)
Zr-C1	2.509(2)
Zr-Cl	2.5376(4)
Zr-C5	2.559(2)
Zr-C2	2.598(2)
Zr-C4	2.661(2)
Zr-C3	2.675(2)
Zr-Si	3.1447(5)
Si-N1	1.7296(14)
Si-C6	1.874(2)
Si-C1	1.873(2)
Si-C7	1.878(2)
N1-C8	1.399(2)
N2-C9	1.399(2)
N2-C14	1.432(2)
N3-C21	1.476(2)
N3-C20	1.477(2)
N3-H3'	0.86(2)
N4-C23	1.477(2)
N4-C22	1.489(2)
N4-H4'	0.94(3)
C1-C2	1.440(2)
C1-C5	1.440(2)
C2-C3	1.413(2)
C2-C2'	1.504(2)
C2'-H2'A	0.89(3)
C2'-H2'B	0.95(3)
C2'-H2'C	0.92(3)
C3-C4	1.420(2)
C3-C3'	1.504(2)
C3'-H3'A	1.00(2)
C3'-H3'B	0.93(3)
C3'-H3'C	0.92(3)
C4-C5	1.420(2)
C4-C4'	1.507(2)
C4'-H4'A	0.94(3)
C4'-H4'B	0.99(3)
C4'-H4'C	0.95(3)
C5-C5'	1.510(2)
C5'-H5'A	0.95(2)
C5'-H5'B	0.96(3)
C5'-H5'C	0.98(3)
C6-H6A	0.92(3)
C6-H6B	0.95(3)
C6-H6C	0.97(3)
C7-H7A	0.90(3)
C7-H7B	0.94(3)
C7-H7C	0.91(3)

C8-C13	1.395(2)
C8-C9	1.422(2)
C9-C10	1.411(2)
C10-C11	1.395(2)
C10-H10	0.98(2)
C11-C12	1.391(3)
C11-H11	0.97(2)
C12-C13	1.395(2)
C12-H12	0.91(2)
C13-H13	0.92(2)
C14-C19	1.395(2)
C14-C15	1.403(2)
C15-C16	1.390(3)
C15-H15	0.96(2)
C16-C17	1.380(3)
C16-H16	0.96(2)
C17-C18	1.384(3)
C17-H17	0.98(2)
C18-C19	1.393(3)
C18-H18	0.94(2)
C19-H19	0.92(2)
C20-H20A	0.96(2)
C20-H20B	1.00(2)
C20-H20C	1.00(2)
C21-H21A	0.95(2)
C21-H21B	0.93(2)
C21-H21C	0.99(3)
C22-H22A	1.02(2)
C22-H22B	0.95(2)
C22-H22C	0.92(2)
C23-H23A	1.00(2)
C23-H23B	1.03(2)
C23-H23C	0.94(2)
N1-Zr-N2	71.84(5)
N1-Zr-N4	97.92(5)
N2-Zr-N4	74.19(5)
N1-Zr-N3	92.33(5)
N2-Zr-N3	74.95(5)
N4-Zr-N3	142.42(5)
N1-Zr-C1	67.90(5)
N2-Zr-C1	139.74(5)
N4-Zr-C1	110.86(5)
N3-Zr-C1	106.52(5)
N1-Zr-Cl	158.74(4)
N2-Zr-Cl	87.13(3)
N4-Zr-Cl	78.73(4)
N3-Zr-Cl	78.82(4)
C1-Zr-Cl	133.06(4)
N1-Zr-C5	87.59(5)
N2-Zr-C5	146.01(5)
N4-Zr-C5	82.51(5)
N3-Zr-C5	134.20(5)
C1-Zr-C5	33.01(5)
Cl-Zr-C5	112.48(4)

N1-Zr-C2	88.75(5)
N2-Zr-C2	148.15(5)
N4-Zr-C2	134.92(5)
N3-Zr-C2	81.07(5)
C1-Zr-C2	32.69(5)
Cl-Zr-C2	108.61(4)
C5-Zr-C2	53.13(5)
N1-Zr-C4	117.99(5)
N2-Zr-C4	160.06(5)
N4-Zr-C4	86.88(5)
N3-Zr-C4	119.62(5)
C1-Zr-C4	53.24(5)
Cl-Zr-C4	82.98(4)
C5-Zr-C4	31.50(5)
C2-Zr-C4	51.78(5)
N1-Zr-C3	118.45(5)
N2-Zr-C3	161.90(5)
N4-Zr-C3	116.37(5)
N3-Zr-C3	89.25(5)
C1-Zr-C3	52.99(5)
Cl-Zr-C3	81.07(4)
C5-Zr-C3	52.08(5)
C2-Zr-C3	31.04(5)
C4-Zr-C3	30.88(5)
N1-Zr-Si	31.35(4)
N2-Zr-Si	103.19(3)
N4-Zr-Si	107.26(4)
N3-Zr-Si	100.21(4)
C1-Zr-Si	36.56(4)
Cl-Zr-Si	169.082(13)
C5-Zr-Si	60.42(4)
C2-Zr-Si	60.63(4)
C4-Zr-Si	88.18(4)
C3-Zr-Si	88.06(4)
N1-Si-C6	114.75(9)
N1-Si-C1	92.64(7)
C6-Si-C1	114.66(10)
N1-Si-C7	113.00(10)
C6-Si-C7	105.98(13)
C1-Si-C7	115.84(9)
N1-Si-Zr	39.72(4)
C6-Si-Zr	127.74(9)
C1-Si-Zr	52.93(5)
C7-Si-Zr	125.44(9)
C8-N1-Si	128.54(11)
C8-N1-Zr	122.50(10)
Si-N1-Zr	108.93(6)
C9-N2-C14	114.71(12)
C9-N2-Zr	115.78(10)
C14-N2-Zr	128.40(10)
C21-N3-C20	110.79(14)
C21-N3-Zr	125.01(12)
C20-N3-Zr	116.79(11)
C21-N3-H3'	105.8(14)

C20-N3-H3'	106.8(14)
Zr-N3-H3'	86(2)
C23-N4-C22	110.03(14)
C23-N4-Zr	127.02(11)
C22-N4-Zr	115.09(10)
C23-N4-H4'	103(2)
C22-N4-H4'	105(2)
Zr-N4-H4'	91(2)
C2-C1-C5	106.42(14)
C2-C1-Si	124.34(12)
C5-C1-Si	122.60(12)
C2-C1-Zr	77.03(9)
C5-C1-Zr	75.39(9)
Si-C1-Zr	90.51(6)
C3-C2-C1	108.67(14)
C3-C2-C2'	124.4(2)
C1-C2-C2'	125.8(2)
C3-C2-Zr	77.49(9)
C1-C2-Zr	70.28(8)
C2'-C2-Zr	127.94(12)
C2-C2'-H2'A	110(2)
C2-C2'-H2'B	113(2)
H2'A-C2'-H2'B	104(2)
C2-C2'-H2'C	116(2)
H2'A-C2'-H2'C	105(2)
H2'B-C2'-H2'C	108(2)
C2-C3-C4	108.34(14)
C2-C3-C3'	127.6(2)
C4-C3-C3'	123.6(2)
C2-C3-Zr	71.47(9)
C4-C3-Zr	74.02(9)
C3'-C3-Zr	126.43(12)
C3-C3'-H3'A	108.9(13)
C3-C3'-H3'B	110(2)
H3'A-C3'-H3'B	110(2)
C3-C3'-H3'C	111(2)
H3'A-C3'-H3'C	107(2)
H3'B-C3'-H3'C	110(2)
C5-C4-C3	108.12(14)
C5-C4-C4'	128.3(2)
C3-C4-C4'	123.0(2)
C5-C4-Zr	70.29(9)
C3-C4-Zr	75.10(9)
C4'-C4-Zr	127.33(12)
C4-C4'-H4'A	110(2)
C4-C4'-H4'B	109.7(14)
H4'A-C4'-H4'B	109(2)
C4-C4'-H4'C	112(2)
H4'A-C4'-H4'C	107(2)
H4'B-C4'-H4'C	109(2)
C4-C5-C1	108.43(14)
C4-C5-C5'	125.6(2)
C1-C5-C5'	125.3(2)
C4-C5-Zr	78.21(10)

C1-C5-Zr	71.61(9)
C5'-C5-Zr	123.65(12)
C5-C5'-H5'A	112.0(13)
C5-C5'-H5'B	114(2)
H5'A-C5'-H5'B	107(2)
C5-C5'-H5'C	113(2)
H5'A-C5'-H5'C	104(2)
H5'B-C5'-H5'C	106(2)
Si-C6-H6A	110(2)
Si-C6-H6B	112(2)
H6A-C6-H6B	107(2)
Si-C6-H6C	111(2)
H6A-C6-H6C	109(3)
H6B-C6-H6C	107(3)
Si-C7-H7A	109(2)
Si-C7-H7B	115(2)
H7A-C7-H7B	105(3)
Si-C7-H7C	113(2)
H7A-C7-H7C	109(2)
H7B-C7-H7C	106(3)
C13-C8-N1	125.1(2)
C13-C8-C9	120.39(14)
N1-C8-C9	114.54(13)
N2-C9-C10	127.1(2)
N2-C9-C8	115.22(13)
C10-C9-C8	117.6(2)
C11-C10-C9	120.9(2)
C11-C10-H10	118.0(12)
C9-C10-H10	121.0(12)
C12-C11-C10	120.9(2)
C12-C11-H11	118.6(12)
C10-C11-H11	120.5(13)
C11-C12-C13	119.0(2)
C11-C12-H12	120.4(13)
C13-C12-H12	120.6(13)
C12-C13-C8	121.1(2)
C12-C13-H13	120.6(12)
C8-C13-H13	118.3(12)
C19-C14-C15	117.1(2)
C19-C14-N2	122.00(14)
C15-C14-N2	120.9(2)
C16-C15-C14	121.4(2)
C16-C15-H15	118.8(13)
C14-C15-H15	119.7(13)
C17-C16-C15	120.4(2)
C17-C16-H16	122(2)
C15-C16-H16	118(2)
C16-C17-C18	119.4(2)
C16-C17-H17	120.8(13)
C18-C17-H17	119.8(13)
C17-C18-C19	120.3(2)
C17-C18-H18	118.9(14)
C19-C18-H18	120.8(14)
C18-C19-C14	121.4(2)

C18-C19-H19	118.5(14)
C14-C19-H19	120.1(14)
N3-C20-H20A	112.2(14)
N3-C20-H20B	109.5(13)
H20A-C20-H20B	105(2)
N3-C20-H20C	109.9(13)
H20A-C20-H20C	113(2)
H20B-C20-H20C	107(2)
N3-C21-H21A	110.9(13)
N3-C21-H21B	108.5(14)
H21A-C21-H21B	112(2)
N3-C21-H21C	107.3(14)
H21A-C21-H21C	110(2)
H21B-C21-H21C	108(2)
N4-C22-H22A	110.6(12)
N4-C22-H22B	110.2(12)
H22A-C22-H22B	108(2)
N4-C22-H22C	109.3(14)
H22A-C22-H22C	106(2)
H22B-C22-H22C	113(2)
N4-C23-H23A	108.8(13)
N4-C23-H23B	107.0(12)
H23A-C23-H23B	111(2)
N4-C23-H23C	109.1(12)
H23A-C23-H23C	107(2)
H23B-C23-H23C	114(2)

Table A4.4. Anisotropic displacement parameters ($A^2 \times 10^3$) for **13**. The anisotropic displacement factor exponent takes the form: $-2\pi^2 [h^2 a^{*2} U11 + ... + 2 h k a^* b^* U12]$

Atom	U11	U22	U33	U23	U13	U12
Zr	15(1)	13(1)	17(1)	0(1)	1(1)	0(1)
Cl	24(1)	16(1)	28(1)	-4(1)	2(1)	-3(1)
Si	20(1)	17(1)	29(1)	-6(1)	-1(1)	-1(1)
N1	18(1)	14(1)	20(1)	-1(1)	1(1)	1(1)
N2	16(1)	18(1)	21(1)	-2(1)	0(1)	0(1)
N3	20(1)	26(1)	22(1)	-1(1)	4(1)	-1(1)
N4	25(1)	22(1)	26(1)	3(1)	7(1)	-1(1)
C1	16(1)	19(1)	22(1)	-1(1)	-2(1)	-2(1)
C2	15(1)	21(1)	24(1)	-1(1)	0(1)	-1(1)
C2'	24(1)	33(1)	29(1)	-1(1)	6(1)	-8(1)
C3	15(1)	20(1)	31(1)	-3(1)	-2(1)	2(1)
C3'	25(1)	29(1)	48(1)	-12(1)	2(1)	6(1)
C4	19(1)	20(1)	33(1)	4(1)	-5(1)	0(1)
C4'	33(1)	25(1)	52(1)	13(1)	-7(1)	2(1)
C5	18(1)	26(1)	23(1)	2(1)	-2(1)	-2(1)
C5'	33(1)	46(1)	22(1)	2(1)	-2(1)	-9(1)
C6	41(1)	47(1)	39(1)	-22(1)	-12(1)	14(1)
C7	33(1)	19(1)	80(2)	5(1)	6(1)	-4(1)
C8	20(1)	17(1)	18(1)	2(1)	2(1)	2(1)
C9	19(1)	20(1)	16(1)	1(1)	2(1)	2(1)
C10	21(1)	29(1)	25(1)	0(1)	-2(1)	4(1)
C11	27(1)	30(1)	29(1)	3(1)	0(1)	12(1)
C12	34(1)	20(1)	28(1)	2(1)	4(1)	10(1)
C13	27(1)	19(1)	24(1)	-1(1)	2(1)	1(1)
C14	17(1)	19(1)	23(1)	1(1)	-2(1)	1(1)
C15	24(1)	44(1)	24(1)	1(1)	-1(1)	-8(1)
C16	28(1)	51(1)	40(1)	12(1)	-6(1)	-17(1)
C17	31(1)	25(1)	53(1)	3(1)	-18(1)	-7(1)
C18	33(1)	29(1)	36(1)	-10(1)	-13(1)	6(1)
C19	23(1)	31(1)	26(1)	-3(1)	-2(1)	4(1)
C20	42(1)	28(1)	23(1)	6(1)	5(1)	6(1)
C21	40(1)	29(1)	25(1)	-4(1)	11(1)	-1(1)
C22	30(1)	31(1)	24(1)	2(1)	9(1)	4(1)
C23	43(1)	25(1)	36(1)	8(1)	9(1)	- 2(1)

Table A4.5. Hydrogen coordinates (x 10^4) and isotropic displacement parameters (A^2 x 10^3) for **13**.

Atom	x	y	z	U(eq)
H3'	8034(19)	662(11)	4317(18)	34(6)
H4'	9331(20)	1409(13)	1588(20)	53(7)
H2'A	4160(24)	61(14)	2852(23)	68(8)
H2'B	5107(24)	-353(17)	3198(24)	77(9)
H2'C	4786(23)	327(15)	3770(24)	71(9)
H3'A	4447(20)	2065(12)	2578(19)	47(6)
H3'B	4727(20)	1556(13)	3571(21)	53(7)
H3'C	5541(21)	2111(14)	3224(21)	56(7)
H4'A	5291(21)	2380(13)	688(20)	56(7)
H4'B	6412(20)	2511(13)	1313(20)	49(7)
H4'C	6350(21)	2240(13)	94(22)	56(7)
H5'A	6107(18)	550(12)	-993(18)	37(6)
H5'B	6748(21)	1241(15)	-867(22)	62(8)
H5'C	7301(23)	519(14)	-624(21)	58(7)
H6A	7185(25)	-1423(17)	-148(24)	81(10)
H6B	6254(25)	-979(15)	-598(24)	70(9)
H6C	7433(26)	-672(16)	-559(26)	79(10)
H7A	6434(23)	-1771(15)	1880(22)	66(8)
H7B	6057(25)	-1324(16)	2775(28)	82(11)
H7C	5335(26)	-1446(15)	1802(24)	75(9)
H10	11262(17)	-244(10)	3307(16)	30(5)
H11	11562(17)	-1444(11)	2957(17)	36(6)
H12	10178(16)	-2125(11)	2166(16)	32(5)
H13	8493(16)	-1624(10)	1680(16)	28(5)
H15	11117(18)	886(11)	1944(19)	38(6)
H16	12473(20)	1654(14)	2524(21)	59(8)
H17	12456(18)	2156(12)	4317(18)	44(6)
H18	10989(18)	1885(12)	5420(18)	39(6)
H19	9618(18)	1127(12)	4826(18)	42(6)
H20A	7509(18)	-302(12)	5316(19)	41(6)
H20B	6618(19)	-436(12)	4417(18)	39(6)
H20C	7877(18)	-506(12)	4077(18)	41(6)
H21A	6947(18)	849(11)	5740(19)	36(6)
H21B	6788(18)	1413(13)	4815(18)	44(6)
H21C	5944(21)	804(11)	4885(19)	45(6)
H22A	10173(19)	972(11)	121(18)	40(6)
H22B	9528(16)	352(11)	700(17)	30(5)
H22C	9043(19)	727(11)	-336(20)	40(6)
H23A	9447(18)	2146(11)	218(18)	40(6)
H23B	8214(17)	1882(11)	-248(18)	35(6)
H23C	8425(17)	2314(11)	911(17)	32(5)

Table A5.1. Crystal data and structure refinement for $Ta[N(CH_3)_2]_3[SO_2(NC(CH_3)_3)_2]$ **17.**

Empirical formula	$C_{14}H_{36}N_5O_2STa$
Formula weight	519.49
Temperature	173(2) K
Wavelength	0.71073 Å
Crystal system	Triclinic
Space group	P-1
Unit cell dimensions	a = 8.9208(1) Å α = 68.917(1)°
	b = 10.0987(1) Å β = 81.182(1)°
	c = 13.7290(1) Å γ = 64.79°
Volume	1044.15(2) Å^3,
Z	2
Density (calculated)	1.652 Mg/m^3
Absorption coefficient	5.378 mm^{-1}
F(000)	520
Crystal size	0.25 x 0.23 x 0.14 mm
θ range for data collection	2.36 to 27.50°
Limiting indices	$-11 \le h \le 10$
	$-13 \le k \le 13$
	$-13 \le l \le 18$
Reflections collected	7278
Independent reflections	4634 [R(int) = 0.0309]
Absorption correction	Empirical
Min. & Man Transmission	0.584, 0.394
Refinement method	Full-matrix least-squares on F^2
Data / restraints / parameters	4634 / 0 / 209
Goodness-of-fit on F^2	0.938
Final R indices [I>2σ(I)]	R1 = 0.0304, wR2 = 0.0770 [4356]
R indices (all data)	R1 = 0.0319, wR2 = 0.0779
Extinction coefficient	0.0039(5)
Largest diff. peak and hole	2.109 and -1.875 e.A^{-3}

Table A5.2. Atomic coordinates (x 10^4) and equivalent isotropic displacement parameters (A^2 x 10^3) for **17**. U(eq) is defined as one third of the trace of the orthogonalized Uij tensor.

Atom	x	y	z	U(eq)
Ta	6712(1)	7891(1)	2392(1)	16(1)
S	3645(1)	7556(1)	2463(1)	20(1)
O1	3187(4)	6496(4)	3356(3)	34(1)
O2	2444(4)	8327(4)	1621(3)	33(1)
N1	5543(4)	6709(4)	2066(2)	17(1)
N2	4117(4)	8738(4)	2752(3)	19(1)
N3	7436(5)	7351(4)	3813(3)	26(1)
N4	6615(5)	9903(4)	1415(3)	24(1)
N5	9005(5)	6762(4)	1948(3)	26(1)
C1	6063(5)	5154(4)	1938(3)	24(1)
C2	6684(7)	3879(5)	2993(4)	39(1)
C3	4661(6)	5038(6)	1517(5)	38(1)
C4	7474(5)	4958(5)	1146(3)	26(1)
C5	2868(5)	9940(5)	3174(4)	29(1)
C6	3756(6)	10810(6)	3378(4)	35(1)
C7	2144(8)	9196(7)	4217(5)	53(2)
C8	1454(7)	11103(6)	2397(6)	53(2)
C9	6732(7)	6512(7)	4727(4)	43(1)
C10	8707(7)	7705(7)	4078(4)	42(1)
C11	5221(6)	11049(5)	722(3)	32(1)
C12	7917(6)	10456(5)	1297(4)	37(1)
C13	9670(6)	7152(6)	884(4)	35(1)
C14	10258(6)	5401(5)	2644(5)	39(1)

Table A5.3. Bond lengths [Å] and angles [°] for **17**.

Ta-N3	1.961(4)
Ta-N4	1.965(3)
Ta-N5	1.996(4)
Ta-N1	2.074(3)
Ta-N2	2.145(3)
Ta-S	2.8799(10)
S-O1	1.446(3)
S-O2	1.452(3)
S-N2	1.606(3)
S-N1	1.648(3)
N1-C1	1.505(5)
N2-C5	1.486(5)
N3-C10	1.453(6)
N3-C9	1.460(6)
N4-C12	1.455(6)
N4-C11	1.462(5)
N5-C14	1.459(6)
N5-C13	1.469(6)
C1-C3	1.520(6)
C1-C4	1.525(6)
C1-C2	1.536(6)
C2-H2A	0.98
C2-H2B	0.98
C2-H2C	0.98
C3-H3A	0.98
C3-H3B	0.98
C3-H3C	0.98
C4-H4A	0.98
C4-H4B	0.98
C4-H4C	0.98
C5-C6	1.522(6)
C5-C8	1.535(7)
C5-C7	1.546(7)
C6-H6A	0.98
C6-H6B	0.98
C6-H6C	0.98
C7-H7A	0.98
C7-H7B	0.98
C7-H7C	0.98
C8-H8A	0.98
C8-H8B	0.98
C8-H8C	0.98
C9-H9A	0.98
C9-H9B	0.98
C9-H9C	0.98
C10-H10A	0.98
C10-H10B	0.98
C10-H10C	0.98
C11-H11A	0.98
C11-H11B	0.98
C11-H11C	0.98

C12-H12A	0.98
C12-H12B	0.98
C12-H12C	0.98
C13-H13A	0.98
C13-H13B	0.98
C13-H13C	0.98
C14-H14A	0.98
C14-H14B	0.98
C14-H14C	0.98
N3-Ta-N4	115.7(2)
N3-Ta-N5	92.4(2)
N4-Ta-N5	92.5(2)
N3-Ta-N1	120.90(14)
N4-Ta-N1	121.45(14)
N5-Ta-N1	98.78(14)
N3-Ta-N2	94.94(14)
N4-Ta-N2	94.65(14)
N5-Ta-N2	166.32(14)
N1-Ta-N2	67.54(12)
N3-Ta-S	109.83(11)
N4-Ta-S	112.23(11)
N5-Ta-S	132.95(11)
N1-Ta-S	34.20(9)
N2-Ta-S	33.39(8)
O1-S-O2	112.4(2)
O1-S-N2	113.7(2)
O2-S-N2	113.0(2)
O1-S-N1	111.7(2)
O2-S-N1	112.3(2)
N2-S-N1	92.3(2)
O1-S-Ta	121.8(2)
O2-S-Ta	125.7(2)
N2-S-Ta	47.32(12)
N1-S-Ta	45.01(11)
C1-N1-S	119.0(3)
C1-N1-Ta	136.3(3)
S-N1-Ta	100.8(2)
C5-N2-S	121.7(3)
C5-N2-Ta	139.0(3)
S-N2-Ta	99.3(2)
C10-N3-C9	113.0(4)
C10-N3-Ta	125.1(3)
C9-N3-Ta	121.9(3)
C12-N4-C11	111.1(3)
C12-N4-Ta	124.3(3)
C11-N4-Ta	124.6(3)
C14-N5-C13	110.2(4)
C14-N5-Ta	124.2(3)
C13-N5-Ta	125.6(3)
N1-C1-C3	111.7(3)
N1-C1-C4	108.3(3)
C3-C1-C4	107.5(4)
N1-C1-C2	108.9(3)
C3-C1-C2	111.1(4)

C4-C1-C2	109.2(4)
C1-C2-H2A	109.5(3)
C1-C2-H2B	109.5(2)
H2A-C2-H2B	109.5
C1-C2-H2C	109.5(3)
H2A-C2-H2C	109.5
H2B-C2-H2C	109.5
C1-C3-H3A	109.5(3)
C1-C3-H3B	109.5(2)
H3A-C3-H3B	109.5
C1-C3-H3C	109.5(3)
H3A-C3-H3C	109.5
H3B-C3-H3C	109.5
C1-C4-H4A	109.5(2)
C1-C4-H4B	109.5(2)
H4A-C4-H4B	109.5
C1-C4-H4C	109.5(2)
H4A-C4-H4C	109.5
H4B-C4-H4C	109.5
N2-C5-C6	107.2(3)
N2-C5-C8	112.0(4)
C6-C5-C8	108.5(4)
N2-C5-C7	111.1(4)
C6-C5-C7	108.4(4)
C8-C5-C7	109.6(5)
C5-C6-H6A	109.5(3)
C5-C6-H6B	109.5(2)
H6A-C6-H6B	109.5
C5-C6-H6C	109.5(3)
H6A-C6-H6C	109.5
H6B-C6-H6C	109.5
C5-C7-H7A	109.5(3)
C5-C7-H7B	109.5(3)
H7A-C7-H7B	109.5
C5-C7-H7C	109.5(3)
H7A-C7-H7C	109.5
H7B-C7-H7C	109.5
C5-C8-H8A	109.5(3)
C5-C8-H8B	109.5(3)
H8A-C8-H8B	109.5
C5-C8-H8C	109.5(3)
H8A-C8-H8C	109.5
H8B-C8-H8C	109.5
N3-C9-H9A	109.5(3)
N3-C9-H9B	109.5(3)
H9A-C9-H9B	109.5
N3-C9-H9C	109.5(3)
H9A-C9-H9C	109.5
H9B-C9-H9C	109.5
N3-C10-H10A	109.5(3)
N3-C10-H10B	109.5(3)
H10A-C10-H10B	109.5
N3-C10-H10C	109.5(3)
H10A-C10-H10C	109.5

H10B-C10-H10C	109.5
N4-C11-H11A	109.5(2)
N4-C11-H11B	109.5(2)
H11A-C11-H11B	109.5
N4-C11-H11C	109.5(2)
H11A-C11-H11C	109.5
H11B-C11-H11C	109.5
N4-C12-H12A	109.5(2)
N4-C12-H12B	109.5(2)
H12A-C12-H12B	109.5
N4-C12-H12C	109.5(3)
H12A-C12-H12C	109.5
H12B-C12-H12C	109.5
N5-C13-H13A	109.5(3)
N5-C13-H13B	109.5(2)
H13A-C13-H13B	109.5
N5-C13-H13C	109.5(3)
H13A-C13-H13C	109.5
H13B-C13-H13C	109.5
N5-C14-H14A	109.5(3)
N5-C14-H14B	109.5(2)
H14A-C14-H14B	109.5
N5-C14-H14C	109.5(3)
H14A-C14-H14C	109.5
H14B-C14-H14C	109.5

Table A5.4. Anisotropic displacement parameters ($A^2 \times 10^3$) for **17**. The anisotropic displacement factor exponent takes the form: $-2\pi^2 [h^2 a^{*2} U11 + ... + 2 h k a^* b^* U12]$

Atom	U11	U22	U33	U23	U13	U12
Ta	16(1)	15(1)	16(1)	-4(1)	0(1)	-8(1)
S	17(1)	21(1)	27(1)	-11(1)	3(1)	-10(1)
O1	35(2)	30(2)	40(2)	-13(1)	14(2)	-21(2)
O2	21(2)	34(2)	45(2)	-21(2)	-9(1)	-4(1)
N1	16(2)	15(1)	23(2)	-7(1)	0(1)	-7(1)
N2	15(2)	20(2)	28(2)	-12(1)	0(1)	-9(1)
N3	26(2)	34(2)	19(2)	-4(2)	-2(1)	-16(2)
N4	32(2)	20(2)	21(2)	-3(1)	-1(1)	-14(2)
N5	21(2)	25(2)	35(2)	-12(2)	6(2)	-12(2)
C1	25(2)	16(2)	33(2)	-9(2)	5(2)	-10(2)
C2	52(3)	19(2)	34(2)	-2(2)	6(2)	-11(2)
C3	31(2)	40(3)	65(3)	-38(3)	9(2)	-21(2)
C4	27(2)	24(2)	32(2)	-15(2)	4(2)	-10(2)
C5	23(2)	31(2)	41(2)	-22(2)	3(2)	-10(2)
C6	34(2)	35(2)	45(3)	-26(2)	5(2)	-14(2)
C7	55(4)	64(4)	62(4)	-44(3)	38(3)	-37(3)
C8	29(3)	39(3)	89(5)	-39(3)	-21(3)	9(2)
C9	48(3)	57(3)	25(2)	3(2)	-5(2)	-33(3)
C10	43(3)	63(3)	33(2)	-13(2)	-9(2)	-32(3)
C11	45(3)	21(2)	26(2)	2(2)	-11(2)	-13(2)
C12	40(3)	27(2)	47(3)	-5(2)	1(2)	-23(2)
C13	35(3)	42(3)	41(3)	-23(2)	18(2)	-24(2)
C14	26(2)	26(2)	66(4)	-18(2)	-8(2)	-7(2)

Table A5.5. Hydrogen coordinates (x 10^4) and isotropic displacement parameters (A^2 x 10^3) for **17**.

Atom	x	y	z	U(eq)
H2A	7586(7)	3980(5)	3247(4)	59
H2B	7089(7)	2861(5)	2907(4)	59
H2C	5772(7)	3984(5)	3498(4)	59
H3A	3732(6)	5160(6)	2010(5)	57
H3B	5050(6)	4023(6)	1428(5)	57
H3C	4295(6)	5856(6)	842(5)	57
H4A	8401(5)	5028(5)	1396(3)	40
H4B	7086(5)	5777(5)	474(3)	40
H4C	7841(5)	3944(5)	1060(3)	40
H6A	4663(6)	10081(6)	3873(4)	52
H6B	2972(6)	11603(6)	3670(4)	52
H6C	4205(6)	11307(6)	2720(4)	52
H7A	1567(8)	8630(7)	4100(5)	79
H7B	1363(8)	10009(7)	4494(5)	79
H7C	3045(8)	8477(7)	4720(5)	79
H8A	870(7)	10559(6)	2258(6)	79
H8B	1912(7)	11599(6)	1743(6)	79
H8C	679(7)	11895(6)	2693(6)	79
H9A	5885(7)	6306(7)	4503(4)	64
H9B	6229(7)	7139(7)	5188(4)	64
H9C	7611(7)	5528(7)	5104(4)	64
H10A	9134(7)	8266(7)	3438(4)	63
H10B	9614(7)	6738(7)	4446(4)	63
H10C	8232(7)	8348(7)	4530(4)	63
H11A	4362(6)	10650(5)	816(3)	48
H11B	5602(6)	11253(5)	-5(3)	48
H11C	4763(6)	12014(5)	888(3)	48
H12A	8836(6)	9668(5)	1769(4)	55
H12B	7477(6)	11416(5)	1467(4)	55
H12C	8317(6)	10655(5)	574(4)	55
H13A	8818(6)	8067(6)	424(4)	53
H13B	9998(6)	6276(6)	630(4)	53
H13C	10637(6)	7371(6)	891(4)	53
H14A	9801(6)	5152(5)	3350(5)	59
H14B	11227(6)	5615(5)	2655(5)	59
H14C	10588(6)	4520(5)	2394(5)	59

LIST OF REFERENCES

1. (a) Kaminsky, W. *Catalysis Today*, **1994**, *20*, 257. (b) Jordan, R. F. *Adv. Organomet. Chem.* **1991**, *32*, 325. (c) Marks T. J. *Acc. Chem. Res.* **1992**, *25*, 57. (d)Mohring, P. C.; Coville, N. J. *J. Organomet. Chem.* **1994**, *479*, 1, and refenreces therein.

2. (a) Arndtsen, B. A.; Bergman, R. G.; Mobley, T. A.; Peterson, T. H. *Acc. Chem. Res.* **1995**, *28*, 154. (b) Jacoby, D.; Isoz, S.; Floriani, C.; Chiesi-Villa, A.; Rizzoli, C. *J. Am. Chem. Soc.* **1995**, *117*, 2805-2816. (c) Cummins, C. C.; Schaller, C. P.; Van Duyne, G. D.; Wolczanski, P. T.; Chan, A. A.; Hoffmann, R. *J. Am. Chem. Soc.* **1991**, *113*, 2985. (d) Schaller, C. P.; Bonanno, J. B.; Wolczanski, P. T. *J. Am. Chem. Soc.* **1994**, *116*, 4133-4134. (e) Thompson, M. E.; Baxter, S. M.; Bulls, A. R.; Burger, B. J.; Nolan, M. C.; Santarsiero, B. D.; Bercaw, J. E. *J. Am. Chem. Soc.* **1987**, *109*, 203.

3. (a) Waymouth, R.; Pino, P. *J. Am. Chem. Soc.* **1990**, *112*, 4911. (b) Broene, R. D.; Buchwald, S. L.; *J. Am. Chem. Soc.* **1993**, *115*, 12569. (c) Buchwald, S. L.; Willoughby, C. A. *J. Am. Soc. Soc.* **1994**, *116*, 11703.

4. (a) Nugent, W. A.; Mayer, J. M. *Metal-Ligand Multiple Bonds*; John Wiley & Sons: New York, 1988. (b) Schrock, R. R.; Rocklage, S.; Wengrovius, J.; Rupprecht, G.; Feldman, J. *J. Mol. Catal.* **1980**, *8*, 73. (c) Ivin, K. J. *Olefin Metathesis*; Academic Press: New York, 1982.

5. (a) Lubben, T. V.; Wolczanski, P. T. *J. Am. Chem. Soc.* **1987**, *109*, 424. (b) Bercaw, J. E.; Wolczanski, P. T. *Acc. Chem. Res.* **1980**, *13*, 121. (c) Cummins, C. C.; Van Duyne, G. D.; Schaller, C. P.; Wolczanski, P. T. *Organometallicc* **1991**, *10*, 164. (d) Floriani, C.; Crscenzi, R.; Solari, E. *Organometallics* **1996**, *15*, 5456. (e) Churchill, M. R.; Li, Y. J.; Blum, L.; Schrock, R. R. *Organometallics* **1984**, *3*, 109.

6. Collman, J. P.; Hegedus, L. S.; Norton, J. R.; Finke, R. G. *Principles and Applications of Organotransition Metal Chemistry*; 2 ed.; University Science Books: Mill Valley, 1987.

7. (a) Coville, N. J.; du Plooy, K. E.; Pickl, W. *Coord. Chem. Rev.* **1992**, *116*, 1 and references therein. (b) Wilkinson, G.; Stone, F. G.; Abel, E.W. (Eds), *Comprehensive Organometallic Chemistry*, Pergamon Press: Oxford, 1982, Vol 3, 1.

8. Okuda, J. *Comments Inorg. Chem.* **1994**, *16*, 185 and references therein.

9. (a) Linden, A.; Schaverien, C.; Meijoboom, N.; Ganter, C.; Orpen, A. G. *J. Am. Chem. Soc.* **1995**, *117*, 3021. (b) Fokken, S.; Spaniol, T. P.; Kang, H. C.; Massa, W.; Okuda, J. *Organometallics* **1996**, *15*, 5069. (c) Fujimura, O.; Mata, de la F. J.; Grubbs, R. *Organometallics* **1996**, 1865. (d) Feher, F.; Tajima, T. L. *J. Am. Chem. Soc.* **1994**, *116*, 2145. (e) Heppert, J. A.; Dietz, S. D.; Eilerts, N. W.; Henning, R. W. Morton, M. D.; Takusagawa, F. *Organometallics 1993*, *12*, 2565.

10. Halterman, R. L. *Chem. Rev.* **1992**, *92*, 965.

11. (a) Crabtree, R. H. *The Organometallic Chemistry of Transition Metals*;, John Wiley & Sons Ed: New York, 1988. (b) Yamamoto, A. *Organotransition Metal Chemistry*; John Wiley & Sons: New York, 1986.

12. (a) Okuda, J. *Topics in Current Chemistry* **1991**, *160*, 97. (b) Janiak, C.; Schumann, H. *Adv. Organomet. Chem.* **1991**, *33*, 291.

13. (a) Ewen, J. A. *Stud. Surf. Sci. & Catal.***1986**, *25*, 271.

14. Bochman, M. *J. Chem. Soc., Dalton Trans.* **1996**, 255 and references therein.

15. Breslow, D. S.; Newburg, N. R. *J. Am. Chem. Soc.***1959**, *81*, 81.

16. (a) Bochmann, M.; Wilson, L. M.; Hurthouse, M. B.; Motevalli, M. *Organometallics* **1988**, *7*, 1148. (b) Jordan, R. F.; Bajgure, C. S.; Willet, R.; Scott, B. *J. Am. Chem. Soc* **1986**, *108*, 7410. (c) Jordan, R. F.; *Adv. Organomet. Chem.* **1991**, *32*, 325.

17. Britzinger, H. H.; Fischer, D.; Mulhaupt, R.; Rieger, B.; Waymouth, R. M. *Angew. Chem. Int. Ed. Engl.* **1995**, *34*, 1143. (and references therein)

18. Waymouth, R. M.; Coates, G. W. *Science* **1995**, *267*, 222.

19. (a) Ewen, J. A.; Jones, R. L.; Razavi, A.; Ferrera, J. D. *J. Am. Chem. Soc.* **1988**, *110*, 6255. (b) Brintzinger, H. H.; Schutenhaus, H. *Angew. Chem., Int. Ed. Engl.* **1979**, *18*, 777. (c) Liinas, G. H. Dong, S. H.; Mallin, D. T.; Rausch, M. D.; Linn, Y. G.; Chien, J. C. *Macromolecules* **1992**, *25*, 1242. (d) Mitchell, J. P.; Hajela, S.; Brookhart, S. K.; Hardcastle, K. I.; Henling, L. M.; Bercaw, J. E. *J. Am. Chem. Soc.* **1996**, *118*, 1045. (e) Lang, H.; Blau, S.; Pritzkow, H.; Zsolnai, L. *Organometallics* **1995**, *14*, 1850. (f) Jordan, R. F.; Christopher, J. N.; Diamond, G. M. *Organometallics* **1996**, *15*, 4038. (g) Hoffman, R.; Lauher, J. W.

J. Am. Chem. Soc. **1976**, *98*, 1729. (h) Hermann, W. A.; Morawietz, M. J.; Priermeier, T. *J. Organomet. Chem.* **1996**, *506*, 351. (i) Diamond, G. M.; Chernega, A. N.; Mountford, P.; Green, M. H. *J. Chem. Soc., Dalton, Tans.* **1996**, 921.

20. (a) Willoughby, C. A.; Buchwald, S. L. *J. Am. Chem. Soc.* **1992**, *114*, 7562. (b) Willoughby, C. A.; Buchwald, S. L. *J. Am. Chem. Soc.* **1994**, *116*, 8952.

21. (a) Halterman, R. L.; Ramsey, T. M. *Organometallics* **1993**, *12*, 2879. (b) Hitchcock, S. R.; Situ, J. J.; Covel, J. A.; Olmstead, M. M.; Nantz, M. H. *Organometallics* **1995**, *14*, 3732.

22. Hong, Y.; Kuntz, B. A.; Collins, S. *Organometallics* **1993**, *12*, 964.

23. Banovetz, J. P.; Stein, K. M.; Waymouth, R. M. *Organometallics* **1991**, *10*, 3430.

24. (a) Shapiro, P. J.; Bunel, E.; Schaefer, W. P.; Bercaw, J. E. *Organometallics* **1990**, *9*, 867. (b) Shapiro, P. M.; Cotter, W. D.; Schaefer, W. P.; Labinger, J. A.; Bercaw, J. E. *J. Am. Chem. Soc.* **1994**, *116*, 4623.

25. (a) Bunel, E.; Burger, B. J.; Bercaw, J. E. *J. Am. Chem. Soc.* **1988**, *110*, 976. (b) Burger, B. J.; Thompson, M. E.; Cotter, W. D.; Bercaw, J. E. *J. Am. Chem. Soc.* **1990**, *112*, , 1566.

26. (a) Canich, J. M. Eur. Patent Appl. EP-420-436-A1, 1991. (b) Canich, J. M. U.S. Patent Appl. 5,026,798, 1991. (c) Canich, J. M.; Hlatky, G. G.; Turner, H. W. PCT Appl. WO92-00333, 1992.

27. Stevens, J. C.; Timmers, F. J.; Wilson, D.R.; Schmidt, G. F.; Nickias, P. N.; Rosen, R. K.; Knight, G. W.; Lai, S. Eur. Patent Appl. EP-416-815-A2, 1991.

28. Carpenetti, D. W.; Kloppenburg, L.; Kupec, J. T.; Petersen, J. L. *Organometallics* **1996**, *15*, 1572.

29. Hughes, A. K.; Meetsma, A.; Tauben, J. H. *Organometallics* **1993**, *12*, 1936.

30. (a) Jutzi, P.; Siemeling, U. *J. Organom. Chem.* **1995**, *500*, 175. (b) Enders, M.; Rudolph, R.; Pritzkow, H. *Chem. Ber.* **1996**, *129*, 459. (c) Mu, Y.; Piers, W. E.; McQuarrie, D. C.; Zaworotko, M. J.; Young, V. G. *Organometallics* **1996**, *15*, 2720. (d) Okuda, J.; Schattermann, F.; Wocadlo, S.; Massa, W. *Organometallicx* **1995**, *14*, 789.

31. (a) du Plooy, K. E.; Moll, U.; Wocaldo, S.; Massa, W.; Okuda, J. *Organometallics* **1995**, *14*, 3129. (b) Okuda, J.; du Plooy, K. E.; Massa, W.; Kang, H.C.; Rose, U. *Chem. Ber.* **1996**, *129*. 275.

32. Kress, J.; Osborn J. A. *Angew. Chem., Int. Ed. Engl.* **1992**, *31*, 1585.

33. Ciruelos, S. Cuenca, T.; Gomez-Sal, P; Manzreno, A.; Royo, P. *Organometallics* **1995**, *14*, 177.

34. Spence, R.; Piers, W. *Organometallics* **1995**, *14*, 4617.

35. (a) Ruwwe, J.; Erker, G.; Frohlich, R. *Angew. Chem. Int. Ed. Engl.* **1996**, *35*, 80. (b) Rottger, D.; Erker, G.; Frohlich, R.; Kotila, S. *Chem. Ber.* **1996**, *129*, 1. (c) Bochmann, M.; Lancaster, S. J.; Robinson, O. B. *J. Chem. Soc., Chem. Commun.* **1995**, 2081.

36. (a) Hermann, W. A.; Baratta, W. *J. Organomet. Chem,.* **1996**, *506*, 357. (b) Hermann, W. A.; Baratta, W.; Morawietz, M. J. *J. Organomet. Chem.* **1995**, *497*, C4.

37. Cotton, A. F.; Wilkinson, G. *Advanced Inorganic Chemistry* 5th ed; John Wiley & Sons: New York, 1988.

38. (a) Trofimenko, S. *J. Am. Chem. Soc.* **1967**, *89*, 3170. (b) Trofimenko, S. *Acc.Chem. Res.* **1971**, *4*, 17. (c) Torfimenko, S. *Chem. Rev.* **1993**, *93*, 943.

39. (a) Stewart, H. F.; Koepsell, D. G.; West, R. *J. Am. Chem. Soc.* **1970**, *92*, 846. (b) Verkade, J. G. *Acc. Chem. Res.* **1993**, *26*, 483. (c) Kempe, R.; Brenner, S.; Arndt, P. *Organometallics* **1996**, *15*, 1071. (d) Kempe, R.; Fuhrmann, H.; Brenner, S.; Arndt, P. *Inorg. Chem.* **1996**, *35*, 6742. (e) Memmler, H.; Walsh, K.; Gade, L. H.; Lauher, J. W. *Inorg. Chem.* **1995**, *34*, 4062. (f) Cloke, G. F. N.; Hitchock, P. B.; Love, J. B. *J. Chem. Soc., Dalton Trans.* **1995**, 25.

40. (a) Uhrhammer, R.; Black, D. G.; Gardner, T. G.; Olsen, J. D.; Jordan, R. F. *J. Am. Soc. Chem.* **1993**, *115*, 8493. (b) Black, D. G.; Swenson, D. C.; Rogers, R. D.; Jordan, R. F. *Organometallics* **1995**, *14*, 3539. (c) Tjaden, E. B.; Swenson, D. C.; Jordan, R. F.; Peterson, J. L. *Organometallics* **1995**, *14*, 371.

41. (a) McConville, D. H.; Scollard, J. D. *J. Am. Chem. Soc.* **1996**, *118*, 1008. (b) McConville, D. H.; Scollard, J. D.; Vittal, J. J. *Organometallics* **1995**, *14*, 5478. (c) Warren, T. H.; Schrock, R. R.; Davis, W. M. *Organometallics* **1996**, *15*, 562.

42. (a) Andersen, R. A. *Inorg. Chem.* **1979**, *18*, 2928. (b) Planalp, R. P.; Andersen, R. A.; Zalkin, A. *Organometallics* **1983**, *2*, 16. (c) Canich, J. A.; Turner, H. W. (Exxon), PCT Int. Appl. WO 92/12162, July 23, 1992. (d) Horton, A. D.; With J. de *J. Chem. Soc. Chem. Commun.* **1996**, 1375.

43. (a) Guérin, F.; McConville, D. H.; Vittal, J. *Organometallics* **1995**, *14*, 3154. (b) Tsuie, B.; Swenson, D. C.; Jordan, R. F. *Organometallics* **1997**, *16*, 1392. (c) Schrock, R. R.; Cai, S. *Inorg. Chem.* **1991**, *30*, 4105.

44. Cloke, F. g.; Tilmann, J. G.; Hitchcock, P. B.; Love, J. *J. Organomet. Chem.* **1996**, *506*, 343.

45. Friedrich, S.; Gade, L. *Organometallics* **1995**, *14*, 5344.

46. Guérin, F.; McConville, D. H.; Vittal, J. *Organometallics* **1997**, *16*, 1491.

47. (a) Aoyagi, K.; Gantzel, K.; Kalai, K.; Tilley, D.T.*Organometallics* **1996**, *15*, 923. (b) Aoyagi, K.; Gantzel, P. K.; Tilley, D. T. *Polyhedron* **1996**, *15*, 4299.

48. (a) Redshaw, C.; Wilkinson, G.; Sweet, T. K.; Hurthouse, M. B. *Polyhedron* **1993**, *12*, 2417. (b) Ling, M.; Maata, E. A. *Inorg. Chem.* **1992**, *31*, 953. (c) Danopoulos, A. A.; Wong, A. C. C.; Wilkinson, G.; Hurthouse, M. B.; Hussain, B. *Chem. Soc., Dalston Trans.* **1990**, 315.

49. (a) Vanderlende, D. D.; Abboud, K. A.; Boncella, J. M. *Organometallics* **1994**, *13*, 3378. (b) Huff, R. L.; Wang, S.S.; Abboud, A. A.; Boncella, J. M. *Organometallics* **1997**, *16*, 1765. (c) Ortiz, C. G.; Abboud, A. A.; Boncella, J. M. Unpublished Results.

50. Feldman J.; Schrock, R. R. *Prog. Inorg. Chem.* **1991**, *39*, 1.

51. Wagener, K. B.; Boncella, J. M.; Nel, J. G. *Macromolecules* **1991**, *24*, 2649.

52. Vaughan, W. M.; Abboud, A. A.; Boncella, J. M. *J. Am. Chem. Soc.* **1995**, *117*, 11015.

53. VanderLende, D. D. Ph. D. Dissertation, University of Florida, 1994.

54. (a) Findeis, B.; Schubart, M.; Gade, L.; Möller, F.; Scowen, I.; McPartlin, M. *J. Chem. Soc., Dalston Trans.* **1996**, 125. (b) Friedrich, S.; Gade, L.; Edwards, A. J.; McPrtlin, M. *Chem. Ber.* **1993**, *126*, 1797. (c) Memmler, H.; Gade, L. H.; Lauher, J. W. *Inorg. Chem.* **1994**, *33*, 3064. (d) Shih, K.Y.; Schrock, R. R.; Kempe, R. *J. Am. Chem. Soc.* **1994**, *116*, 8804.

55. (a) Freundlich, J. K.; Schrock, R. R.; Davis, W. M. *J. Am. Chem. Soc.* **1996**, *118*, 3643. (b) Zanetti, N. C.; Schrock, R. R.; Davis, W. M. *Angew. Chem. Int. Ed. Engl.* **1995**, *34*, 2044. (c) Shih, K.Y.; Totland, K.; Ceidel, S. W.; Schrock, R. R. *J. Am. Chem. Soc.* **1994**, *116*, 12103.

56. Friedrich, S.; Memmler, H.; Gade, L. H.; Li, W. S.; Scowen, I.; McPertlin, M.; Housecroft, C. E. *Inorg. Chem.* **1996**, *35*, 2433.

57. Cummins, C. C.; Scrck, R. R.; Davis, W. M. *Inorg. Chem.* **1994**, *33*, 1448.

58. (a) Glassman, T. E.; Vale, M. G.; Schrock, R. R. *Organometallics* **1991**, *10*, 4046. (b) Glassman, T. E.; Vale, M. G.; Schrock, R. R. *J. Am. Chem. Soc.* **1991**, *113*, 725.

59. (a) Casey, C. P.; Jordan, R .F.; Rheingold, A. L. *J. Am. Chem. Soc.* **1983**, *105*, 665. (b) Casey, C. P.; Jordan, R. F.; Rheingold, A. L. *Organometallics* **1984**, *3*, 504. (c) Casey, C. P. *J. Organomet. Chem.* **1990**, *400*, 205.

60. (a) Johnson, L. K.; Virgil, S. C.; Grubbs, R. H. *J. Am. Chem. Soc.* **1990**, *112*, 5384. (b) Schrock, R. R.; De Pue, R. T.; Feldman, J.; Yap, K. B.; Yang, D. C.; Davis, W. M.; Park, L.; DiMare, M.; Schofield, M.; Anhaus, J.; Walborsky, E.; Evitt, E.; Kruger, C.; Betz, P. *Organometallics* **1990**, *9*, 2262. (c) Kress, J.; Osborn, J. A.; Greene, R. M. E.; Ivin, K. J.; Rooney, J. J. *J. Am. Chem. Soc.* **1987**, *109*, 899. (d) Bryan, J. C.; Mayer, J. M. *J. Am. Chem. Soc.* **1990**, *112*, 2298. (e) Legzins, P.; Phillips, E. C.; Sanchez, L. *Organometallics* **1989**, *8*, 940. (f) Cundari, T. R.; Gordon, M. S. *Organometallics* **1992**, *11*, 55. (g) Schattenmann, F. J.; Schrock, R. R. *J. Am. Chem. Soc.* **1996**, *118*, 3295. (h) Oskam, J. H.; Fox, H. H.; Yap, K. B.; McConvill, D. M.; O'Dell, R.; Lichtenstein, B. J.; Schrock, R. R. *J. Organomet. Chem.* **1993**, *459*, 185.

61. (a) Wengrovius, J. H.; Sancho, J.; Schrock, R. R. *J. Am. Chem. Soc.* **1981**, *103*, 3932. (b) Sancho, J.; Schrock, R. R. *J. Mol. Catal.* **1982**, *15*, 75. (c) McCallough, L. G.; Schrock, R. R. *J. Am. Chem. Soc.* **1984**, *106*, 4067. (d) Pedersen, S. F.; Churchill, M. R.; Wasserman, H.; Schrock, R. R. *J. Am. Chem. Soc.* **1982**, *104*, 6808. (e) McCullough, L. G.; Dewan, J. C.; Murdezk, J. C.; Schrock, R. R. *J. Am. Chem. Soc.* **1985**, *107*, 5987. (f) Churchill, M. R.; Ziller, J. W.; McCullough, L.; Pedersen, F.; Schrock, *Organometallics* **1983**, *2*, 1046.

62. Weiss, K.; Schubert, U.; Schrock, R. R. *Organometallics* **1986**, *5*, 397.

63. Freudenberger, J. H.; Schrock, R. R. *Organometallics* **1986**, *5*, 398.

64. (a) Schrock, R. R. *Acc. Chem. Res.* **1986**, *19*, 342. (b) Rocklage, S. M.; Churchill, M. R.; Wasserman, H. J.; Schrock, R. R. *Organometallics* **1982**, *1*, 1332. (c) Freudenberger, J. H.; Schrock, R. R. *Organometallics* **1985**, *4*, 1937.

(d) Schaverien, C. J.; Dewan, J. C.; Schrock, R. R. *J. Am. Chem. Soc.* **1986**, *108*, 2771.

65. (a) Blosch, L. L.; Abboud, K. A.; Boncella, J. M. *J. Am. Chem. Soc.* **1991**, *113*, 7066. (b) Blosch, L. L.; Gamble, A. S.; Abboud, K A.; Boncella, J. M. *Organometallics* **1992**, *11*, 2342. (c) Gamble, A. S.; Boncella, J. M. *Organometallicss* **1993**, *12*, 2814. (d) Blosch, L. L. Ph. D. Dissertation, University of Florida, July 1993.

66. (a) Vaughan, W. M.; Abboud, K. A.; Boncella, J. M. *Organometallics* **1995**, *14*, 1567. (b) Vaughan, W. M.; Abboud, A. A.; Boncella, J. M. *J. Organomet. Chem.* **1995**, *485*, 37.

67. (a) Schrock, R. R.; Crowe, W. E.; Bazan, G. C.; DiMare, M.; O'Regan, M. B.; Schofield, M. H. *Organometallics* **1991**, *10*, 1832. (b) Oskam, H. J.; Schrock, R. R. *J. Am. Chem. Soc.* **1993**, *115*, 11831. (c) Osborn, J. A.; Kress, J. *J. Am. Chem. Soc.* **1987**, *109*, 3953.

68. Churchill, M. R.; Li, Y. J. *J. Organomet. Chem.* **1985**, *282*, 239.

69. (a) Wigley, D. E.; Morrison, D. L. *Inorg. Chem.* **1995**, *34*, 2610. (b) Chao, Y. W.; Rodgers, P. M.; Wigley, D. E. *J. Am. Chem. Soc.* **1991**, *113*, 6326.

70. (a) Schrock, R. R. *J. Organomet. Chem.* **1986**, *300*, 249. (b) Schrock, R. R.; SePue, R. T.; Feldman, J.; Schaverien, C. J.; Dewan, J. C.; Liu, A. H. *J. Am. Chem. Soc.* **1988**, *110*, 1423. (c) Schrock, R. R.; Murdzek, J. S.; Bazan, G. C.; Robbins, J.; DiMare, M.; O'Regan, M. *J. Am. Chem. Soc.* **1990**, *112*, 3875.

71. Hinkle, R. J.; Stang, P. J.; Arif, A. M. *Organometallics* **1993**, *12*, 3510.

72. Derome, A. *Modern NMR Techniques for Chemistry Research*, Pergamon Press: New York, 1987.

73. (a) Powell, K. R.; Pérez, P. J.; Luan, L.; Feng, S. G.; White, P. S.; Brookhart, M.; Templeton, J. L. *Organometallics* **1994**, *13*, 1851. (b) Gunnoe, T. B.; White, P. S.; Templeton, J. L. *J. Am. Chem. Soc.* **1996**, *118*, 6916.

74. (a) Nugent, W. A.; Harlow, R. L. *Inorg. Chem.* **1980**, *19*, 777. (b) Cahn, D. M.; Fultz, W. C.; Nugent, W. A.; Roe, C. D.; Tulip, T. *J. Am. Chem. Soc.* **1985**, *107*, 251.

75. Arzoumanian, H.; Krentzien, H.; Teruel, H. *J. Chem. Soc., Chem. Commun.* **1991**, 55.

76. Hoffman, D. M.; Wierda, D. A. *J. Am. Chem. Soc.* **1990**, *112*, 7056.

77. Boncella, J. M.; Cajigal, M. L.; Abboud, K. A. *Organometallics* **1996**, *15*, 1905.

78. Erikson, T. K. G.; Mayer, J. *Angew. Chem., Int. Ed. Engl.* **1988**, *27*, 1527.

79. Schrock, R. R.; Clark, N. D.; Sancho, J.; Wengrovius, J. H.; Rocklage, S. M.; Pedersen, S. F. *Organometallics* **1982**, *1*, 1645.

80. Schrock, R. R.; LaPointe, A. M. *Organometallics* **1995**, *14*, 1875.

81. (a) Davis, W. M.; Weinstock, I. A.; Scrock, R. R. *J. Am. Chem. Soc.* **1991**,*113*, 135. (b) Edwards, D. S.; Blondi, L. V.; Ziller, J. W.; Churchill, M. R.; Scrock, R. R. *Organometallcis* **1983**, *2*, 1505.

82. Jutzi, P. *Chem. Rev.* **1986**, *86*, 983.

83. (a) Bermann, M.; Wazer, J. R. *Synthesis* **1972**, 576. (b) Stowell, J. C. *J. Org. Chem.* **1967**, *32*, 2360. (c) Sharpless, B. K.; Hawkins, J. M. *J. Org. Chem.* **1984**, *49*, 3862.

84. (a) Kemmit, R. D.; Mason, S.; Moore, M. R.; Fawcett, J.; Russell, D. R. *J. Chem. Soc., Chem. Commun.* **1990**, 1535. (b) Parkin, I. P.; Slawin, A.; Williams, D. J.; Woollins, J. D. *J. Chem. Soc., Chem. Commun.* **1989**, 1060. (c) Parkin, I. P.; Woollins, D. J. *J. Chem. Soc, Dalton Trans.* **1990**, 519. (d) Cowley, A. H.; Mehropta, S. K.; Roesky, H. W. *Inorg. Chem.* **1981**, *20*, 712.

85. Sandström, J. *Dynamic NMR Spectroscopy* Academic Press: New York, 1982.

86. (a) Diamond, G. M.; Jordan, R. F.; Petersen, J. L. *J. Am. Chem. Soc.* **1996***118*, 8024. (b) Diamond, G. M.; Jordan, R. F. *Organometallics* **1996**, *15*, 4030. (c) Christopher, J. N.; Diamond, G. M.; Jordan, R. F. *Organometallics* **1996**, *15*, 4038. (d) Diamond, G. M.; Jordan, R. F.; Petersen, J. L. *Organometallics* **1996**, *15*, 4045.

87. Johnson, A. R.; Davis, M.W.; Cummins, C. C. *Organometallics* **1996**, *15*, 3825.

88. Boncella, J. M.; Andersen, R. A. *Organometallics* **1985**, *4*, 205.

89. Sheldrick, G. M. *SHELLXT*; Nicolet XRD: Madison, WI. 1986

BIOGRAPHICAL SKETCH

Percefoni Doufou was born on January 30, 1970, in Thessaloniki, Greece. At the age of eleven she took her first chemistry class as it is customary in Greek schools and soon thereafter, she announced to her parents that she wanted to be a chemist when she grew up. While finishing her last year in Anatolia College, an American high school in her home town, and after some helpful talks with the president of the school, William McGrew, she decided to apply to College of Wooster. She received her acceptance to the college with mixed feelings of joy and sadness since, she would have to leave her family behind to pursue a better education.

Doufou enjoyed chemistry in Wooster, especially her junior and senior year. She also managed to minor in archaeology, a field that always fascinated her. The summer of 1991, she came to the University of Florida for the summer undergraduate research program and conducted research under the supervision of Dr. James M. Boncella. Returning to Wooster, she worked on her Senior Independent Thesis under the supervision of Dr. Paul L. Gaus. She received her B.A. in May of 1992.

She then returned to the University of Florida as a graduate student, and joined the research group of Dr. Boncella. Her research involved two areas. The first part focused on the synthesis, characterization, and mechanistic studies of intramolecular proton transfer in a series of trispyrazolyl borate tungsten amido neopentylidyne complexes. The second project involved the synthesis of (bis)sulfamido and cyclopentadienyl-*o*-phenylenediamido ligands, and their reactions with group IV and V metal complexes. She graduated with her Ph.D. in August 1997.

I certify that I have read this study and that in my opinion it conforms to acceptable standards of scholarly presentation and is fully adequate, in scope and quality, as a dissertation for the degree of Doctor of Philosophy.

James M. Boncella, Chairman
Associate Professor of Chemistry

I certify that I have read this study and that in my opinion it conforms to acceptable standards of scholarly presentation and is fully adequate, in scope and quality, as a dissertation for the degree of Doctor of Philosophy.

David E. Richardson
Professor Chemistry

I certify that I have read this study and that in my opinion it conforms to acceptable standards of scholarly presentation and is fully adequate, in scope and quality, as a dissertation for the degree of Doctor of Philosophy.

Kenneth B. Wagener
Professor of Chemistry

I certify that I have read this study and that in my opinion it conforms to acceptable standards of scholarly presentation and is fully adequate, in scope and quality, as a dissertation for the degree of Doctor of Philosophy.

Russell S. Drago
Graduate Research Professor of Chemistry

I certify that I have read this study and that in my opinion it conforms to acceptable standards of scholarly presentation and is fully adequate, in scope and quality, as a dissertation for the degree of Doctor of Philosophy.

Anthony B. Brennan
Associate Professor of Materials Science and Engineering

This dissertation was submitted to the Graduate Faculty of the Department of Chemistry of the College of Liberal Arts and Sciences and to the Graduate School and was accepted as partial fulfillment of the requirements for the degree of Doctor of Philosophy.

August, 1997

Dean, Graduate School